UNIVERSITY OF OKLAHOMA

GRADUATE COLLEGE

FAIR RESOURCE ALLOCATION IN MACROSCOPIC EVACUATION PLANNING USING MATHEMATICAL PROGRAMMING: MODELING AND OPTIMIZATION

A DISSERTATION

SUBMITTED TO THE GRADUATE FACULTY

in partial fulfillment of the requirements for the

Degree of

DOCTOR OF PHILOSOPHY

By

HAMOUD SULTAN BIN OBAID

Norman, Oklahoma

2020

FAIR RESOURCE ALLOCATION IN MACROSCOPIC EVACUATION PLANNING USING MATHEMATICAL PROGRAMMING: MODELING AND OPTIMIZATION

A DISSERTATION APPROVED FOR THE
SCHOOL OF INDUSTRIAL AND SYSTEMS ENGINEERING

BY THE COMMITTEE CONSISTING OF

Dr. Theodore B. Trafalis, Chair

Dr. Sridhar Radhakrishnan

Dr. Kash Barker

Dr. Andres Gonzalez

Dr. Charles Nicholson

To my family

My wife Amjad, my mother Eitidal and my father Sultan, and my brothers and sisters

Acknowledgments

First and foremost, thanks to God for his countless blessings. To my friends, faculty and staff at the University of Oklahoma, no words can describe my deep appreciation to your support and encouragement during my pursuit of my doctoral degree.

I would like to express my deepest appreciation for my family members for their support. No words can describe my gratitude to my wife for standing next to me and supporting me to achieve my goals. She helped me go through the difficulties during my studies.

I am grateful to my advisor, Dr. Theodore B. Trafalis, for his continuous support, kindness, and responsiveness. Without his continuous help and guidance, the work in this dissertation would not be possible.

I would like to extend my special thanks to the members of my committee Dr. Sridhar Radhakrishnan, Dr. Kash Barker, Dr. Andres Gonzalez, and Dr. Charles Nicholson for their support, assistance, and feedback.

I would like to acknowledge my sponsor, King Saud University, for giving me the opportunity to pursue higher education. The thanks are extended to the Saudi Arabian Cultural Mission (SACM) for being the coordinator of my sponsorship.

Finally, I would like to thank the School of Industrial and Systems Engineering at the University of Oklahoma, its faculty, staff, and my colleagues whom I consider as my family during my journey.

Table of Contents

List of Tables

List of Figures

List of Acronyms

ACR	ant colony routing
AET	average evacuation time
ATC	air traffic control
ATM	asynchronous transfer mode
ATT	average travel time
BFW	bi-conjugate Frank-Wolfe
BPR	Bureau public roads
CFW	conjugate Frank-Wolfe
COV	coefficient of variation
CSO	constrained system optimal
CTM	cell transmission model
DTA	dynamic traffic assignment
FIFO	first-in-first-out
FW	Frank-Wolfe
GA	genetic algorithm
GP	gradient projection
IP	Internet protocol
LBM	latency based model
LP	linear programming
MAD	maximum of absolute deviations
MAE	mean absolute error
MILP	mixed integer linear programming
MMF	max-min fairness
MPLS	multi-protocol label switching
NA	nearest allocation
NCT	network clearance time
PFA	*progressive-filling* algorithm
POF	price of fairness
PQ	point queue
REE	robust efficient evacuation
RFEE	robust fair-efficient evacuation
RGS	route guidance system
SAD	sum of the absolute deviation
SO	system optimal
SPD	sum of the positive deviation
SSD	sum-of-squared deviations
TET	total evacuation time
TTT	total travel time
UE	user equilibrium
UFP	unsplittable flow problem
UWSN	underwater sensor networks

Abstract

Evacuation is essential in the case of natural and manmade disasters such as hurricanes, nuclear disasters, fire accidents, and terrorism epidemics. Random evacuation plans can increase risks and incur more losses. Hence, numerous simulation and mathematical programming models have been developed over the past few decades to help transportation planners make decisions to reduce costs and protect lives. However, the dynamic transportation process is inherently complex. Thus, modeling this process can be challenging and computationally demanding. The objective of this dissertation is to build a balanced model that reflects the realism of the dynamic transportation process and still be computationally tractable to be implemented in reality by the decision-makers. On the other hand, the users of the transportation network require reasonable travel time within the network to reach their destinations.

This dissertation introduces a novel framework in the fields of fairness in network optimization and evacuation to provide better insight into the evacuation process and assist with decision making. The user of the transportation network is a critical element in this research. Thus, fairness and efficiency are the two primary objectives addressed in the work by considering the limited capacity of roads of the transportation network. Specifically, an approximation approach to the max-min fairness (MMF) problem is presented that provides lower computational time and high-quality output compared to the original algorithm. In addition, a new algorithm is developed to find the MMF resource allocation output in nonconvex structure problems. MMF is the fairness policy used in this research since it considers fairness and efficiency and gives priority to fairness. In addition, a new dynamic evacuation modeling approach is introduced that

is capable of reporting more information about the evacuees compared to the conventional evacuation models such as their travel time, evacuation time, and departure time. Thus, the contribution of this dissertation is in the two areas of fairness and evacuation.

The first part of the contribution of this dissertation is in the field of fairness. The objective in MMF is to allocate resources fairly among multiple demands given limited resources while utilizing the resources for higher efficiency. Fairness and efficiency are contradicting objectives, so they are translated into a bi-objective mathematical programming model and solved using the ϵ-constraint method, introduced by Vira and Haimes (1983). Although the solution is an approximation to the MMF, the model produces quality solutions, when ϵ is properly selected, in less computational time compared to the *progressive-filling* algorithm (PFA). In addition, a new algorithm is developed in this research called the θ*-progressive-filling* algorithm that finds the MMF in resource allocation for general problems and works on problems with the nonconvex structure problems.

The second part of the contribution is in evacuation modeling. The common dynamic evacuation models lack a piece of essential information for achieving fairness, which is the time each evacuee or group of evacuees spend in the network. Most evacuation models compute the total time for all evacuees to move from the endangered zone to the safe destination. Lack of information about the users of the transportation network is the motivation to develop a new optimization model that reports more information about the users of the network. The model finds the travel time, evacuation time, departure time, and the route selected for each group of evacuees. Given that the travel time function is a non-linear convex function of the traffic volume, the function is linearized through a piecewise linear approximation. The developed model is a mixed-integer linear programming (MILP) model with high complexity. Hence, the

model is not capable of solving large scale problems. The complexity of the model was reduced by introducing a linear programming (LP) version of the full model. The complexity is significantly reduced while maintaining the exact output.

In addition, the new θ-*progressive-filling* algorithm was implemented on the evacuation model to find a fair and efficient evacuation plan. The algorithm is also used to identify the optimal routes in the transportation network. Moreover, the robustness of the evacuation model was tested against demand uncertainty to observe the model behavior when the demand is uncertain. Finally, the robustness of the model is tested when the traffic flow is uncontrolled. In this case, the model's only decision is to distribute the evacuees on routes and has no control over the departure time.

Chapter 1: Introduction

1.1 Overview

The average number of world natural catastrophes over the past 30 years (from 1987 to 2016) is 490 with average fatalities of 53,000 and $130 billion in losses as reported by Re (2018), and Max (2016). However, the number of catastrophes has been increasing with 710 events in 2016 most of which require mass evacuation to protect lives and properties. In addition, evacuation is essential for some manmade disasters such as nuclear disasters, fire accidents, and terrorism epidemics. The definition of evacuation is the removal of persons or things from an endangered area. The endangered area can be a building, neighborhood, city, or state. Evacuation is a natural reaction in emergencies to protect lives, and random evacuation plans can increase the risks and incur further losses.

Hence, numerous simulation and mathematical models have been proposed over the past few decades to help transportation planners make decisions to reduce costs and protect lives. However, the dynamic transportation process is inherently complex, and modeling this process can be challenging and computationally demanding. Simulation models can overcome these challenges, but they may fail to guarantee optimality. The objective is to build a balanced mathematical model that reflects the realism of the dynamic transportation process and still be computationally tractable to be implemented in reality by the decision-makers. On the other hand, the users of the transportation network require reasonable travel times within the network to reach their destinations. The output of the model should confirm with the decision-maker and the user requirements.

1.2 Problem Statement

The transportation in evacuations is quite different than transportation in normal conditions. Due to the sudden surge in demand to evacuate, the roads become massively congested, raising the risks of loss in properties and lives. For example, evacuation of a vast region including Houston, Texas, in hurricane Rita caused massive congestion where evacuees spent long times is traffic causing more fatalities than the actual hurricane, as reported by Litman (2006). Large-scale evacuations are a necessity to protect lives and properties. Hence, optimizing these evacuations can significantly reduce congestions and minimize costs.

The first objective of this dissertation is to develop a novel modeling approach to enhance the evacuation process and to help decision-makers allocate demands on the available capacity resources to reduce the congestion effect and find the optimal network clearance time. Specifically, a mixed-integer linear programming (MILP) model is developed as a dynamic traffic assignment (DTA) model that we call latency-based model (LBM). To the best of our knowledge, there is no mathematical programming modeling approach that computes the estimated time each group of evacuees spends on each route. Most of the mathematical programming DTA models find the network clearance time (NCT), and some models compute the estimated average travel time (ATT) and average evacuation time (AET) of the evacuees (Bish et al., 2014). In this proposed model, evacuees use the set of shortest routes to reach the destination. There are many algorithms to find the set of shortest routes (Rhodes, 2016), for example. The travel time on any road segment is load-dependent as a function of the flow. The function used is a modified version of the Bureau of Public Roads (1964) function proposed by Mtoi and Moses (2014). Our model is capable of propagating the delay that takes place in downstream road segments to the upstream segments along the predefined routes. However, the

developed model's complexity is high, leading us to develop a smaller version of the original model with lower complexity and exact output. Using small network examples, the results of the model are compared with the cell transmission model (CTM) introduced by Daganzo (1994, 1995), which is later modified to a linear programming (LP) model by Ziliaskopoulos (2000). We also show that the CTM model regulates the entrance to a road segment rather than slowing the traffic along the road segment, which indicates that the CTM model is insensitive to the length of a congested road segment. The model is also tested on a real-world network, and the results are compared with the CTM. Further, sensitivity analysis is implemented by changing the number of groups to observe the behavior of the ATT and AET.

The second objective in this dissertation is to allocate resources of the transportation network fairly among the users in the evacuation process. First, a new approach to finding an approximation to the MMF is presented to find a fair-efficient resource allocation. The model is developed as a multicriteria optimization model, and the output is compared with the *progressive-filling* algorithm (PFA) output. In addition, a new algorithm is developed to find the MMF resource allocation. The new algorithm, called θ*-progressive-filling* algorithm, does not rely on the complementary slackness condition to identify the saturated demands. Hence, the θ*-progressive-filling* algorithm is capable of finding the MMF resource allocation in nonconvex structure problems and can find the MMF resource allocation in general problems.

In addition, the new θ*-progressive-filling* algorithm is implemented to the LBM model to find the MMF evacuation time for all groups of evacuees. The results of the algorithm are compared with different objectives, such as the NCT and AET. Moreover, the θ*-progressive-filling* algorithm is capable of finding the optimal routes in the transportation network since the algorithm works on problems with the nonconvex structure. The sum of absolute deviations

(SAD) is used as a performance measure to compare fairness, and the AET is used to compare the efficiency of different objectives.

Finally, the model robustness is tested by assuming that the number of evacuees is uncertain, and the underlying distribution of the demand is unknown. The robust counterpart of the LBM model is introduced based on the box uncertainty set. The main objective is to maintain the model feasibility under different scenarios since that infeasible model is useless. In addition, the iterative θ-*progressive-filling* algorithm is tested to achieve a robust fair and efficient distribution of evacuees by finding the MMF evacuation times on the given set of used routes. The other objective tested is the AET, which finds the most efficient evacuation plan. The mean, standard deviation, and maximum NCT, AET, and SAD are reported for the tested networks. The evacuation time and the number of evacuees are plotted for robust efficient and robust fair-efficient objectives. The assumption is that the flow is controlled. However, the flow, in reality, is uncontrolled because the departure time is mostly the decision of the evacuee. Hence, the model is tested when the flow of evacuees is uncontrolled, given that the model decision is on distributing the evacuees on the predefined routes.

1.3 Assumptions

The evacuation model is developed based on a few assumptions as follows:

1- The road capacities are constant with the assumption that road capacities are not affected by accidents such as car crashes, building collapses, or medical conditions that add to the expected delay.
2- All evacuees follow the route guidance system (RGS) to achieve the optimal evacuation plan.

3- The destination nodes are uncapacitated. Hence, there are no restrictions on how many evacuees can be sent to a specific destination.
4- All communities are treated fairly, assuming that the threat level is equal for all communities.

1.4 Main Contributions

This dissertation introduces a set of novel approaches, algorithms, and models to optimize the evacuation process with the objective of MMF. The contributions in this dissertation are highlighted in this section.

1- A bi-objective optimization model is developed to find an approximate MMF resource allocation for general problems. The efficiency is maximized in one objective, and the difference between commodities is minimized in the second objective. The application used is a static bandwidth allocation with multiple demands.
2- A new MILP latency-based evacuation model, we call it LBM, is developed as a DTA model to optimize the evacuation process. The travel time is a piecewise approximation to the nonlinear traffic volume function.
3- A new LP latency-based DTA evacuation model is developed as a less complex version of the original model in contribution 2. The model complexity is significantly reduced while maintaining the exact output of the original model. The model is then compared with the known CTM.
4- A new algorithm called θ-*progressive-filling* algorithm is developed to find the MMF resource allocation for general problems. The algorithm does not rely on the complementary slackness condition to identify the blocking demands. Hence, it is

capable of finding the MMF resource allocation for nonconvex structure problems. In addition, the algorithm can be used to find the optimal routes in transportation networks.

5- The *θ-progressive-filling* algorithm is implemented on the LBM model. We use an illustrative example to show the effectiveness of the algorithm and how it can achieve a fair and efficient solution. The algorithm is also tested on convex and nonconvex structure, and the output of the two models are compared.

6- The robust counterpart of the LBM model is introduced. The model's robustness is tested by assuming that the demand to evacuate is uncertain. We show that the robust model outperforms the nominal model in its worst case. The mean, standard deviation, and maximum of NCT, AET, and SAD are presented for three networks. In addition, we assume that the flow of evacuees is uncontrolled, i.e., the evacuee decides its departure time. So, the only decision the model makes is allocating evacuees on routes. The results are reported and compared with controlled flow evacuees.

1.5 Dissertation Organization

This dissertation is composed of 8 chapters. In chapter 1, an overview of the evacuation problem is introduced, the problem statement is addressed, and the main contributions are listed. In chapter 2, a general literature review is discussed in two parts. In section 2.1, a literature review of fairness in resource allocation is discussed. In section 2.2, the evacuation modeling literature review is presented. Next, an approximation approach using bi-objective optimization to solve the MMF problem is presented in chapter 3. Then, a new approach to model the evacuation process is introduced in chapter 4. Afterward, the LBM evacuation model complexity is reduced while maintaining the exact original model output in chapter 5. In chapter 6, a new iterative algorithm that finds the MMF is introduced and implemented to the LBM evacuation model.

Next, the LBM robustness is tested under demand uncertainty with the controlled and uncontrolled flow, comparing the efficient and fair-efficient outputs in chapter 7. Afterward, the contribution of this dissertation is summarized in addition to recommendations for future research in chapter 8. Finally, additional figures from chapters 3 and 7 are listed in Appendix A.

Chapter 2: Literature Review

In this chapter, an overview of two fields is presented. The first field is fairness, and the second field is evacuation.

2.1 Fairness in Resource Allocation

Fairness has been gaining great interest in the past few decades. The decision-maker objective is to maximize efficiency, but if fairness is not considered, the service receivers are not satisfied and claim that it is an unfair or unjust distribution of resources. However, if the objective is to distribute resources fairly, the decision-maker may not be satisfied if the resources are not fully utilized. A balanced solution between fairness and efficiency is the goal of fair resource allocation. Fairness, in its early development, was applied in the microeconomics of social welfare. Every individual or demand is assigned a utility function *u* based on the preference of the individual assuming that the decision-maker is aware of the preferences of each individual. The set of resources *X* is to be distributed among individuals. Given that $x \in X$ is a feasible allocation of resources among the individuals chosen by the decision-maker, then $f_i(x)$ is the utility of individual *i* for every $i = 1,..,n$. This leads to the utility set *U* for all individuals:

$$U = \{u_i = f_i(x), \forall\, i = 1,..,n\} \tag{2-1}$$

Fair distribution of resources was initiated by observing and measuring the differences in the level of income of individuals in a society or a country by the statistician Gini (1912). Gini developed the measure Gini index or the Gini coefficient to measure income inequality. Then he discussed the relationship between the Gini index and the Lorenz curve in Gini (1914). Later, fair division of resources was introduced by Steinhaus (1948) through the Cake Cutting Problem, where resources are distributed fairly or what is called an envy-free division. Fairness has gained

significant interest, and many approaches have been developed to allocate resources fairly. The scope of this chapter is to review fair resource allocation approaches in general and, more specifically, in networks.

The chapter is organized as follows. In section 2.1.1, the early development of fairness in resource distribution is discussed. In section 2.1.2, some measures of fairness are explored. Policies for resource sharing such as Lexicographic ordering, max-min fairness (MMF), proportional fairness, and (p, α)-proportional fairness are discussed in section 2.1.3. In section 2.1.4, MMF is discussed in detail. Finally, some applications in fairness are presented in section 2.1.5.

In section 2.1.5.1, fairness in communication networks is discussed. In section 2.1.5.2, fairness in facility location is discussed. In section 2.1.5.3, fairness in air traffic control is reviewed. Fairness in job scheduling is discussed in section 2.1.5.4. In section 2.1.5.5, fairness in evacuation and traffic management is reviewed.

2.1.1 Fairness Early Development

The classical fair division of an object between two partners is by letting one partner halve the object and the other to choose their half. The first partner is satisfied by being allowed to split the object into two halves, and the other is pleased by being given the freedom to choose one of the two halves. This problem is known by the cake cutting problem or envy-free division, and an example of a divisible object is a land (pasture or field). Using this method becomes complicated if the number of partners is more than three. Steinhaus (1948) has proposed an approach to solving this problem for *n* partners proposed by B. Knaster and S. Banach. Every partner has the right to cut a part of the cake until the last one cuts the last piece he touched, then he is

eliminated. The remaining $n - 1$ repeat the same procedure until two partners are left, then the classical rule is applied. Examples of divisible resources are salary, bonus, performance incentives, and severance pay.

Steinhaus then proposed an approach to fairly divide indivisible objects such as houses, animals, cars, etc. among n partners. Every partner estimates the value of each object, and then every object value is decided by the highest estimated value and attributed to the partner who estimated it. Then, partners who received higher-value objects compensate the partners with the lower-value objects to reduce the differences to zero. See Brams and Taylor (1996) and Golovin (2005) for more details.

Fairness has been applied in the microeconomic theory of social welfare (Mas-Colell et al., 1995). Every consumer is assigned a utility function based on their preferences of the desired commodities, then all utility functions of all consumers are aggregated into a social welfare function. The objective is to maximize the social welfare function with respect to fairness and justice. A way to fairly maximize the utility functions of all consumers is to maximize the worst-off utility function or to rank alternatives based on their worst outcomes, given their probabilities. This approach is called maximin or Rawlsian social welfare function by Rawls (1971), but it is not Pareto optimal in most cases. Another approach is the leximin ordering of social welfare function by using lexicographical ordering by Chen (2000), and it provides a Pareto optimal solution for the optimal leximin social welfare function. Lexicographical ordering will be discussed in detail in a later section. Finally, max-min fairness is the most widely accepted approach since it fairly distributes resources and maximizes the utilization of the system. The relationship between Leximin maximum and the max-min fair solution will be discussed in detail in section 2.1.3.

2.1.2 Fairness Measures

In this section, some measures are used to determine the variability in the distributed resources among the set of demands. However, some of these measures can be employed as objectives.

2.1.2.1 Basic Fairness Measures

To measure equity or fairness, simple statistical measures such as the mean, standard deviation, and variance can give an excellent indication of how the resource is distributed on individual demands. The resource can be bandwidth in communication networks, distance in facility location, or processing time in job scheduling. In addition, these measures can be set as objectives in mathematical programming. Some of the basic statistical measures discussed in Leclerc et al. (2012) are the maximum of absolute deviations (MAD), the sum-of-squared deviations (SSD), and the sum of the absolute deviations (SAD). Note that u_i is the resource assigned to demand *i* given that the number of demands is *n*, and $\bar{u}$ is the average resource of all the *n* demands.

$$MAD = \max_{i=1,2,..,n} |u_i - \bar{u}| \tag{2-2}$$

$$SSD = \sum_{i=1}^{n} (u_i - \bar{u})^2 \tag{2-3}$$

$$SAD = \sum_{i=1}^{n} |u_i - \bar{u}| \tag{2-4}$$

These measures perform well as objectives in mathematical programming. However, there are drawbacks associated with these measures if they are employed as objectives. These measures can produce superior results with low total deviation but with poor efficiency. All demands can be assigned zero resources and still provide excellent results. Another drawback is that some demands are assigned zero resources at the cost of improving other demands with more

resources. These measures quantify the differences on average and not considering every demand independently.

2.1.2.2 Gini Index

One of the measures to measure the income inequality in a society developed by Gini (1912) is the Gini index or Gini coefficient, as shown in (2-5). We denote by u_i the level of income of individual *i*. If the income of all individuals is equal, the absolute difference among incomes is zero indicating perfect equality. However, if one individual receives all the income and all others receive zero income, the Gini index equals one, as seen in (2-6). Values greater than one are possible if the utility function of an individual is negative.

$$\mathcal{G} = \frac{\sum_{j=1}^{n} \sum_{i=1}^{n} |u_i - u_j|}{2n \sum_{i=1}^{n} u_i} \tag{2-5}$$

$$0 \leq \mathcal{G} \leq 1 \tag{2-6}$$

To find the Gini index value from the Lorenz curve shown in Figure 2-1, the shaded area is divided by both the shaded and the striped areas under the curve. If the Lorenz curve falls on the line of equality, then the shaded area becomes zero resulting in the Gini index value of zero. See Gastwirth (1972) for more details.

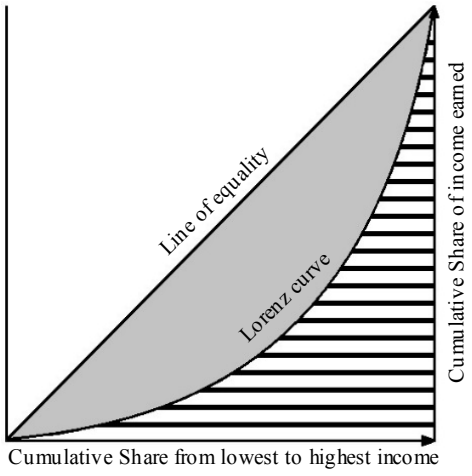

Figure 2-1: Lorenz curve

2.1.2.3 Jain's Index

Jain's index, illustrated in (2-7), is derived from the coefficient of variation (*COV*). The variability of a series of numbers is measured independently by the *COV*. See Abdi (2010) for more illustration. Jain's index is equal to $1/(1 + COV^2)$, indicating a negative correlation with the *COV*. Jain's index is bounded by $\frac{1}{n}$ and 1, and the higher the index, the fairer the solution is, as shown in (2-8). If *k* out of *n* demands are allocated resources fairly, Jain's index is equal to k/n, meaning that it is very intuitive. See Jain et al. (1999) for more details.

$$\mathcal{J} = \frac{(\sum_{i=1}^{n} u_i)^2}{n \sum_{i=1}^{n} u_i^2} \tag{2-7}$$

$$\frac{1}{n} \leq \mathcal{J} \leq 1 \tag{2-8}$$

2.1.2.4 Unfairness

The unfairness measure provides an insight into the maximum difference between the highest value, and the lowest value of the assigned resource in the form of a fraction is the unfairness $u(x)$ Correa et al. (2007). $v_i(x)$ is the cost of the resource $x_i \; \forall \; i \in D$ given *D* is the set of demands, as shown in (2-9). The lower bound of the fraction is one indicating perfect fairness, as seen in (2-10).

$$U(x) = max\left\{\frac{v_i(x)}{v_j(x)} : i, j \in D, \; x_i, x_j > 0\right\} \tag{2-9}$$

$$u(x) \geq 1 \tag{2-10}$$

There are four variations of the unfairness measure. These fairness measures are loaded unfairness, normal unfairness, user equilibrium unfairness, and free-flow unfairness. In loaded unfairness, the ratio is the entity travel time to the fastest traveler on the same source-destination

pair. Normal unfairness delivers the ratio of the length of the entity path to the shortest path of the same source-destination pair. User equilibrium unfairness provides the ratio of the entity travel time to the travel time on the same source-destination pair under user equilibrium. Finally, the ratio of the entity travel time to the length of the fastest path for the same source-destination pair is found by the free-flow unfairness, for more details see Jahn (2005).

2.1.2.5 Price of Fairness (POF)

The price of fairness is a measure of the percentage of utilization lost when fairness is incorporated in the model (Bertsimas and Farias, 2011). To find an efficient solution and its optimal allocation, the model (2-11)-(2-12) is solved, and the optimal value is denoted with SYSTEM(U).

$$Max\ e^T u \tag{2-11}$$

subject to

$$u \in U \tag{2-12}$$

If the decision-maker objective is to distribute the resources among demands fairly, the sum of utilities is denoted by $\text{FAIR}(U;\Phi) = e^T\Phi(U)$. Since efficiency and fairness are conflicting objectives, the sum of utilities will mostly decrease, resulting in a loss in efficiency. The percentage of loss can be measured by the price of fairness $\text{POF}(U;\ \Phi)$ in (2-13). The closer the POF to 0, the lower efficiency compromised.

$$\text{POF}(U;\ \Phi) = \frac{\text{SYSTEM}(U) - \text{FAIR}(U;\Phi)}{\text{SYSTEM}(U)} \tag{2-13}$$

The upper bounds of the POF when MMF and PF are the fairness schemes considered as seen in (2-14) and (2-15). See Bertsimas and Farias (2011) for more details.

$$\mathrm{POF}(U;\Phi^{PF}) \leq 1 - \frac{2\sqrt{n}-1}{n}, \tag{2-14}$$

$$\mathrm{POF}(U;\Phi^{MMF}) \leq 1 - \frac{4n}{(n+1)^2}, \tag{2-15}$$

where Φ^{PF} is the proportional fairness scheme, and Φ^{MMF} is the max-min fairness scheme.

2.1.3 Policies for Resource Sharing

2.1.3.1 Lexicographic Ordering

To find an equitable solution using lexicographic ordering, the lexicographic minimax model (2-16) is applied.

$$\underset{x}{Min}\left\{\underset{j=1,..,n}{Max}\, f_j(x), x \in \mathcal{X}\right\}, \tag{2-16}$$

where $\mathcal{X}$ is the set of feasible solutions, and $f_j, j = 1,..,$ n are the objective functions. The model (2-16) is solved to find the lexicographic minimax vector of optimal solutions. A vector is leximin larger than another vector if the non-decreasing ordered vector is lexicographically larger than the other non-decreasing ordered vector. The vector x is said to be lexicographically greater than the vector y ($x \succ y$) if $x_i = y_i$ and $x_j > y_j$ for all $j > i$. The vector x is said to be lexicographically greater than or equal the vector y ($x \succcurlyeq y$) if $x \succ y$ or $x = y$. The relationship between the MMF vector and lexmin maximal vector can be described by the following statement. If a vector $x \in \mathcal{X}$ is MMF over the set $\mathcal{X}$, then the vector is lexmin maximal over the set $\mathcal{X}$. A vector x is lexmin maximal over the set $\mathcal{X}$ if for all $y \in \mathcal{X}$, $x \succcurlyeq y$. However, the opposite relationship is not always true. The lexmin maximal vector x is not necessarily MMF vector over the set $\mathcal{X}$ since the lexmin maximal vector x is not necessarily unique. For example,

Figure 2-2 A does not have an MMF solution since the two points (2,4) and (4,2) contradict the MMF definition, as we will discuss in the next section. However, these two points are leximin maximal solutions. Although Figure 2-2 B has a unique leximin maximal point (4,2), it is not MMF since x_2 can be increased by decreasing x_1. See Radunović and Boudec (2007) for more details.

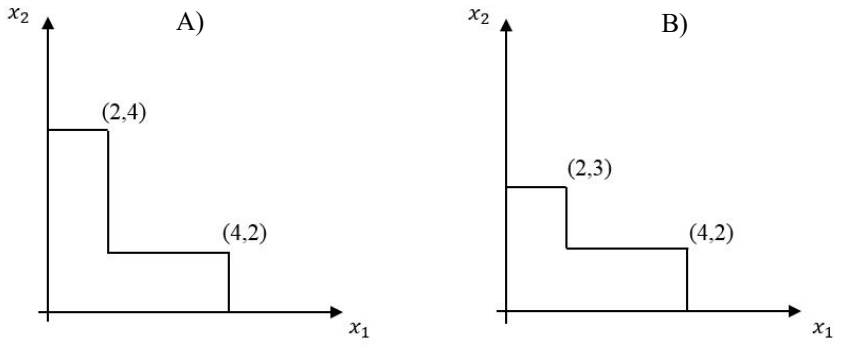

Figure 2-2: two-dimensional examples to illustrate the difference between leximin maximum solution and MMF solution

2.1.3.2 Max-Min Fairness

MMF is a state where all resources are utilized with the fairest possible allocation. A vector $\gamma \in \Gamma$ is said to be max-min fair if it is feasible, and if there exists $\gamma_s' > \gamma_s$ for $s \in \{1, \dots, n\}$, then $\gamma_t' < \gamma_t \leq \gamma_s$ for $t \in \{1, \dots, n\}$. Let us assume that the vector γ is MMF on the set Γ. A component γ_s in the vector γ cannot be increased without worsening another component γ_t that is less than or equal to γ_s on the same set. *Water-filling* or *progressive-filling* algorithm is an algorithm that gives the MMF solution introduced by Bertsekas and Gallager (1987). See Nace (2008) for more illustration. MMF solution is unique and provides the fairest solution with the highest efficiency. As a result, it is a widely accepted approach to find a fair and efficient resource allocation solution. The algorithm is called *water filling* or *progressive-filling* since it starts filling the lowest capacity components with the available

resource until the component is filled, then it proceeds with the other components until the resource is consumed or all components are filled. Suppose there is a set of demands *K*, and the goal is to supply these demands with the resource α. At iteration $n = 0$, the set of blocking demands B_n is an empty set meaning that the resource in all demands in constraint (2-18) is maximized when maximizing α in the objective function (2-17).

$$Max\ \alpha, \tag{2-17}$$

subject to

$$f_k(x) \geq \alpha, \qquad \forall\ k \in K \backslash B_n \tag{2-18}$$

$$f_k(x) \geq \lambda_k, \qquad \forall\ k \in B_n \tag{2-19}$$

$$x \in \mathrm{X}. \tag{2-20}$$

The *progressive-filling* algorithm to find the max-min fair solution is defined as follows:

- Set n := 0 and $L_0 = \emptyset$;

- While $L_n \neq K$ do:

  - Set $n = n+1$. Solve the LP problem P_n, compute α;
  - Identify the set K_n of saturated demands in iteration n, set $\lambda_k = \alpha\ \forall k \in K_n$ and $B_n = B_{n-1} \cup K_n$.

The flow vector obtained at the last step is leximin maximal, and the obtained multicommodity flow is thus a max-min fair one.

The iterative approach to find MMF flow in networks is very common, but there are some challenges related to it. The first challenge with this approach is solving the LP model a number

of times that can be computationally demanding, depending on the size of the network. Another challenge is in identifying the blocking constraints. The method to identify the blocking constraints in MMF is to identify the binding constraints through the dual variables. The corresponding dual variables to the binding constraints are positive according to the strict complementary slackness theorem, but the complementary slackness condition is not necessary. As a result, only a subset of the binding constraints is identified in each iteration leading to degeneracy since $\alpha_n = \alpha_{n+1} = \alpha_{n+2} = \cdots$. This would lead to higher computational time, but convergence is guaranteed. In addition, the *water filling* algorithm has some limitations depending on the structure of the problem. The feasible space has to be convex, and the utility function is concave for the water filling algorithm to work. Bin Obaid and Trafalis (2016) introduced an approximation model to find the max-min fair solution for bandwidth allocation in communication networks. The model works on convex and non-convex problems. However, the max-min fair solution is not guaranteed based on the structure of the problem. Next, we discuss the concept of proportional fairness as an alternative fairness concept.

2.1.3.3 Proportional Fairness (PF)

Given a set of users *K*, a vector of rates x with components $x_k, k \in K$ is proportionally fair if it is feasible and if for any other vector of rates y with components $y_k, k \in K$, the aggregate proportional changes are less than or equal to zero as seen in (2-21).

$$\sum_{k \in K} \frac{y_k - x_k}{x_k} \leq 0 \tag{2-21}$$

Proportional fairness is applied when the service received is proportional to the amount paid by the service receiver. Suppose bandwidth is sent to a set of demands *K* through a network with a set of capacitated resources *J* of capacity *C*, and a set *A* given $A_{jk} = 1$ if demand *k* uses resource

j. The objective (2-22) is to maximize the utility function for all demands subject to capacity constraints (2-23) and non-negativity constraints (2-24).

$$Max \sum_{k \in K} U_k(x_k), \tag{2-22}$$

subject to

$$Ax \leq C, \tag{2-23}$$

$$x \geq 0. \tag{2-24}$$

Assume that the amount paid w_k per unit time is decided by user *k* and receives flow x_k proportional to m_k given that $x_k = m_k/\lambda_k$ where λ_k is the cost per unit of time. Now the objective (2-25) is to maximize the utility of user *k* and minimize the amount paid by every user given that the amount paid is non-negative (2-26).

$$Max\ U_k\left(\frac{m_k}{\lambda_k}\right) - m_k, \tag{2-25}$$

subject to

$$m_i \geq 0. \tag{2-26}$$

Suppose that the vector *m* is known. The optimal solution of the objective (2-27) subject to the constraints (2-28) and (2-29) is proportionally fair. See Bonald et al. (2006) for more details. If $m_k = 1\ \forall\ k \in K$, the vector of rates is a Nash bargaining solution. See Kelly (1997) and Kelly et al. (1998) for more details.

$$Max \sum_{k \in K} m_k \log x_k, \tag{2-27}$$

subject to

$$Ax \leq C, \tag{2-28}$$

$$x \geq 0. \tag{2-29}$$

2.1.3.4 (p, α) - Proportional Fairness

Let $p = (p_1, p_2, \dots, p_R)$ and α are positive numbers. A vector of rates x with components $x_k, k \in K$ is (p, α) proportionally fair if it is feasible and for any other vector y with components $y_k, k \in K$ the aggregate proportional changes are less than or equal to zero as shown in (2-30).

$$\sum_{k \in K} p_k \frac{y_k - x_k}{x_k^{\alpha}} \leq 0 \tag{2-30}$$

Although max-min fairness is a widely accepted approach for fair and efficient resource allocation, some researchers claim that max-min fairness gives absolute priority to fairness. (p, α) – proportional fairness is a generalization of max-min fairness and proportional fairness. Since fairness and utilization are contradicting objectives, (p, α)-proportional fairness compromises between resource utilization, in objective (2-22), and proportional fair solution in objective (2-27). Note that (p, α) – proportional fairness, as shown in (2-31), is a generalization to proportional fairness (Mo, 2000). For α = 0, the maximum utilization is found $U(0) = \sum_{k \in K} x_k$, and for α = 1, the result is the proportional fair solution $U(1) = \sum_{k \in K} \log(x_k)$.

$$U_k(x_k, \alpha) = \begin{cases} \dfrac{x_k^{1-\alpha}}{1-\alpha} & for\ \alpha \neq 1 \\ \log(x_k) & for\ \alpha = 1 \end{cases} \tag{2-31}$$

As α goes to ∞, the solution converges to max-min fairness. See Mo and Walrand (2000) for more details.

2.1.4 Max-Min Fairness in Resources Allocation

Among the policies of resource sharing, MMF is the fairest policy since it starts with the least fortunate group of individuals or demands, then proceeds with the next group to improve efficiency. MMF in networks early exploration by Megiddo (1974) introduces the concept of distributing the flow fairly, based on lexicographic ordering, instead of maximizing the overall flow in the network. In addition, Bertsekas et al. (1992) were among the first to explore MMF for multicommodity flow networks. Leximin ordering and its applications, such as microeconomic theories in social welfare, are discussed in the literature. See Hulme and Mosley (1996), for example. A vector is leximin larger than another vector if the non-decreasing ordered vector is lexicographically larger than the other non-decreasing ordered vector. The vector x is said to be lexicographically greater than the vector y ($x \succ y$) if $x_i = y_i$ and $x_j > y_j$ for all $j > i$. The vector x is said to be lexicographically greater than or equal the vector y ($x \succcurlyeq y$) if $x \succ y$ or $x = y$. The relationship between MMF vector and lexmin maximal vector can be described by the following statement. If a vector $x \in \mathcal{X}$ is MMF over the set $\mathcal{X}$, then the vector is lexmin maximal over the set $\mathcal{X}$. A vector x is lexmin maximal over the set $\mathcal{X}$ if for all $y \in \mathcal{X}$, $x \succcurlyeq y$. However, the opposite relationship is not always true. The lexmin maximal vector x is not necessarily MMF vector over the set $\mathcal{X}$ since lexmin maximal vector x is not necessarily unique. Hence, an MMF vector x is lexmin maximal vector over the set $\mathcal{X}$ and unique. The reader is referred to Radunovic and Le Boudec (2007). The most common approach to find MMF flow in a multicommodity network is using the PFA. To find MMF in multicommodity network, each commodity is assigned a fixed path, and all commodity flows are increased simultaneously until a blocking commodity is reached, then the blocking commodity flow and the capacity it is occupying are removed from the network. See Nace (2006) for more details. This process is

repeated until all commodity flows are removed from the network. Another method to find MMF in resource allocation in flow networks introduced by Retvari et al (2007) is the polyhedral approach. Geometry is used to find MMF flows in networks where the number of commodities represents the number of dimensions of the polyhedron. Changing the flow of one commodity would result in a change in the flow of other commodities sharing the same capacity of the network, forming a polyhedron. The MMF flow solution point in the polyhedron can be located by maximizing the distance between the point and the zero axes for each commodity. The drawbacks of this approach are that the path for each commodity has to be predefined to identify the right-hand side values of the constraints, and the model is solved iteratively, which can lead to high computational time. A paper by Amaldi et al. (2014) introduce an approach to find the max throughput subject to MMF flow by building an MIP model. Each commodity follows a single path that is predefined as a parameter, and a 0-1 variable represents each commodity to follow one path among a number of possible paths. Another 0-1 variable is defined to indicate whether a link is a bottleneck in addition to flow variables of the links and the commodities. This problem rises to an exponential number of variables as the network's size increases. As a result, the author suggests a branch and price to solve the problem. Moreover, the network topology is an important factor in the fair distribution of commodity flows, as illustrated by Carvalho (2012). Semi-analytical methods were used to solve the problem on the nearest neighbor graph using the shortest path flow, where the distance between the source and sink is a function of the shortest paths. Bashllari et al. (2007) have explored the rerouting of flow under disruption in two scenarios, partial rerouting, and global rerouting. Their approach to solving the problem is by dynamic programming solving an LP model in each iteration. A number of papers deal with the dynamic flow, and others optimize the static flow (offline). It is infeasible to update the traffic

routing depending on the traffic distribution variation since operators cannot afford it. However, the commodity flow demand can be forecasted in the average or worst-case scenario to optimize under static flow as discussed by Nace and Pi (2012). The flow of bandwidth in the internet protocol (IP) network is measured by Mbs/sec and required to be unsplittable leading to higher complexity. The unsplittable flow problem (UFP) complexity is NP-complete. However, multi-protocol label switching (MPLS) technology allows the bandwidth traffic to be split among multiple paths. In the next chapter, the assumption is that the traffic is static (offline), and the multicommodity flow can be split among different routes.

2.1.5 Applications in Fairness

2.1.5.1 Fairness in Communication networks

Recently, more than 90% of the literature of fair resource allocation has been extensively applied specifically in communication networks and networks in general. Megiddo (1974) has introduced fairness to networks. He finds the optimal solution to the fair and maximum flows using the lexicographical ordering of the individual flows for sources and sinks. Nace and Pióro (2008) discuss the max-min fairness approach and its variations to fairly distribute bandwidth among a set of demands in communication networks. Max-min fair bandwidth allocation is studied in different network structures such as multi-channel wireless mesh networks, wireless multihop networks, cellular networks, and packet switches and routers by Tang et al. (2006), Thulasiraman et al. (2011), Boche et al. (2007), and Pan and Yang (2007) respectively. When the bandwidth demand is very high, the network or routers become congested. Mahajan et al. (2001) and Siu and Tzeng (1995) explore congestion in routers and asynchronous transfer mode (ATM) networks, respectively.

Another application is in communication networks, where fairness in resource allocation is applied in the area of wireless sensor networks. Wireless sensors are placed in remote and hard to reach areas to sense the environment such as temperature, wind speed, humidity, etc. Then, send the data to the server through the shortest path to optimize the energy. The source of energy for these sensors is from solar panels or wind propellers. Some sensors sense and send the information while other sensors sense information, receive information from different sensors, and send the information to other sensors or the server, and these processes require energy. The objective is to maximize the utilization and fairly sense the data from all the sensors in the network. Sridharan and Krishnamachari (2009) uses max-min fairness to maximize the utilization and fairly collect information from all sensors in the network. Hsu et al. (2010) claim that it is inefficient to use max-min fairness for underwater sensor networks (UWSN) and proposes MILP model to find a max-min fair solution.

2.1.5.2 Fairness in Facility Location

Fairness in resource allocation is applied to other applications in networks. Fairness is applied in facility location and location-allocation problems. When placing public facilities such as schools, libraries, or outpatient clinics, minimizing the distance from the facility to the service receivers is the main objective. However, minimizing the total distances may result in placing the facility very far from some service receivers and very close to others, which may drive some service receivers to claim that it is unfair or unjust. Beheshtifar and Alimoahmmadi (2015) develop a model with multiple objectives to determine optimal sites for new clinics. Two of the objectives are minimizing the total distance to reach the clinics and minimizing the inequity to access the clinics. Buzna et al. (2014) propose an approach to solve the facility location problem using a lexicographic minimax objective to find an equitable and efficient solution.

However, when placing fire stations, police departments, or ambulance stations, modeling the problem can be slightly different. The problem becomes a set covering problem since the response time is a vital factor in the rescue process. Goldberg (2004) develops a mixed-integer programming (MIP) model that determines the optimal location and dispatching process of ambulances. The model maximizes the number of potential patients covered locations (within nine minutes distance) and fairly allocates the patients to the ambulance locations by distributing the demand fairly among the ambulance locations. We conclude that fairness can be applied not only to service receivers but also to service providers. Another example of locating facilities fairly is by Erkut et al. (2008). They introduced a multicriteria facility location model for solid waste, and one of the objectives is to locate the facilities fairly.

2.1.5.3 Fairness in Air Traffic Control (ATC)

The demand for air transportation has been increasing significantly, leading to air traffic congestion and more challenging scheduling tasks. The scheduling process starts with strategic planning, where flights are assigned takeoff and landing slots. Before execution, tactical planning takes place due to uncontrolled delays caused by inclement weather or technical issues. These delays incur a cost in billions of dollars. Decision-making tools are being developed to improve the scheduling process. The majority of the optimization models fail in considering the distribution of delay equally among the airline carriers. As a result, minimizing the total delay minutes (or total cost) is an efficient solution, but it remains unimplemented due to the lack of fairness. Jonker et al. (2005) have proposed an MIP model imposing fairness using real-world data spanning across six days. Since fairness and efficiency are contradicting objectives, they achieved fairness, compromising less than 10% of the total cost. See Jonker et al. (2005) for more details.

2.1.5.4 Fairness in Job Scheduling

Job scheduling on parallel processors has been extensively studied in the past few decades. Job scheduling can become very challenging as the number of jobs increases since they are scheduled over time and space. In addition, jobs are scheduled on multiple threads, which leads to an extremely large number of combinations. As a result, the model complexity is NP-complete. Hence, approximation models and heuristics have been introduced in the literature. See Feitelson and Rudolph (1995) and Schwiegelshohn and Yahyapour (1998) for more details. Due to the high demand of different size job processing, the fairness issue has arisen. Algorithms and heuristics are introduced for fair job scheduling. See Wang et al. (2013) and Zaharia et al. (2010). Another application of fair scheduling is applied in heterogeneous vehicular networks by Zhang et al. (2016). They used a max-min fair scheduling approach to maximize the mobile service amount. See Thawari et al. (2012) and Zhang (2016) for more details.

2.1.5.5 Fairness in Evacuation and Traffic Management

Fairness has been applied to evacuation processes and traffic management. The objective of fair evacuation models is to minimize the total evacuation time and fairly allocate evacuees to the shortest route with minimum travel time. The delay experienced by the evacuees due to congestion is a main factor in the evacuation process. A very common approach to model an evacuation model is the CTM developed by Daganzo (1993). The objective in CTM is to minimize the NCT, or system optimal (SO), neglecting fairness in routing the evacuees, which may cause high congestion in some parts of the network and lead to further losses in lives and properties. User equilibrium (UE) or Wardrop's rule by Wardrop (1952) is the optimal fair solution that schedules travelers on the shortest routes such that no traveler can improve their

travel time by changing routes. The result is a fair distribution of resources and minimum congestion over the network.

2.1.6 Summary

Fairness is applicable in applications with multiple demands. The set of demands are assigned utility functions based on their preferences. Then the utilities are maximized fairly for a fair-efficient solution given that fairness is more important than efficiency in some applications. There is no single method to find a fair and efficient resource allocation. Every approach has its strength points and weaknesses. Using basic statistical measures may not give the fairest, or the most efficient solution since the average or total deviation is minimized, disregarding the individual allocations. Gini index, Jain's index, and unfairness are non-linear functions and can lead to more computational complexity. Max-min fairness can be computationally demanding with the problem size if the *progressive-filling* algorithm is used. Finding a proportional fair or (p, α) – proportional fair solution can be challenging. Lagrangean duality is one of the approaches to find a proportional fair solution.

2.2 Evacuation Modeling

2.2.1 Evacuation Overview

An early exploration of evacuation process improvement in theatre buildings by Smith (1882) was by redesigning the doorways, hallways, and stairways of a theatre to preventing congestion in case of emergencies. The author's approach to preventing clogging the exit doors and hallways is by dividing them by partitions allowing only one person to fit forming a line of people to avoid body contact. Evacuation has been gaining great interest in the past few decades, and simulation and mathematical programming models have been developed. A wide variety of evacuation

models has been explored with different objectives. Evacuation models are categorized under two main categories; vehicle-based evacuation and structure evacuation. Structure evacuation covers the evacuation of pedestrians from buildings such as stadiums, skyscrapers, and theaters. See Kiski and Francis (1985) for example. On the other hand, vehicle-based evacuation includes private vehicle evacuation and mass-transit evacuation such as bus-based evacuation by Bish et al. (2014) and Margulis et al. (2006) respectively. Based on a specific objective, evacuation procedures are modeled as microscopic or macroscopic by Parisi and Dorso (2005) Yusoff et al. (2008) respectively. Microscopic focuses on the movement of individual entities while the macroscopic focuses on the overall flow of evacuees. Mesoscopic models cover both microscopic and macroscopic as proposed by Di Gangi (2011). The evacuation models are also classified as static and dynamic models. In static models, the time has no effect on the model by Kagaris (1999) while dynamic evacuation models incorporate time in the model by Kaufman et al. (1998).

2.2.2 Objectives of Evacuation Models in Flow Networks

There are several objectives in these evacuation models such as system optimal (SO), user equilibrium (UE), nearest allocation (NA), and constrained system optimal (CSO). The objective in SO as defined by Wardrop (1952) is to minimize the total evacuation time of evacuees to minimize the NCT. In UE, the evacuation time for each group or individual on all routes is minimized so that no individual can improve their travel time by changing routes (Nash equilibrium). Evacuees are assigned to the nearest shelter or safe destination in NA by Southworth (1991). The models SO and UE/NA are contradicting since the SO does not consider the distribution of the individual evacuation times.

2.2.2.1 Wardrop's First Principle

The objectives in most mathematical programming traffic assignment models are the NCT known as SO, or the UE. UE or the First Wardrop principle by Wardrop (1952) is that the evacuation time of all evacuees is minimized, and no individual evacuee can improve their travel time by changing routes. This objective provides the best solution for each individual. Nash equilibrium is another fair resource allocation approach introduced by Nash (1951) in network games. An n-person game consists of n players, and each player has a finite set of strategies and a payoff function p_i. The Nash equilibrium point solution is when each player maximizes their strategy if the other players' strategies are fixed. Hence, each player has an optimal strategy against other players. Charnes and Cooper (1961) observed the relationship between Wardrop equilibrium and Nash equilibrium. Nash equilibrium converges to Wardrop equilibrium as the number of players increases in a network game with a finite number of players as proved by Haurie and Marcotte (1985). For more illustration, see Correa and Stier-Moses (2011). UE is equivalent to MMF, where the maximum evacuation time of all evacuees is minimized until it cannot be improved any further. Then the next group of evacuees' evacuation time that can be improved is minimized until they cannot be improved. This process is repeated until all travel times are minimized to obtain an optimal MMF solution. In the MMF solution, no individual can improve their travel time without worsening another individual's travel time that is less than or equal to them. See Friesz et al. (1993) and Smith (1993) for example. To find the MMF solution, the *water filling* or *progressive-filling* algorithm, introduced by Bertsekas (1987), is used. The *progressive-filling* algorithm works only on convex problem since it uses the complementary slackness to identify the evacuation time that cannot be improved any further. In some cases,

MMF flow may not use routes shorter than the used ones. However, the Nash equilibrium does not leave shorter routes unused. See Correa et al. (2007) for more details.

Selfish routing regained a great interest in the recent years after Wardrop's first principle UE. Lack of fairness can motivate evacuees to act selfishly to reach their destination in the shortest time possible. Game theory or network games is the common approach that addresses selfish routing. See Anshelevich and Ukkusuri (2009), Hayrapetyan et al. (2007), Nikolova and Stier-Moses (2011), and van Essen et al. (2016).

2.2.2.2 Wardrop's Second Principle

SO or the second Wardrop's principle introduced by Wardrop (1952) in the traffic assignment models is the NCT in the optimization models. In SO, the maximum evacuation time on any route is minimized to maximize the evacuation efficiency disregarding the individual travel times. However, SO results in unfair assignment of traffic on the same or different origin-destination pairs. See Tuydes-Yaman and Ziliaskopoulos (2014) for example. Modeling the congestion effect in the problem is a challenging task since it contributes greatly to the model complexity as the load dependent travel time is a non-linear function of the traffic volume. In addition, minimizing the maximum travel time of the traffic in flow networks is an NP-hard problem even with linear latency functions and with a single source and terminal as shown by Correa et al. (2007). The drawback of SO is that the model does not consider the congestion in different parts of the network as the model objective is to minimize the network clearance time. Hence, parts of the network can be highly congested leading to longer evacuation time. See Correa (2007) for more illustration.

CSO, which is a compromised objective between SO and UE, has been explored by Jahn et al. (2005) to balance the system efficiency and the fairness in static traffic assignment networks.

Lujak et al. (2015) proposed a static traffic assignment modeling approach to find a fair-efficient solution based on Nash Welfare optimization. Finding a fair and efficient solution using CSO is also applicable in facility location. Bayram et al. (2015) introduce a non-linear static model with CSO objective to compromise system efficiency and users' interest in shelter location in evacuation which is an application under evacuation and facility location.

Other objectives are tested by Bish et al. (2014) in the evacuation model. Minimizing the ATT and the average evacuation time (AET) of evacuees results in different optimal solutions. Minimizing the ATT is ideal in normal traffic congestion control while minimizing the AET is suitable for emergency evacuation.

2.2.3 Evacuation Modeling Approaches

Most evacuation models using mathematical programming are based on static or dynamic traffic assignment. See Jahn et al. (2005), Janson (1991), Jayakrishnan (1995), Kachroo and Sastry (2016) Kaufman et al. (1998), and Wie et al. (1990) for static and dynamic traffic assignment examples. In this section, static and dynamic modeling approaches are discussed.

2.2.3.1 Static Evacuation models

Nemours algorithms have been proposed to solve the UE static traffic assignment problem. One of the most widely accepted algorithms is Frank-Wolfe (FW). This algorithm finds a UE approximation by solving a set of convex linear programming problems iteratively as an approximation method. See LeBlanc (1975) for more details. Modified versions of the FW method were proposed to improve the efficiency of the FW method such as the conjugate Frank-Wolfe (CFW), and bi-conjugate Frank-Wolfe (BFW). Mitradjieva Lindberg (2013) perform a comparison between these algorithms and show that CFW and BFW outperform the FW method. Path based algorithms such as gradient projection (GP) method developed by Rosen (1960) is

widely used in communication networks. Forian et al. (2009) introduce an algorithm that decomposes the O-D pairs into subproblem, and each subproblem is solved based on the GP method to find the equilibrium traffic assignment. Some network design models and algorithms are biologically inspired and used for traffic assignment such as genetic algorithm (GA), ant colony routing (ACR) algorithm, and Physarum algorithm. Ceylan and Bell (2005) applied the GA to solve a signalized road network under congestion as the upper level and applied stochastic user equilibrium traffic assignment as the lower level. Cong et al. (2013) implemented an online ACR optimization heuristic to update the traffic distribution on routes by determining the splitting rates on each node. Xu et al. (2018) propose a modified version of the Physarum algorithm to solve the user equilibrium traffic assignment model based on the origin nodes. Most models and algorithms assume a static traffic assignment. However, static traffic assignment models have a limitation in capturing the traffic evolution and congestion propagation effect which could lead to erroneous solutions. Another limitation is in capturing the traffic interaction in adjacent links. For example, static traffic assignment model solution may result in expanding two parallel links leading to creating a bottleneck since most of these models' objective is based on the sum of the travel times on all links. Hence, dynamic evacuation models are closer to traffic evolution reality than the static traffic assignment models.

2.2.3.2 Dynamic Evacuation Models

Pioneering work in the DTA simulation modeling is developed by Yagar (1971). The travel time between two nodes in the transportation network is dependent on the flow volume in DTA models. Hence, the travel time is a nonlinear convex function of the flow. The drawback of this modeling approach is that the travel time is overestimated as the travel time function is convex as

observed by Nie and Zhang (2005). As a result, the optimization community shifted to other evacuation modeling approaches. See Mahmassani (2001) for a survey on simulation models.

Among the first attempts to model the DTA as a discrete-time SO mathematical program was by Merchant and Nemhauser (1978a, 1987b). The M-N model captures the traffic propagation due to congestion through a link exit function, and the travel time is represented through the link performance function of the traffic volume. The model has been extended and investigated with different exit flow functions, link travel time models, and first-in-first-out (FIFO) property by Carey (1986), Wie et al. (1995) and Carey and McCartney (2002). In general networks, additional constraints of non-convex structure are imposed to maintain the FIFO requirement that can lead to greater computational complexity as discussed by Carey (1992). Another issue that is common to occur in discrete SO-DTA is the traffic holding-back, where the traffic on one route is delayed for unreasonable time in favor of other traffic since there is no restriction on how long a group of evacuees can be delayed. Both FIFO and traffic holding-back are discussed by Carey and Subrahmanian (2000). Another modeling approach of the DTA is the point queue (PQ) model. The assumption in this model is that the time spent in the network is the travel time in free-flow speed plus the waiting time in queue. The vehicle waits on an exit queue on the link until it is possible to move forward to the next link based on the capacity and the cost of the link. See Drissi-Kaïtouni and Hameda-Benchekroun (1992) and Li et al. (2000) for more illustration on PQ models.

The relationships among the traffic flow characteristics such as flow, volume, speed on long crowded roads were explored in an early theoretical study by Lighthill and Whitham (1955a) (1955b). The shock waves were introduced to the macroscopic traffic flow model a year later by Richards (1956) to be known as the LWR hydrodynamic model. Based on the LWR

hydrodynamic model, the CTM was developed by Daganzo (1993) and (1995). The network is preprocessed by dividing the roads into homogenous sections or cells. With the tick of a clock, the evacuees or part of the evacuees advance to the next cell once the capacity allows them to move forward. Otherwise, they wait in the cell until the capacity allows them to move forward. To model the congestion effect, the capacity of the cells changes with time based on the number of vehicles in the preceding cell, the capacity flow into the cell, and the empty space in the next cell. Ziliaskopoulos (2000) modified the CTM and formulate it as an LP with a single destination and SO objective or NCT defined as the time from the beginning of the evacuation process until the last group of evacuees reaches the safe destination. Ukkusuri and Waller (2008) implemented the UE objective as a DTA using the CTM and compare the results with the SO output. See Bayram (2016) for a literature survey on optimization models for large scale evacuation.

2.2.3.2.1 The Cell Transmission Model

A network (N, A) is given with a set of nodes N and a set of arcs A. The set of nodes is categorized into three sets; the set of source nodes N_S, the set of road segment nodes N_R, and the set of sink or terminal nodes N_T. It requires a one-time interval ρ to travel a road segment, and the time horizon for evacuation planning is composed of total time intervals T.

Sets and Parameters

K set of communities based on the sink capacity

D_{ik} number of evacuees of community k at source node i

D total number of evacuees

C_{jk} capacity of sink j for evacuees from community k

Q_i maximum number of vehicles that can enter of leave a road segment i in one time interval

J_i maximum number of vehicles that road segment *i* can hold

δ_i free-flow speed to the shockwave speed ratio w/v for road segment *i* to propagate the congestion effect to the upstream road segments, where *w* is the speed when the traffic is congested, or backward wave speed, *v* is the free-flow speed, and $0 \leq \delta_i \leq 1$. See Daganzo (1995) for more illustration.

Variables

x_i^{tk} the number of evacuees of community *k* at node *i* at the beginning of the time interval *t*

y_{ij}^{tk} the number of evacuees of community *k* traveling on arc (*i, j*) at time interval *t*

E^t binary variable equals 1 if the evacuation is still in process during time interval t, and equals 0 otherwise

n number of time intervals required for all evacuees to reach destination

The objective in CTM is to minimize the NCT which is the sum of the indicator variables E^t as shown in the objective function (2-32) and constraint (2-33). The problem that CTM solves is as follows:

$$Min\ NCT = n \tag{2-32}$$

subject to

$$n = \sum_{t=1}^{T} E^t \tag{2-33}$$

$$E^t \geq 1 - \sum_{k \in K} \sum_{j \in N_T} x_j^{(t+1)k} / D \qquad t = 1, \dots, T \tag{2-34}$$

$$x_i^{1k} = D_{ik} \qquad \forall i \in N_S, k \in K \tag{2-35}$$

$$x_i^{1k} = 0 \qquad \forall i \in N_R \cup N_T, k \in K \tag{2-36}$$

$$x_i^{(t+1)k} = x_i^{tk} + \sum_{j|(j,i)\in A} y_{ji}^{tk} - \sum_{j|(i,j)\in A} y_{ij}^{tk} \qquad \forall i \in N, k \in K, \; t = 1, \dots, T-1 \tag{2-37}$$

$$\sum_{j|(i,j)\in A} y_{ij}^{tk} \le x_i^{tk} \qquad \forall i \in N, k \in K, \; t = 1, \dots, T \tag{2-38}$$

$$\sum_{i|(i,j)\in A} \sum_{k\in K} y_{ij}^{tk} \le Q_j \qquad \forall j \in N_R, \; t = 1, \dots, T \tag{2-39}$$

$$\sum_{j|(i,j)\in A} \sum_{k\in K} y_{ij}^{tk} \le Q_i \qquad \forall i \in N_R, \; t = 1, \dots, T \tag{2-40}$$

$$\sum_{i|(i,j)\in A} \sum_{k\in K} y_{ij}^{tk} \le \delta_j \left(J_j - \sum_{k\in K} x_j^{tk} \right) \qquad \forall j \in N_R, t = 1, \dots, T \tag{2-41}$$

$$\sum_{t=1}^{T} \sum_{i|(i,j)\in A} y_{ij}^{tk} \le C_{jk} \qquad \forall j \in N_T, k \in K \tag{2-42}$$

$$x_i^{tk} \ge 0 \qquad \forall i \in N, k \in K, \; t = 1, \dots, T \tag{2-43}$$

$$y_{ij}^{tk} \ge 0 \qquad \forall (i,j) \in A, k \in K, \; t = 1, \dots, T \tag{2-44}$$

$$E^t \in \{0,1\} \qquad t = 1, \dots, T \tag{2-45}$$

The variable E^t becomes 0 once all evacuees reach their destination as shown in constraint (2-34). The demand starts from the source nodes in constraint (2-35) making sure that the network is empty at the beginning of the evacuation process as shown in constraint (2-36). The flow conservation constraint (2-37) transfers evacuees from a cell to the next cell when possible, and the number of evacuees traversing the link cannot exceed the number of evacuees within the node as seen in constraint (2-38). Constraints (2-39) and (2-40) regulate the number of vehicles

that can enter or leave the road segment respectively. Constraint (2-41) regulates the entrance to a road segment based on the shockwave speed to simulate the congestion propagation effect. The capacity of the road segment is set in constraint (2-42), and the non-negativity constraints are (2-43), (2-44), and (2-45).

However, the M-N model and the CTM are based on a similar concept of traffic movement and delay propagation. Nie (2011) shows that incorporating additional constraints to the linearized M-N model results in relaxed CTM and proposes an algorithm to solve the issue of flow holding back. Therefore, both models are generally similar in the basic concept since CTM can be derived from the original M-N model. Essential information lacking in these models is the total time each group of evacuees spends in the network until they reach their destination.

2.2.3.2.2 The Cell Transmission Model Weakness Points

Similar to any evacuation modeling approach, the cell transmission model has several weakness points. These weak points are listed as follows:

1- In the CTM model, the ratio of the free-flow speed to the shockwave speed parameter δ_i for road segment *i* is set and updated manually. The parameter δ_i regulates the entry of evacuees to the next cell by simulating the congestion. Thus, the congestion of any road segment must be known prior to the evacuation to set the value of δ_i, which may not be accurate, given the dynamic nature of the process.

2- The CTM model is insensitive to the length of the road. The CTM leans more towards the simulation of tolls, not congestion simulation. Hence, an evacuee can travel in free-flow speed once passes the bottleneck or toll point if not delayed by another one. In reality, the transportation network user is delayed based on the volume traffic, even if there is no bottleneck. An illustrative example is discussed in section 5.3.1.1.

3- The CTM model does not keep track of the time evacuees spend in the network. The CTM model sends evacuees then finds the total time evacuees spend from the beginning of the evacuation process until the last evacuee reaches the destination. This modeling approach is suitable for efficient evacuation. However, some evacuees may spend a very long time in the network, while others reach the destination is a short time since the individual evacuation time for each evacuee is not an objective in the CTM model.

2.2.4 Uncertainty in Evacuation

In emergencies, the congestion takes place in parts of the road network due to the surge in demand and need to evacuate. Most evacuation models are modeled as nominal by assuming deterministic input data. Recently, incorporating uncertainty in evacuation models has been gaining a great interest with the objective of more robust models that can control uncertainty. Uncertainty is generally modeled as stochastic programming or robust optimization.

2.2.4.1 Stochastic Programming

Stochastic programming models require a known probability distribution of the uncertain parameters. If the probability distribution is known, scenario based through Monte Carlo simulation or chance constraint programming can be implemented. Kimms and Maiwald (2018) use a scenario based approach to address the uncertainty in the road capacities using bi-objective optimization. Wang et al. (2016) focus on the evacuation plans by implementing a scenario based approach assuming that the travel times and road capacities are uncertain. Waller and Ziliaskopoulos (2006) implement a chance constrained modeling approach assuming uncertain demands with a known probability distribution. Yazici and Ozbay (2010) incorporated the uncertainty in both the demand and the road capacity in the model using individual and joint chance constraint stochastic programming. Ukkusuri and Waller (2008) developed a linear model

to help decision makers allocate budget on capacity improvement based on uncertain demand using chance constraint and two stage resource model stochastic programming. Then they compare the output of the model with the output of the nominal model for user and system optimum. However, collecting data is challenging in evacuation processes. Robust optimization is used if the probability distribution of the uncertain parameter is unknown. In robust optimization, the feasible set is controlled to maintain the model feasibility in the worst case scenarios.

2.2.4.2 Robust Optimization

Robust optimization is the proper approach when the probability distribution of the data is unknown. Feasibility is the most concern in robust optimization since the infeasible model is useless. Robust solutions are tolerant, to some extent, to the variability of the parameters to maintain feasibility. Soyster (1973) introduced the concept of inexact linear programming. The feasible region is defined as set containment instead of convex inequalities known as box uncertainty set. Box uncertainty is simple to implement but it is too conservative as it compromises a considerable portion of the feasible space since all parameters are set to their worst value. Ben-Tal and Nemirovski (1998) introduce the ellipsoidal uncertainty set to control the level of conservatism. The drawback of the ellipsoidal uncertainty approach is that it can become computationally intractable since it is solved using conic quadratic models. Later, the polyhedral uncertainty set was introduced by Bertsimas and Sim (2004). The polyhedral approach is linear, computationally tractable, and easy to implement. The level of conservatism can be controlled by the parameter Γ_i of the i^{th} constraint. This approach is a generalization to the box uncertainty as the model becomes nominal if $\Gamma_i = 0$, and the model becomes Soyter's if the parameter $\Gamma_i = |J_i|$ given that J_i is the set of uncertain coefficients. Hence, the level is

conservatism is controlled by adjusting the parameter Γ_i within the interval $\Gamma_i \in [0, |J_i|]$. The drawback of this approach is that the interpretation of the parameter Γ_i is ambiguous. See Bertsimas and Sim (2004) for more illustration. Do Chung et al. (2011) implement robust optimization using the box uncertainty approach in the evacuation process to improve the road capacities with limited budget given uncertain demand. Ren et al. (2013) develop an integrated model to assign evacuees to routes and optimize traffic signals with uncertain demand using the ellipsoidal uncertainty set. Yao et al. (2009) develop a linear programming model based on a robust optimization approach to reduce the infeasibility cost due to the uncertainty in demand. Ben-Tal et al. (2011) use the polyhedral uncertainty set for the uncertain demand in evacuation and humanitarian relief supply chain model. Reliability-based optimization is another approach used disregarding the probability distribution of the uncertain parameters. Ng and Waller (2010) present a reliability based approach by providing a probabilistic guarantee on the resulting evacuation plan, i.e. infeasibility is allowed with a prespecified tolerance, given that the uncertainty is in demand and road capacity with the unknown underlying distribution. Lim et al. (2015) present a reliability based evacuation route planning model to find the relationship between the clearance time, the number of evacuation routes, and the congestion probability assuming that the capacity of the road links is uncertain, and its probability distribution is known.

In some cases, the probability distribution of one of the model parameters can be partially known. Lim et al. (2019) propose a distributionally robust chance constrained model assuming that the demand underlying distribution is partially known. Do Chung et al. (2012) proposed an approximate joint-chance constrained Cell Transmission model assuming that the underlying probability distribution of the demand is partially known.

Chapter 3: Approximation to Max-Min Fairness in Multi Commodity Networks

3.1 Introduction

The most common approach to find MMF resource allocation, as illustrated in detail by Nace and Pi (2008), in a problem is to start with the lowest capacity objects of a system to fill with the available resource to its maximum capacity. Then fill the second-lowest object continuing with the next lowest object until the available resource is consumed or maximum capacity is reached. MMF ensures the resource is fairly distributed among the available objects while utilizing the available resources. This algorithm is called PFA introduced by Bertsekas and Gallager (1987). MMF is widely applied in traffic engineering and load-balancing problems. IP is an extensively studied application using MMF, where the goal is to maximize the throughput subject to a fair distribution of resources. A different approach is presented in this chapter to help find MMF flow in large scale multicommodity network topologies and provide a better insight into the network structure. The two objectives of MMF are transformed into a bi-objective mathematical optimization model to help the decision-maker to select the level of throughput and utilization.

Firstly, we will start by exploring related work to MMF. Specifically, in section 3.2, we will provide the definition to MMF, discuss the common approach to solve MMF problems in multicommodity flow networks, and discuss some challenges related to this approach. In section 3.3, a new approach combining MMF knowledge with multicriteria optimization is introduced including a small illustrative example. In section 3.4, experiments are applied to real and random network topologies to give a better understanding of the new approach. In section 3.5, the output of the *progressive-filling* algorithm and the multicriteria model are compared.

3.2 The *Progressive-Filling* Algorithm

In this section, the MMF definition is provided, the PFA algorithm is studied including the LP model, and the challenges in using this algorithm are discussed.

3.2.1 MMF Definition

We first define the MMF vector. A vector $\gamma \in \Gamma$ is said to be max-min fair that has the property that if there exist a $\gamma_s' > \gamma_s$ for $s \in \{1, \dots, n\}$, then $\gamma_t' < \gamma_t \leq \gamma_s$ for $t \in \{1, \dots, n\}$. Let us assume that the vector γ is MMF on the set Γ. A component γ_s in the vector γ cannot be increased without worsening another component γ_t that is less than or equal to γ_s on the same set. The same definition is valid for the MMF flow in networks. A multicommodity network is MMF if a commodity flow cannot be increased without worsening another commodity flow that is less than or equal to it in the same network since commodity flows share the same network capacity.

3.2.2 The MMF LP Model

3.2.2.1 Sets and Parameters:

N Set of vertices, indexed by $i \in N$

A Set of arcs, indexed by $(i, j) \in A$

C Set of capacities for each arc, indexed by $(i, j) \in A$

K Set of commodities, indexed by $k \in K$

K_n Set of commodities saturated simultaneously at iteration n

B_n Set of demands saturated during the first n iterations

P_n The LP model of iteration n

3.2.2.2 Decision Variables:

f The maximum flow at any iteration

γ_k The maximum flow of commodity $k \in K$

x_{ij}^k The flow on arc $(i,j) \in A$ of commodity $k \in K$

The LP model P_n objective (3-1) is to maximize the flow of all commodities. Each link has a capacity for all commodities, as seen in constraint (3-2). The flow conservation constraints for transshipment nodes is illustrated in (3-3), the flow conservation at the source and terminal for the blocking flows is illustrated in constraint (3-4), and the flow conservation to maximize the flow at the source and terminal nodes are illustrated in constraint (3-5) and (3-6). Finally, constraints (3-7) is the non-negativity constraints. The dual variable can be seen for each constraint to be used to identify the blocking commodities.

$$Max\ CF = f \tag{3-1}$$

subject to

$$(\delta_{i,j}) \qquad \sum_{k \in K} x_{ij}^k \leq C_{ij} \qquad \forall (i,j) \in A \tag{3-2}$$

$$(\lambda_{i,k}) \qquad \sum_{j:(i,j)\in A} x_{ij}^k - \sum_{j:(j,i)\in A} x_{ji}^k = 0 \qquad \forall k \in K, i \notin \{s^k, t^k\} \tag{3-3}$$

$$(\lambda_{i,k}) \qquad \sum_{j:(i,j)\in A} x_{ij}^k - \sum_{j:(j,i)\in A} x_{ji}^k = \begin{cases} \gamma_k, i = s^k \\ -\gamma_k, i = t^k \end{cases} \qquad \forall k \in B_{n-1}, \forall i \in N \tag{3-4}$$

$$(\lambda_{s^k,k}) \qquad \sum_{j:(j,i)\in A} x_{ji}^k - \sum_{j:(i,j)\in A} x_{ij}^k + f \leq 0 \qquad \forall k \in K \backslash B_{n-1}, i = s^k \tag{3-5}$$

$$(\lambda_{t^k,k}) \qquad \sum_{j:(i,j)\in A} x_{ij}^k - \sum_{j:(j,i)\in A} x_{ji}^k + f \leq 0 \qquad \forall k \in K \backslash B_{n-1}, i = t^k \tag{3-6}$$

$$x_{ij}^k \geq 0 \qquad \forall k \in K, \forall (i,j) \in A \tag{3-7}$$

The iterative process to solve the MMF problem starts with maximizing the flow in the model P_n until the blocking commodity flows are reached. Then the blocking constraints are identified using the strict complementary slackness. The slacks of the blocking constraints become zeros resulting in positive corresponding dual variables according to the complementary slackness theorem. The next step is to set the identified blocking constraints in (4) equal to γ_k where $\gamma_k = f$. Then, the model P_{n+1} is maximized to find the next set of blocking constraints K_{n+1} and set them to γ_k. This process is repeated until all flow constraints become blocking constraints. This algorithm ensures that by increasing the flow of a subset of commodities, the lower flow commodities set to constant flow do not decrease or worsen.

Table 3-1: The *progressive-filling* algorithm

Algorithm:	**Find the MMF multicommodity flow and the associated flow vector**
Step 1	Set $n = 0$ and $B_0 = \emptyset$
Step 2	If $B_n = K$, stop. Otherwise set $n = n+1$, then find the minimum f by solving the problem P_n
Step 3	Identify the set K_n of blocking commodities at iteration n, set $\gamma_k = f \ \forall k \in K_n$ and $B_n = B_{n-1} \cup K_n$.
Step 6	Go to step 2

3.2.3 Challenges with the PFA Algorithm

The iterative approach to find an MMF flow in networks is very common, but there are some challenges related to it. This first challenge with this approach is solving the LP model a number of times that can be computationally demanding, depending on the size of the network. Another challenge is in identifying the blocking constraints. In the MMF algorithm, the method to identify the blocking constraints is to identify the binding constraints through the dual variables.

The corresponding dual variables to the binding constraints are positive according to the complementary slackness theorem, but the complementary slackness condition is unnecessary. As a result, only a subset of the blocking constraints is identified in each iteration leading to degeneracy since $f_n = f_{n+1} = f_{n+2} = \cdots$, which could lead to higher computational time, but convergence is guaranteed. Danna et al. (2012) developed a new method called binary search, which is used to identify the blocking constraints to overcome this challenge. Still, a limitation of access rates is a condition for the algorithm to work. Furthermore, if changes occur to the network, the model requires to be solved with the new network since it does not have the capability to reroute the flow through the remaining links.

3.3 MMF and Multicriteria Optimization

In this section, we present an approximation approach to find MMF flow in multicommodity networks that have not been explored based on our knowledge. In addition, we discuss a small illustrative example.

3.3.1 Model Definition

We assume a network N is given, described through the graph $G = (N, A)$ with the set of nodes N and a set of directed arcs A. Each arc $a \in A$ where $a = (i, j)$ and $i, j \in N$. $s, t \in N$ where s is a supply node, and t is a terminal node. S is the set of supply nodes, and T is the set of terminal nodes where $s \in N_S$ and $t \in N_T$. The model is composed of hard and soft constraints since a goal programming approach is used.

3.3.1.1 Parameters and Sets

C_{ij} The capacity of the arc $(i, j) \in A$

β The minimum flow for all commodities

3.3.1.2 Set of Variables

x_{ij}^k The flow of commodity k on arc $(i,j) \in A$

f_i^k The incoming/outgoing flow of commodity k at node $i \in N$

d^{kl} The positive difference in flow between the commodities k and l

3.3.2 Constraints

3.3.2.1 Flow Conservation Constraints

The set of constraints (3-8) are the flow conservation constraints where x_{ij}^k is the flow of commodity k from node i to node j. If the incoming flow is greater than the outgoing flow at node i, then node i is a sink node. The node i is a source node if the outgoing flow is greater than the incoming flow at node i. If the incoming and outgoing flows are equal at node i, the node i is a transshipment node.

$$\sum_{j \in N} x_{ij}^k - x_{ji}^k = \begin{cases} f_i^k, & if\ i = s^k \\ -f_i^k, & if\ i = t^k \\ 0, & else \end{cases} \qquad \forall\ i \in N, k \in \mathrm{K}_i \tag{3-8}$$

3.3.2.2 Capacity Constraints

With the additional index k, each commodity flows in a distinct network. However, the set of capacity constraints (3-9) links all the commodity flows to one network to share the same capacity resource. It ensures that all the commodity flows pass through the arc $a = (i,j)$ in both directions but do not exceed the capacity of it given that $C_{ij} = C_{ji}$.

$$\sum_{k \in K} x_{ij}^k + x_{ji}^k \leq C_{ij} \qquad \forall\ (i,j) \in A, i > j \tag{3-9}$$

3.3.2.3 Fairness Constraints

The set of soft constraints (3-10) provides a way to reduce the difference among the commodity flows, resulting in a fair allocation of commodity flows. The variable d^{kl} is the deviation variable of commodity flow *k* compared with commodity flow *l*. These deviation variables make up the difference between two commodity flows.

$$f_i^k - f_j^l + d^{kl} - d^{lk} = 0 \qquad \forall\, k,l \in K, \forall\, (i,j) \in N \qquad (3\text{-}10)$$

A lower bound to the flow of each commodity is set in the set of constraints (3-11) to guarantee that all commodities receive at least the minimum flow.

$$f_i^k \geq \beta \qquad \forall i \in N, k \in K \qquad (3\text{-}11)$$

3.3.2.4 Non-Negativity Constrains

If the deviation variables are minimized to 0, all the commodity flows are equal and said to be fairly distributed. The set of constraints (3-12) are the non-negativity constraints.

$$x_{ij}^k, f_i^k, d^{kl} \geq 0 \qquad \forall (i,j) \in A\,, i \in N, k \in K \qquad (3\text{-}12)$$

3.3.3 Objective Functions

The first objective (3-13) is to maximize the overall flow to utilize the available capacity resources. Maximizing the first objective does not lead to a fair distribution of flow. However, maximizing the flow as a first step is useful to adjust the value of ϵ. When the first objective is set as a constraint using the ϵ-constraint method by Vira and Haimes (1983), the sum of deviation is minimized in the second objective (3-14).

$$Max\ CF = \sum_{i \in N, k \in K} f_i^k \tag{3-13}$$

$$Min\ SAD = \sum_{k,l \in K} d^{kl} \tag{3-14}$$

There is a number of approaches to measure fairness or equity. See Leclerc et al. (2012) for more illustration. In this model, the sum of absolute deviations (3-15) is used to measure the equity between commodities since it is efficient and linear. The function (3-15) is converted to the set of constraints (3-10).

$$SAD = \sum_{j} \sum_{i \geq j} |f_i - f_j| \tag{3-15}$$

The difference between the second objective function (14) and the Gini coefficient (15) is that the objective function is not divided by the total flow of commodities. The absolute difference between commodity flow is divided by the total flow after running the model to preserve the linearity of the model.

The decision-maker then decides what level of fairness is desired, considering the tradeoff between fairness and maximum flow. Maximizing the throughput in a network comes from the desire to utilize the network capacity. Hence, the utilization (3-16) of the network is considered as a performance measure helping the set the desired level of throughput.

$$U = \frac{\sum_{k \in K} \sum_{(i,j) \in A} x_{ij}^k}{0.5 \sum_{(i,j) \in A} C_{ij}} \tag{3-16}$$

3.4 Illustration and Experimentation

In this section, a trivial example is used to illustrate the approximation model. In addition, experimentations are implemented on the benchmark and randomly generated networks with different sizes.

3.4.1 Illustrative Example

Let us consider the simple example of a network (N1) used by Nace and Pi (2008) where we have three routers A, B, and C and three links AB, BC, and AC with capacities 2 MB/sec, 3 MB/sec, and 1 MB/sec respectively. If the flow is maximized, the resulting flow is illustrated in Figure 3-1 (a). The total throughput is 6.

The value of the maximum flow is determined. The next step is to set the first objective (3-13) as a constraint using the ϵ-constraint method (Vira and Haimes, 1983).

$$Min\ SAD = \sum_{k,l \epsilon K} d^{kl} \tag{3-17}$$

subject to

$$\sum_{i \in N, k \in K} f_i^k \geq \epsilon \tag{3-18}$$

$$\sum_{j:(i,j)\in A} x_{ij}^k - x_{ji}^k = \begin{cases} f_i^k, & if\ i = s^k \\ -f_i^k, & if\ i = t^k \\ 0, & else \end{cases} \qquad \forall\, i \in N, k \in K \tag{3-19}$$

$$\sum_{k \in K} x_{ij}^k \leq C_{ij} \qquad \forall (i,j) \in A, k \in K \tag{3-20}$$

$$\sum_{i \in S} f_i^k - \sum_{j \in S} f_j^l + d^{kl} - d^{lk} = 0 \qquad \forall\, k \in K \tag{3-21}$$

$$U = \frac{\sum_{k \in K} \sum_{(i,j) \in A} x_{ji}^{k}}{\sum_{(i,j) \in A} C_{ij}} \tag{3-22}$$

$$f_i^k \geq \beta \qquad \forall\, i \in N, k \in K \tag{3-23}$$

$$x_{ij}^k, f_i^k, d^{kl} \geq 0 \qquad \forall (i,j) \in A, i \in N, k \in K \tag{3-24}$$

When the ϵ value is set to 6, the maximum flow, in this case, the minimum sum of the deviation obtained is 4. If ϵ is reduced to 5.5, the resulting minimum sum of deviations is 2 as shown in Figure 3-1 (b).

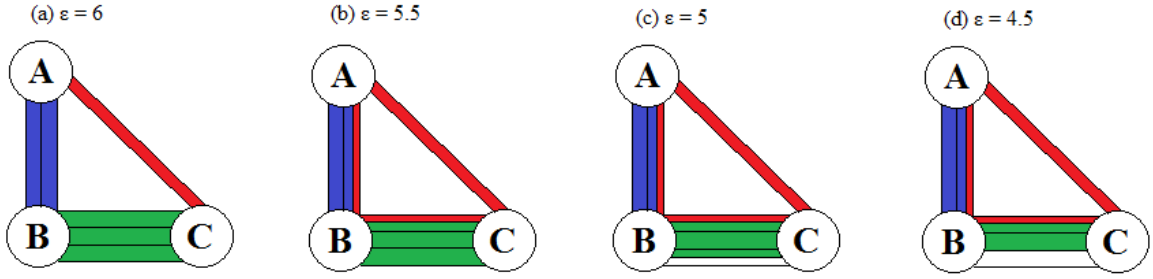

Figure 3-1: The result when maximizing the overall throughput.

However, the minimum sum of deviations becomes 1 if we set ϵ to 5, but the set of capacity constraints (20) are no longer binding, which indicates that the capacity resource is not fully utilized. Table 3-2 summarizes the results of the tested example. The deviation can be minimized to zero if the ϵ value is set to 4.5, resulting in equal flows for all commodities with some non-binding capacity constraints as seen in Figure 3-1 (c), and (d).

Table 3-2: Summary of example 1 results using different values of ϵ

ϵ (Total flow)	6		5.5		5		4.5	
Commodity	**Path**	**Flow**	**Path**	**Flow**	**Path**	**Flow**	**Path**	**Flow**
A ⟶ B	A-B	2	A-B	1.5	A-B	1.5	A-B	1.5
A ⟶ C	A-C	1	A-B-C+A-C	1.5	A-B-C+A-C	1.5	A-B-C+A-C	1.5
B ⟶ C	B-C	3	B-C	2.5	B-C	2	B-C	1.5
Min deviation	4		2		1		0	
Utilization	1		1		0.9166		0.8333	

We can observe the results in Table 3-2, where the sum of deviational variables decreases as the ϵ value decreases. Reducing the flow reduces the congestion resulted from the competing commodities trying reach to their destinations resulting in giving some space for sharing, as seen in the example above.

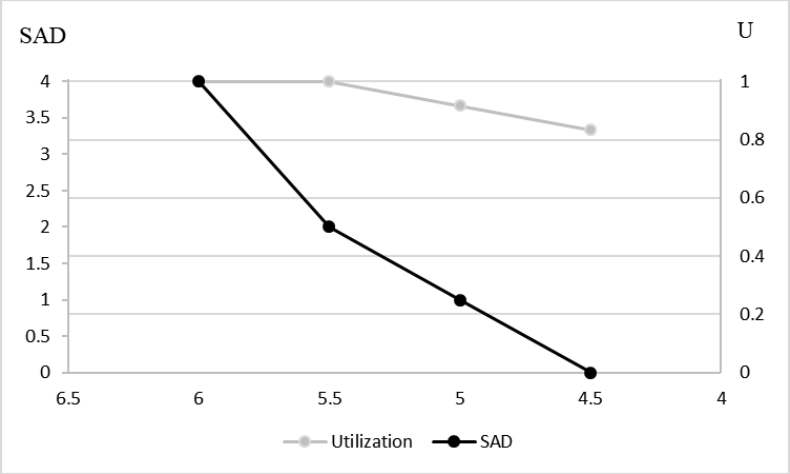

Figure 3-2: Pareto front and utilization of different ϵ values in Table 3-2

In Figure 3-2, there are infinite non-dominated solutions forming a Pareto front. Additionally, this proposed approach requires less computational time and provides high flexibility in terms of decision-making. It can be noticed that the slope is different in the intervals [4.5, 5.5) and (5.5, 6]. Rationally, if the ϵ value is decreased below the value 5.5, the gain in fairness is not substantial compared to the gain acquired by creating space for sharing. The most attractive value of ϵ is 5.5, which is the value we would obtain if the MMF algorithm was implemented. The reason that 5.5 is the most attractive value is that it gains most of the two competing objectives. The value of fairness equals 1 when the flow is maximum and 0 when all commodity flows are equal. It can be noticed that the network utilization is 1 for all $\epsilon \geq 5.5$ giving another measure to help to decide the choice of the desired ϵ value.

3.4.2 Experimentation

The model is tested on several networks that have been studied in the literature, including randomly generated networks. The network topologies obtained from the SND library by Orlowski (2010) are Abilene, Atlanta, France, Nobel-US, and Brain. In addition, two random networks are used for comparison purposes. All the network capacities are set to 1000. In Table 3-3, the information of the networks is seen in the first column. p is the percentage of flows given that 1 is the maximum flow of the network. The total flow column provides the values of ϵ used in the model to compute the non-dominated solutions forming the Pareto front, which will be discussed later. Every run time (seconds) is shown in the time column for every ϵ value, and the total run time (seconds) is shown in the total time column. The outputs of the models are illustrated in the sum absolute deviation and utilization columns.

3.4.3 The Selection of ϵ Value

The two objectives of MMF are utilizing the network and minimizing the difference in flow between commodities. In Table 3-3, it can be seen that when reducing the total flow of commodities ϵ, the deviation and the utilization decrease in a behavior that is highly dependent on the network topology. The utilization of the network is added to help to select the value of ϵ value.

Table 3-3: experimentation results for every percentage of the flow *p* of the benchmark networks with CPU time in seconds

Network	*p*	Total Flow (ϵ)	SAD	Utilization	CPU Time	Total Time
Abilene	0	0	0.00	0.00	0.91	6.57
	0.2	3000	0.00	0.50	1.03	
|N|= 12	0.4	6000	202842.11	0.82	1.12	
|A|= 15	0.6	9000	563373.74	1	1.22	
|K|= 132	0.8	12000	1039777.78	1	1.15	
	1	15000	1530000.00	1	1.09	
Atlanta	0	0	0.00	0.00	2.25	19.28
	0.2	4400	0.00	0.50	2.35	
|N|= 15	0.4	8800	487582.88	0.87	2.86	
|A|= 22	0.6	13200	1373887.01	1	3.72	
|K|= 210	0.8	17600	2506465.28	1	4.10	
	1	22000	3652000.00	1	3.93	
France	0	0	0.00	0.00	5.28	49.68
	0.2	4400	0.00	0.26	6.30	
|N|= 25	0.4	8800	0.00	0.52	7.28	
|A|= 45	0.6	13200	757301.54	0.72	7.69	
|K|= 300	0.8	17600	1917968.86	0.84	10.04	
	1	22000	3160421.89	0.92	13.02	
Nobel-US	0	0	0.00	0.00	2.30	20.18
	0.2	4200	0.00	0.43	2.76	
|N|= 14	0.4	8400	50000.00	0.86	4.58	
|A|= 21	0.6	12600	419003.64	1	3.93	
|K|= 91	0.8	16800	942334.62	1	3.85	
	1	21000	1470000.00	1	2.73	
Brain	0	8250	10563853.1	0.49993330	1546.654	15739
	0.2	9900	14980895.1	0.49993124	1562.262	
|N|= 161	0.4	11550	19416687	0.49993305	1863.42	
|A|= 332	0.6	13200	23911321.8	0.49993486	2742.34	
|K|=14311	0.8	14850	28417386.1	0.50064574	3717.558	
	1	16500	33165672.8	0.50812858	4305.429	

For example, the ϵ of the Abilene network can be reduced to 0.6 of the total flow utilizing 100% of the network capacity and reducing the sum of absolute deviations to 0.37 of its maximum. For Atlanta, the ϵ value suggested is 0.6 of the maximum total flow, similar to the network Abilene.

The deviation can be brought down to 0.38 of its maximum, utilizing 100% of the network capacity, as shown in Figure 3-3. Reducing the flow in France network improves the sum absolute deviation value but decreases the utilization. As a result, the maximum flow is suggested to be the optimal solution since it utilizes the network capacity. Nobel-US behaves similarly to the networks Abilene and Atlanta when reducing the flow to 0.6 of its maximum resulting in 0.29 of the maximum deviation. The values of ϵ can be adjusted more accurately. However, in this experimentation, the intervals between ϵ values selected to be 0.2 ranging from the maximum flow to the minimum flow.

Table 3-4: experimentation results of every flow percentage *p* of the randomly generated networks with CPU time in seconds

Network	p	Total Flow (ϵ)	SAD	Utilization	CPU Time	Total Time
Net70	0	0	0.00	0.00	67.87	683.21
	0.2	29033.4	0.00	0.26	82.31	
|N|= 70	0.4	58066.8	0.00	0.51	81.96	
|A|= 518	0.6	87100.2	449408.80	0.77	89.90	
|K|= 679	0.8	116133.6	6512444.67	1	180.15	
	1	145167	60883964.44	1	180.96	
Net26	0	0	0.00	0.00	0.75	7.78
	0.2	8200	0.00	0.27	0.91	
|V|= 26	0.4	16400	0.00	0.54	1.12	
|E|= 84	0.6	24600	51350.59	0.84	1.32	
|D|= 109	0.8	32800	717096.56	0.99	1.85	
	1	41000	2003000.00	0.98	1.78	

The random network topology Net70 ϵ gives the MMF flow of 0.8, resulting in 100% utilization and less than 0.11 of the maximum deviation. The random network topology Net26 MMF flow can be obtained by setting ϵ to 0.8, reducing the sum absolute deviation to 0.35 of its maximum. The range of the value of ϵ can be decreased for more accuracy when the initial value of ϵ is

acquired. The results of the benchmark networks in Table 3-3 are plotted in Figure 3-3 to help visualize the Pareto front and select the critical ϵ value for the MMF resource allocation solution.

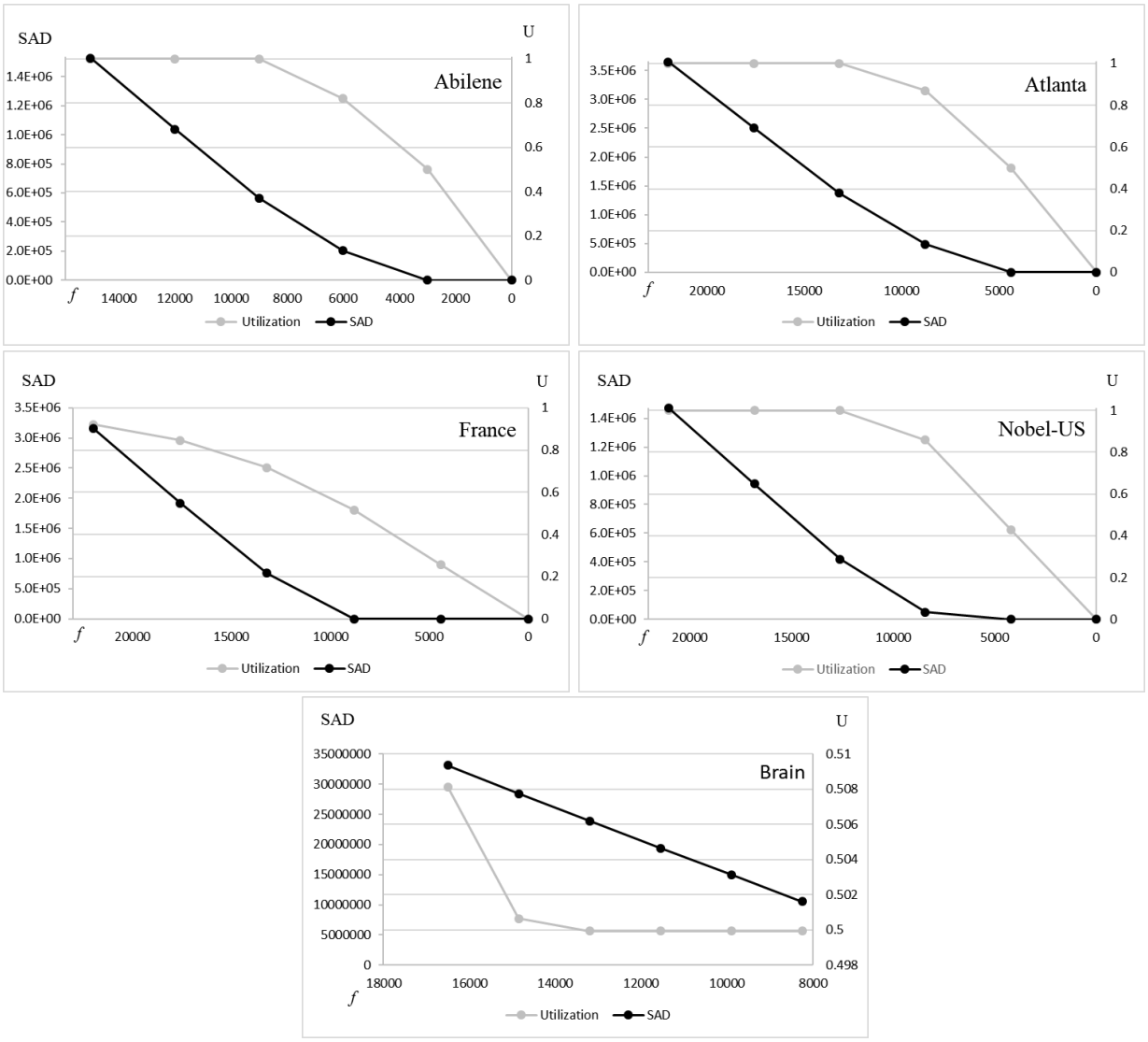

Figure 3-3: The Pareto front of the two objectives the SAD and the flow f in addition to the utilization U for the benchmark networks

The results of the random networks in Table 3-4 are plotted in Figure 3-4. Note that a slight reduction in the flow results in a significant improvement in fairness while maintaining full utilization of the network capacity.

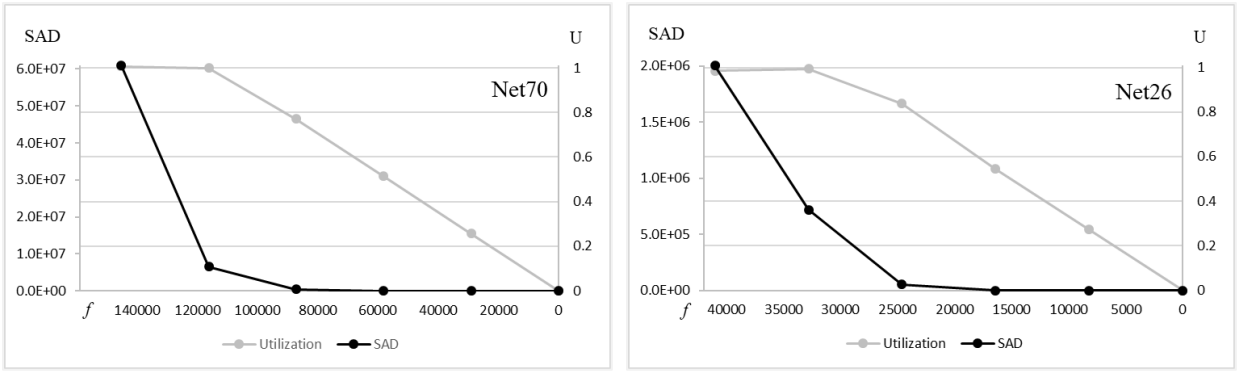

Figure 3-4: The Pareto front of the two objectives the SAD and the flow f in addition to the utilization U for the randomly generated networks

3.5 Comparison Between the Multi-Objective Model and the Progressive-Filling Algorithm

The networks tested in section 3.4 were tested using the PFA algorithm. The number of iterations n is not controlled in the PFA algorithm. However, the number of Pareto solutions $\hat{n}$ between the two objectives in the bi-objective model is controlled. The number of solutions $\hat{n}$ is 5 and can be higher for more accurate approximation.

Table 3-5: The computational time of the PFA compared with the bi-objective model for the tested networks

Network	**PFA time (s)**	$\boldsymbol{n}$	**Bi-objective time (s)**	$\hat{\boldsymbol{n}}$
Abilene	4.4	11	1.22	5
Atlanta	13.59	13	2.73	5
France	54	23	5.06	5
Nobel - US	3.4	9	0.65	5
Net26	14.29	20	4.6	5
Net70	4623	5	365.28	5
Brain	65842.15	22	14191.19	5

The quality of the output compared with the exact solution is highly dependent on the structure of the network. The mean absolute error (MAE) of the bi-objective solution compared with the PFA MMF solution for the tested networks is illustrated in Table 3-6. The highest error is

observed as 0.2190 in the network France while the lowest error of 0.0009 is the result in the random network Net70. The Average MAE of the tested networks is 0.1102.

Table 3-6: The MAE and computational time reduction of the bi-objective model compared with the PFA

Network	MAE	CPU Time Reduction (%)
Abilene	0.1189	72.27
Atlanta	0.1791	79.91
France	0.2190	90.63
Nobel - US	0.1491	80.88
Net26	0.0937	67.81
Net70	0.0009	92.09
Brain	0.0110	78.44
Average	**0.1102**	**80.29**

The number of commodities in each bandwidth interval for the networks France and Net70 (the networks with highest and lowest MAE respectively) is illustrated in Figure 3-5. Note that the allocation of the bi-objective model yields very similar results compared with the PFA output.

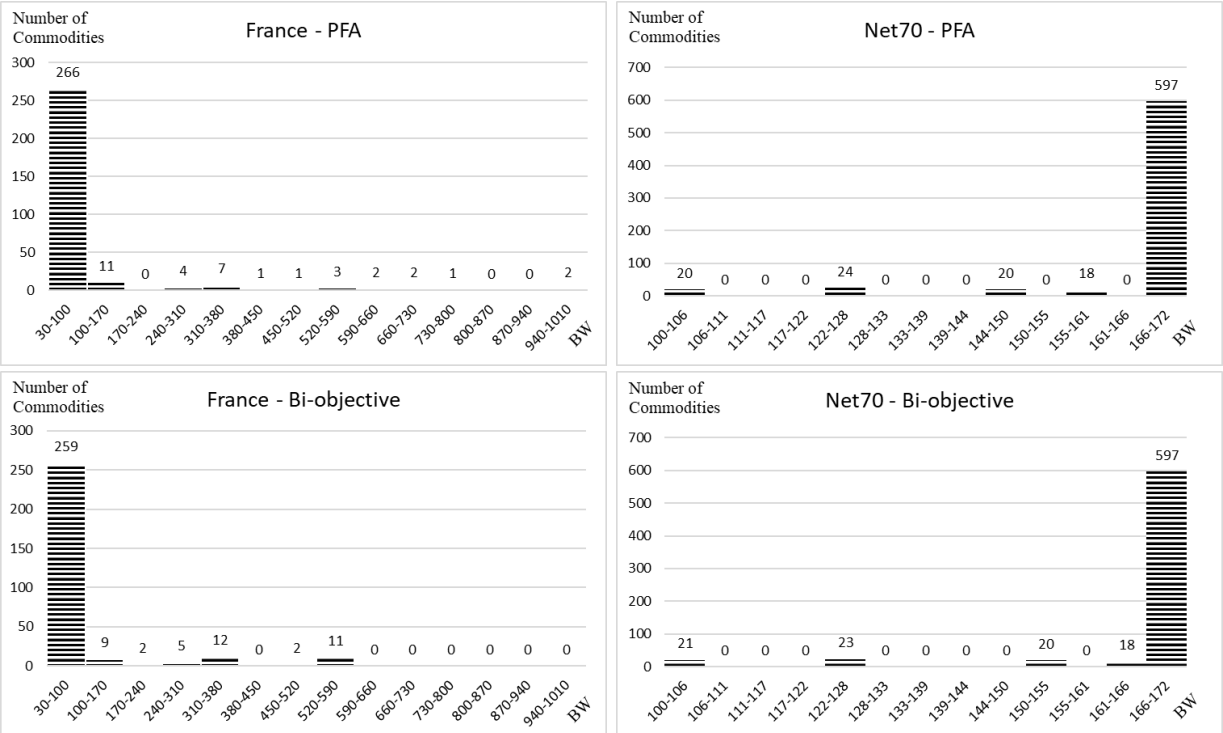

Figure 3-5: The histogram of the bandwidths allocated for the set of demands of the PFA and bi-objective model solutions

3.6 Computational Complexity

The proposed approach requires less computational, achieves an excellent approximation to the MMF resource allocation, and provides high flexibility in terms of decision making. The problem is solved in polynomial time, as illustrated by Cohen and Megiddo (1991). An approximation to the MMF resource allocation is achieved using a bi-objective model where the flow is maximized in one objective, and the differences in resources between commodities are minimized for a fairer solution. The bi-objective model is implemented on seven networks. Then the results are compared with the output of the PFA. The MAE is found by comparing each commodity with its correspondent, and the total computational time is compared for both models. The average MAE is around 0.1, and it can be as low as 0.001. On the other hand, the computational time is reduced to around 80%, and it can be as high as 92%.

Chapter 4: Modeling Latency-Based Evacuation Process: Routing and Scheduling

4.1 Introduction

In this chapter, we propose a novel approach to model the evacuation process in order to help decision-makers allocate demands on the available capacity resources to reduce the congestion effect and find the optimal network clearance time. Specifically, an MILP model is developed as a DTA model that we call LBM. To the best of our knowledge, there is no mathematical programming modeling approach that computes the estimated time each group of evacuees spends on each route. Most of the mathematical programming DTA models find the NCT, and some models compute the estimated ATT and AET of the evacuees.

The motivation of the research in this chapter is that the current evacuation models do not provide enough information about the evacuees. The time for the evacuees, for example, to reach the destination is unknown in CTM, which can lead to unfair distribution of evacuees and selfish reactions by the evacuees. In addition, other objectives are incorporated to compare them with the network clearance time. Moreover, the congestion modeling approach may not reflect the reality in other evacuation optimization models. Hence, a new approach is introduced to express the congestion in a more obvious and realistic way.

This chapter is organized as follows. In the next section, a new modeling approach is introduced and discussed. In section 4.3, a toy example is used to illustrate the model in addition to experimentation and computational results reporting. The computational complexity is discussed in 4.4.

4.2 Evacuation Model

In this section, a novel evacuation modeling approach is introduced. Before running the model, the network is preprocessed by identifying all the hub nodes in the network and adding artificial hub nodes if necessary. Then the shortest routes from source nodes to terminal nodes are identified. The hub nodes are identified or added so that the travel time in free-flow speed between each consecutive pair of hub nodes is constant. Once a group of evacuees passes through a hub node on a certain route, this group enters a new road segment with time increments of one time unit. The time unit is decided by the traveling time between two consecutive hub nodes in free-flow speed. However, the evacuees may be delayed by more than one time unit to travel between two hub nodes due to congestion.

Since the travel time is load dependent, the travel time function (4-1) is incorporated into the model. The travel time function, also known as Bureau Public Roads (BPR) function, describes the relationship between the volume of the traffic and the travel time used by the U.S. Department of Commerce Bureau of Public Roads in Bureau (1964). The travel time $T(f)$ with traffic volume f on a road segment is described as follows:

$$T(f) = T^0\left(1 + \alpha\left(\frac{f}{c}\right)^{\beta}\right), \tag{4-1}$$

where, T^0 is the travel time on a road segment in free-flow speed in normal road conditions given the capacity c of the road segment, and α and β are turning parameters describing road characteristics with $\alpha \geq 0$ and $\beta \geq 0$; those parameters are set to 0.15 and 4 respectively by the U.S. Department of Commerce Bureau of Public Roads.

Since this function is non-linear, we approximate it through a linear piecewise approximation given that each linear segment is represented by a slope and intercept as shown in Figure 4-1. Note that f is the flow volume, and $T(f)$ is the travel time function (4-1). The accuracy of the output increases as the number of the linear segments increase.

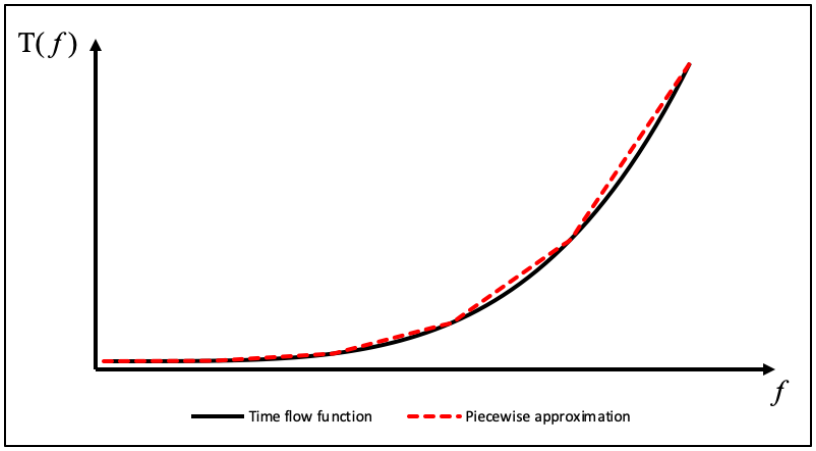

Figure 4-1 Linearizing the BPR travel time function using piecewise approximation

4.2.1 Model Definition

Given a graph $G = (N, A)$ with a set of nodes N and a set of directed arcs A, each arc $a \in A$ connects two nodes $i, j \in N$ where $a = (i, j)$. The nodes of the network are composed of a set of source nodes $N_S \subset N$, a set of terminal nodes $N_T \subset N$, and a set of hub nodes $N_H \subset N$ given that $N_S \subset N_H$ and $N_T \subset N_H$ since the evacuees are allowed to enter or exit through a hub node. Given a set of communities K to be evacuated, R_k is the set of routes that community k can use where R is the set of routes in the networks from N_S to N_T. $T = \{1, \dots, t_e\}$ is the set of times when evacuees are evacuated given that t_e is the time, where the last group of evacuees are evacuated, and $H = \{1, \dots, h_e\}$ is the set of times evacuees are spending in the network given that h_e is the time when the last group of evacuees reached the safe destination. When the time $t \in T$ equals 1, the evacuation process starts. The time path forms a network, and each time segment connects two hubs $h, g \in H$ where $(h, g) \in H_P$. The set V is the traffic volume set, and each element of

this set is decided based on the number of vehicles passing per time unit. The link (i, j) on a route is linked to the time of evacuation *t* from hub *h* to hub *g* through the tuple *S* given that $(i, j, t, h, g) \in S$. More illustration of time path constraints will be given in the example in section 4.3.1.

4.2.1.1 Parameters and Sets:

K The set of communities

R The set of shortest routes from the source nodes to the terminal nodes

V The set of traffic volumes

U_B The set of upper bounds based on road capacity where u^v is the upper bound of the traffic volume $v \in V$

L_B The set of lower bounds based on road capacity where l^v is the lower bound of traffic volume $v \in V$

D The set of linear segments of the piecewise approximation to the BPR function

m^d The slope of the linear segment $d \in D$ of the piecewise approximation

b^d The intercept of the linear segment $d \in D$ of the piecewise approximation

μ The minimum number of evacuees to be evacuated in any group

ρ The time in minutes to travel from one hub to the next hub and the system clock

c_{ij} The time to travel from node *i* to node *j* on the link $(i, j) \in A$ in free-flow speed

C_r The time to travel on route *r* from source to destination in free-flow speed

Q_k The population of community *k*

4.2.1.2 Set of Variables:

x_{ijhg}^{ktrv} The number of evacuees from community *k* evacuated at time *t* on route *r* with traffic volume *v* on arc *(i, j)* on time path segment *(h, g)*.

x'_{ijh} The number of evacuees on arc *(i, j)* at hub h

f_r^{kt} The number of evacuees of community k on route r evacuated at time t

y_{ijh}^{v} Binary variable equals 1 if the evacuees on arc *(i, j)* at hub h is within traffic volume v

z_{ijhg}^{ktrv} Binary variable equals 1 if the evacuees in community k evacuated at time t are allowed to pass on arc (i, j) on route r at time path segment (h, g) within traffic volume v and 0 otherwise

τ_{ijh} The latency on arc (i, j) at hub h transferred to the group of evacuees that follows

$\hat{\tau}_{ijh}$ The slack latency on arc (i, j) at hub h not transferred to the group of evacuees that follows

τ'^{ktr}_{ijh} The latency of the group evacuated from community k on route r at time t on arc (i, j) at hub h

s_{ijh}^{ktr} The slack variable to complement the latency of the group evacuated from community k on route r at time t on arc (i, j) at hub h

l_r^{kt} The latency on a full route r of a community k evacuated at time t

e_r^{kt} The travel time of community k on route r evacuated at time t

e'^{kt}_r The evacuation time of community k on route r evacuated at time t

E Network clearance time

4.2.2 Constraints

4.2.2.1 Flow Conservation Constraints

In the flow conservation constraints (4-2), evacuees' hub $\hat{g}$ is greater than h since the evacuees pass through a hub node. The hub $\hat{g}$ equals h if the evacuees pass through a non-hub node in the flow conservation constraint (4-3). Hence, exiting evacuees from node *i* follow one time path. Every community to be evacuated has a population size $of\ Q_k$ as seen in constraint (4-4).

$$\sum_{\hat{g}|(h,g)\in H_P} x_{i\hat{j}h\hat{g}}^{ktrv} - \sum_{g|(g,h)\in H_P} x_{jigh}^{ktrv} = \begin{cases} f_r^{kt} \; if \; i \in N_S \\ -f_r^{kt} \; if \; i \in N_T \\ 0, otherwise \end{cases} \quad \begin{array}{l} \forall \; k \in K, v \in V \; r \in R, \\ (j,i),(i,\hat{j}) \in r, \hat{j} \in N_H \\ t,h,g|(i,j,t,h,g) \in S \end{array} \tag{4-2}$$

$$x_{i\hat{j}h\hat{g}}^{ktrv} - \sum_{g|(g,h)\in H_P} x_{jigh}^{ktrv} = 0 \quad \begin{array}{l} \forall \; k \in K, v \in V \; r \in R, \\ (j,i),(i,\hat{j}) \in r, \hat{j} \notin N_H \\ t,h,g|(i,j,t,h,g) \in S \end{array} \tag{4-3}$$

$$\sum_{t\in T}\sum_{r\in R} f_r^{kt} = Q_k \qquad \forall \; k \; \in K \tag{4-4}$$

4.2.2.2 Networks Link Constraints

Since all the evacuees share the same road network, constraint (4-5) sums all evacuees from all communities *k* evacuated at different times *t* with all traffic volumes v using all the routes *r* passing through the arc (i,j) at hub *h* to the variable x'_{ijh}.

$$x'_{ijh} = \sum_{r\in R}\sum_{k\in K}\sum_{v\in V}\sum_{t|(i,j,t,h,g)\in S} x_{ijhg}^{ktrv} \qquad \forall \; (i,j) \in A, h, g|(i,j,t,h,g) \in S \tag{4-5}$$

4.2.2.3 Flow Volume Constraints

The amount of the flow passing through arc (i,j) is decided by the traffic volume variable y_{ijh}^{v}. If the flow x'_{ijh} falls between the upper bound u^r and the lower bound l^v of traffic volume *v*, then y_{ijh}^{v} equals 1 as shown in constraints (4-6) and (4-7) given that *M* is a significantly large number. The evacuees passing on arc (i,j) at hub *h* are allowed to pass through one traffic volume as seen in constraint (4-8).

$$x'_{ijh} \geq \sum_{v\in V} l^v y_{ijh}^{v} \qquad \forall \; (i,j) \in A, h \in H \tag{4-6}$$

$$x'_{ijh} \leq \sum_{v \in V} u^v y^v_{ijh} + M(1 - y^v_{ijh}) \qquad \forall (i,j) \in A, h \in H \qquad (4\text{-}7)$$

$$\sum_{v \in V} y^v_{ijh} \leq 1 \qquad \forall (i,j) \in A, h \in H \qquad (4\text{-}8)$$

4.2.2.4 Path Latency Constraints

To find the latency τ_{ijh} on arc *(i, j)* at hub h, the inventory constraint (4-9) is used. The latency of an arc *(i, j)* at hub h equals the required time for evacuees to travel on the arc based on their volume adding the latency of the evacuees on the same arc at time $h-1$ and subtracting the time they would spend in a free-flow speed. It can be noticed that $\hat{\tau}_{ijh}$ in (4-10) is bounded by the time evacuees spend on the arc in free-flow speed, but it can be less in case no evacuees are passing on the arc to maintain the constraint feasibility. The initial latency of the arc *(i, j)* equals 0 in constraint (4-11).

Note that constraint (4-9) transfers the effect of congestion to the following group of evacuees. As the link becomes more congested, the latency increases then added to the total latency of the following group of evacuees. Although the evacuees are not delayed by the earlier groups on the upstream links of the congested link, the delay is added once they pass on the congested road segment. Constraint (4-9) creates the propagation effect of congestion on the evacuees passing on upstream links.

$$\tau_{ijh} = c_{ij} t_{ijh} + \tau_{ijh-1} - \hat{\tau}_{ijh} \qquad \forall (i,j) \in A, h \in H \qquad (4\text{-}9)$$

$$\hat{\tau}_{ijh} \leq c_{ij} \qquad \forall (i,j) \in A, h \in H \qquad (4\text{-}10)$$

$$\tau_{ijh} = 0 \qquad \forall (i,j) \in A, h = 0 \qquad (4\text{-}11)$$

To find the travel time on a road segment based on the traffic volume, the piecewise approximation to the BPR convex function is used. Since the function is convex, the travel time t_{ijh} on arc (i,j) at hub h can be found as seen in constraint (4-12).

$$t_{ijh} \geq m^d x'_{ijh} + b^d \qquad \forall\, (i,j) \in A, h \in H, d \in D \qquad (4\text{-}12)$$

4.2.2.5 Time Path Constraints

In constraint (4-13), all evacuees of community *k* on arc (*i, j*) at time *h* evacuated at time *t* on route *r* can pass through one time path as shown in constraint (4-14) given that *M* is a sufficiently large number; meaning that no part of the group is delayed or outrun the rest of the group. In constraint (4-15), each group of evacuees is bounded by a minimum number μ decided by the decision maker. In constraint (4-16), the evacuees follow one time path based on the traffic volume decided by the set of constraints (4-6) and (4-7).

$$x_{ijhg}^{ktrv} \leq M z_{ijhg}^{ktrv} \qquad \forall\, (i,j) \in A, r \in R, t \in T, h \in H, k \in K, v \in V \qquad (4\text{-}13)$$

$$x_{ijrhg}^{ktrv} \geq \mu\, z_{ijhg}^{ktrv} \qquad \forall\, (i,j) \in A, r \in R\ t \in T, h \in H, k \in K \qquad (4\text{-}14)$$

$$\sum_{v \in V} z_{ijhg}^{ktrv} \leq 1 \qquad \forall\, (i,j) \in A, r \in R, t \in T, k \in K \qquad (4\text{-}15)$$

$$x_{jihg}^{ktrv} \leq M y_{ijh}^{v} \qquad \forall\, (i,j) \in A, r \in R\ t \in T, (h,g) \in H_P, k \in K, v \in V \qquad (4\text{-}16)$$

4.2.2.6 Evacuees Latency Constraints

The latency on a route *r* of a community *k* evacuated at time *t* in constraint (4-17) is the sum of the latencies (transferred and non-transferred) of the evacuees on that route in the network. Since

all communities evacuated in various times using different routes share the same network, the latency of a community *k* on route *r* is a subset of the latencies of the network. To extract the latencies of a specific group of evacuees, the variable z_{ijhg}^{ktrv} is used to identify the time path that the evacuees followed as shown in constraints (4-18)-(4-20)

$$l_r^{kt} = \sum_{(i,j)\in r} \sum_{h\in H} \tau'^{ktr}_{ijh} \qquad \forall\, t \in T, r \in R_k, k \in K \tag{4-17}$$

$$\tau_{ijh} + \hat{\tau}_{ijh} = \tau'^{ktr}_{ijh} + s_{ijh}^{ktr} \qquad \forall\, (i,j), r \in R, \in A, t \in T, h \in H, k \in K \tag{4-18}$$

$$\tau'^{ktr}_{ijh} \leq M z_{ijhg}^{ktrv} \qquad \forall\, (i,j) \in A, p \in P, t \in T, h \in H, k \in K \tag{4-19}$$

$$s_{ijh}^{ktr} \leq M(1 - z_{ijhg}^{ktrv}) \qquad \forall\, (i,j) \in A, r \in R\ t \in T, h \in H, k \in K \tag{4-20}$$

4.2.2.7 Evacuation Constraints

The time required to travel for each group of evacuees evacuated from community *k* on route *r* at time *t* to reach their destination is the travel time on route *r* in free-flow speed in addition to the latency as shown in constraint (4-21). The evacuation time for each group of evacuees evacuated from community *k* on route r at time *t* to reach their destination is the waiting time since the start of evacuation process, the travel time on route *r* in free-flow speed, and the latencies on the route as seen in constraint (4-22). To minimize the network clearance time, the maximum evacuation time is minimized as shown in constraint (4-23).

$$e_r^{kt} = C_r z_{ijhg}^{ktrv} + l_r^{kt} \qquad \forall\, k \in K, r \in R, (\, i,j) \in r, i \in N_S, t, h, g | (i,j,t,h,g) \in S \tag{4-21}$$

$$e'^{kt}_r = \rho(t-1)z^{ktrv}_{ijhg} + C_r z^{ktrv}_{ijhg} + l^{kt}_r \qquad \forall\, k \in K, r \in R, (\,i,j) \in r, i \in N_S, \; t,h,g|(i,j,t,h,g) \in S \tag{4-22}$$

$$e'^{kt}_r \leq E \qquad \forall\, k \in K, r \in R, t \in T \tag{4-23}$$

The set of constraints (4-24) prevents later evacuees from preceding earlier evacuees on the same route stating that the volume of the later evacuees is greater than or equal to the previous evacuees or no evacuees follow them.

$$y^v_{ijh} \leq \sum_{q \in V | q \geq v} y^q_{ij(h+1)} + y^0_{ij(h+1)} \qquad \forall (i,j) \in A, h = 1,..,t_e - 1, \; v \in V \tag{4-24}$$

Lastly, the following are non-negativity constraints (4-25) and binary variables constraints (4-26).

$$x^{ktrv}_{ijhg}, x'_{ijh}, f^{kt}_r, \tau_{ijh}, \hat{\tau}_{ijh}, \tau'^{ktr}_{ijh}, s^{ktr}_{ijh}, l^{kt}_r, e^{kt}_r, e'^{kt}_r, E \geq 0 \qquad \forall\, k \in K, r \in R, (i,j) \in A, v \in V, \; t,h,g|(i,j,t,h,g) \in S \tag{4-25}$$

$$y^v_{ijh}, z^{ktrv}_{ijhg} \in \{0,1\} \qquad \forall\, k \in K, r \in R, (i,j) \in A, v \in V, \; t,h,g|(i,j,t,h,g) \in S \tag{4-26}$$

Before building the MILP model, all the possibilities of all groups of evacuees passing through road and time networks are enumerated and stored into sets. When building the model, the constraints refer to these sets. The advantage of this procedure is that the problem size can be reduced by limiting the feasible space as will be seen in the next section.

4.2.3 Objective Functions

The objective of the model is to minimize the NCT *E*, where *E* is the total travel time of the last group arriving to the safe destination since the beginning of the evacuation process as see in the objective function (4-27).

$$Min\ NCT = E \tag{4-27}$$

However, different objectives are experimented. The ATT and the AET for each group of evacuees are incorporated in the model as seen in the objectives (4-28) and (4-29) respectively given that the sum of z_{ijhg}^{ktrv} for all $i \in N_S$ is the number of groups to be evacuated given that the minimum number of groups to be evacuated is one group.

$$Min\ ATT = \frac{\sum_{k\in K}\sum_{r\in R}\sum_{t\in T} e_r^{kt}}{\sum_{k\in K}\sum_{r\in R}\sum_{(i,j)\in r|i\in N_S}\sum_{t,h,g|(i,j,t,h,g)\in S} z_{ijhg}^{ktrv}} \tag{4-28}$$

$$Min\ AET = \frac{\sum_{k\in K}\sum_{r\in R}\sum_{t\in T} e'^{kt}_r}{\sum_{k\in K}\sum_{r\in R}\sum_{(i,j)\in r|i\in N_S}\sum_{t,h,g|(i,j,t,h,g)\in S} z_{ijhg}^{ktrv}} \tag{4-29}$$

4.3 Illustration and Experimentation

In this section, a trivial network is used to illustrate the model. In addition, a real world small network is used for illustration and experimentation.

4.3.1 Illustrative Example

Consider a network with 5 nodes and 4 arcs as shown in Figure 4-2. Suppose that the population in the source node n1 is evacuated to the shelter in the terminal node n5. Node n1 is a source node, node n5 is a terminal node, and n1, n2, n4, n5 are hub nodes. The time to travel from n1 to n2 in free-flow speed is 60 minutes, and the time to travel from n2 to n4 is 60 minutes

disregarding the time to travel to and from node n3 since it is not a hub node. The total travel time from n1 to n5 is 180 minutes.

The travel time of each linear segment is shown in Table 4-1 given the lower and upper bounds of flows for each segment d.

Table 4-1: Travel time between each pair of hub nodes based on the flow volume

d	L	U	Travel time (m)*60
1	1	3200	60
2	3201	3600	75
3	3601	3900	100
4	3901	4100	120
5	4101	4200	160

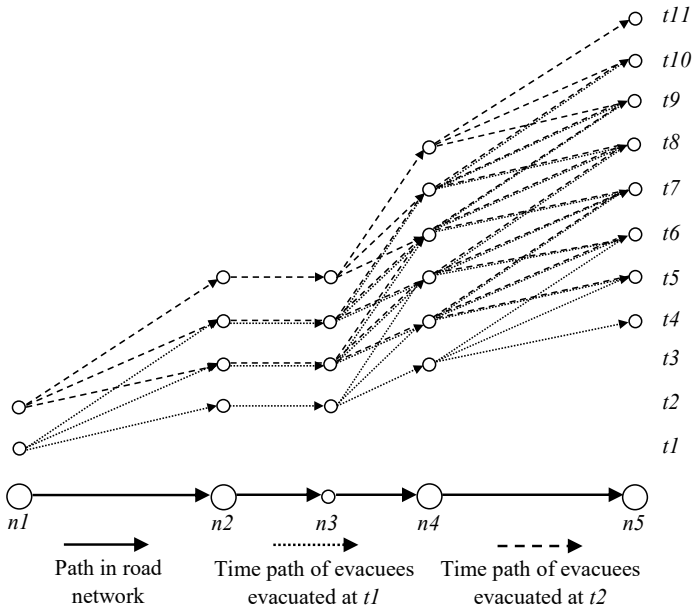

Figure 4-2: A small network example with 5 nodes and 4 arcs

The model is tested on three different population sizes in three scenarios A, B, and C assuming that in each scenario the population is divided into two groups. The first group is evacuated at *t1* and the second group is evacuated at *t2*. As shown in scenario A in Table 4-2, the population of 8500 is divided into two groups of 4350 and 4150 evacuees with the same traffic volume. The

latency of the first group is 180 minutes resulted from a delay of 60 minutes between every two consecutive hub nodes. The second group latency is 163.54 minutes resulted from the delay by their own congestion. The delay of the first group is not transferred to the second group since that the latency of the first group is less than or equal the travel time in free-flow speed, as seen in constraint (4-10). In scenario B, the population is 9500, and the first group of evacuee's traffic volume is 2 resulting in a delay of 254.7 minutes. The second group of evacuees falls in the traffic volume 3 with a latency of 385.5 minutes delayed partially by the first group of evacuees since there is a gap of time between them. The first group in scenario C is delayed in 180 minutes between every pair of consecutive hub nodes with a total of 540 minutes. The second group is delayed by 540 minutes in addition to the transferred delay from the first group of 360 minutes. The travel time is the latency in addition to the travel time in free-flow speed, the evacuation time is the travel time in addition to the waiting time of 60 minutes, and the NCT is the maximum evacuation time.

Table 4-2: Results of the example network of the 3 scenarios

Scenario	Population Size	time	Number of Evacuees	Latency	Travel Time	Evacuation Time	NCT
A	8500	1	4350	180.00	360.00	360.00	403.54
		2	4150	163.54	343.54	403.54	
B	9500	1	4599	254.70	434.70	434.70	625.50
		2	4901	385.50	565.50	625.50	
C	10400	1	5200	540.00	720.00	720.00	1140.00
		2	5200	900.00	1080.00	1140.00	

Figure 4-3 illustrates the time path of the groups of evacuees in all three scenarios. In the experimentation section, other objectives are tested resulting in different distribution of evacuees with the same network clearance time.

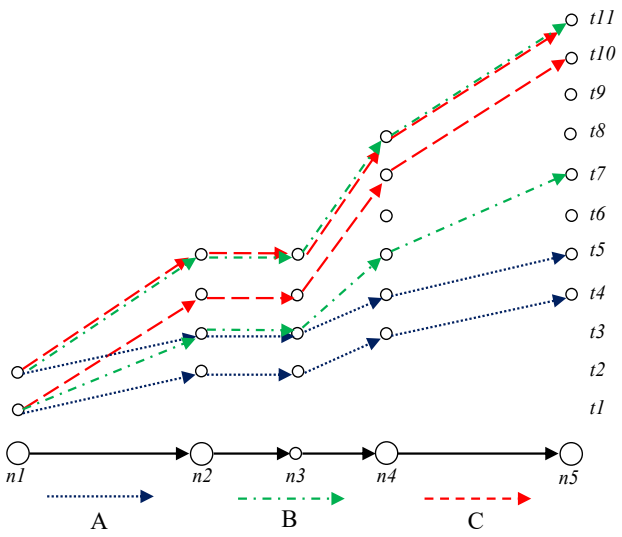

Figure 4-3: Results of the example network of the 3 scenarios

4.3.2 Experimentation

The network experimented in this section is the Tampa City, Florida and is obtained from Google Maps (2014). Suppose nodes 1 and 2 populations are evacuated to the uncapacitated safe zone in nodes 21 - 25 as shown in Figure 4-4. First, the nodes are identified as hub or non-hub nodes. The non-hub nodes set is $N \backslash N_H = \{4, 6, 7, 8, 14, 17\}$, and the remainder of the nodes are hub nodes N_H. Note that nodes 11 and 15 are examples of artificial nodes that have been added to the network as hubs to give a time increment by one unit of time to the evacuees passing through them, and the unit of time selected is 30 minutes based on the size of the network. The number of all possible simple routes, eliminating loops, from the source node 0 to the terminal node 26 is 17. All routes can be used, but in an evacuation process, the set of routes used is the set of shortest routes to minimize the travel time reach to a safe destination. After identifying the hub nodes and shortest routes, the model builds the time path for each route. The selected set of shortest routes are shown in Table 4-3.

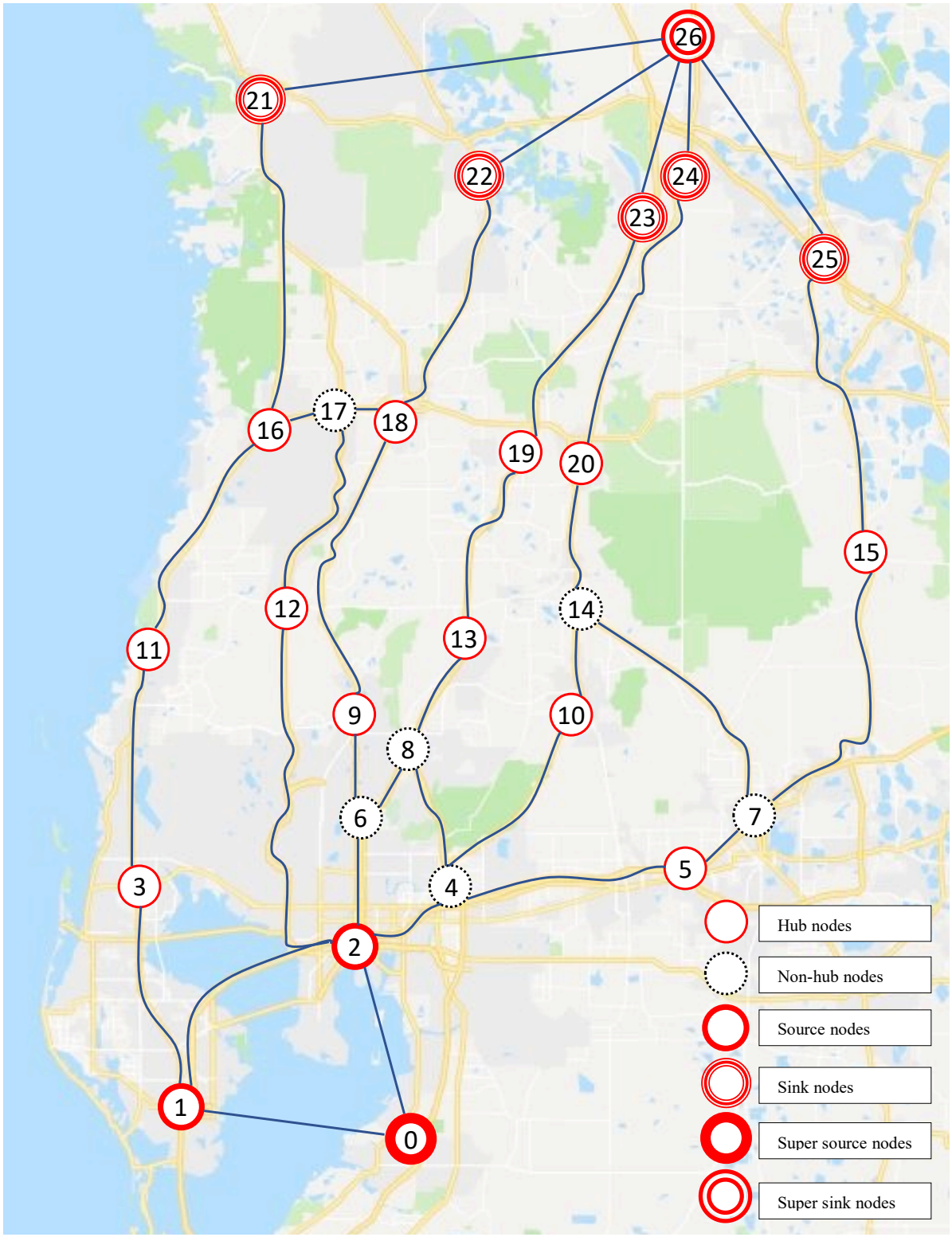

Figure 4-4: Tampa City network with 27 nodes and 43 bidirected arcs

Table 4-3: The set of shortest routes in Tampa City network from the source node 0 to destination node 26

r	Route	Length (minutes)
0	0 – 1 – 3 – 11 – 16 – 21 – 26	120
1	0 – 2 – 12 – 17 – 16 – 21 – 26	90
2	0 – 2 – 12 – 17 – 18 – 22 – 26	90
3	0 – 2 – 6 – 9 – 18 – 22 – 26	90
4	0 – 2 – 6 – 8 – 13 – 19 – 23 – 26	90
5	0 – 2 – 4 – 10 – 14 – 20 – 24 – 26	90
6	0 – 2 – 4 – 5 – 7 – 15 – 25 – 26	90

The number of evacuees in the two communities in nodes 1 and 2 is 20,000 evacuees. When minimizing the network clearance time *E*, the model requires 3-time units, which is equivalent to 1.5 hours to evacuate all the evacuees from the endangered area. In addition, the minimum network clearance time is 240 minutes, 4 hours until the last group of evacuees reaches the destination as shown in Table 4-4.

To find the optimal ATT and AET, the $\epsilon - constraint$ method is used since the range of the number of groups is known. In Tampa City network, the evacuation time is 3-time units when the NCT is minimized. The maximum number of groups to be evacuated is 21 when fixing the evacuation time to 3 units given that the number of routes is 7. The following model is solved to find the optimal solution of ATT:

$$Min\ TTT = \sum_{k\in K}\sum_{r\in R}\sum_{t\in T_E} e_r^{kt} \tag{4-30}$$

subject to

$$\sum_{k\in K}\sum_{r\in R}\sum_{t\in T}\sum_{h\in H}\sum_{(i,j)\in r} z_{ijrh}^{kt} = \epsilon \tag{4-31}$$

Constraints (4-2) - (4-26)

Since the range of ϵ is known, the total travel time (TTT) in the objective function (4-30) is minimized while changing the total number of groups in constraint (4-31). The result is illustrated in Figure 4-5.

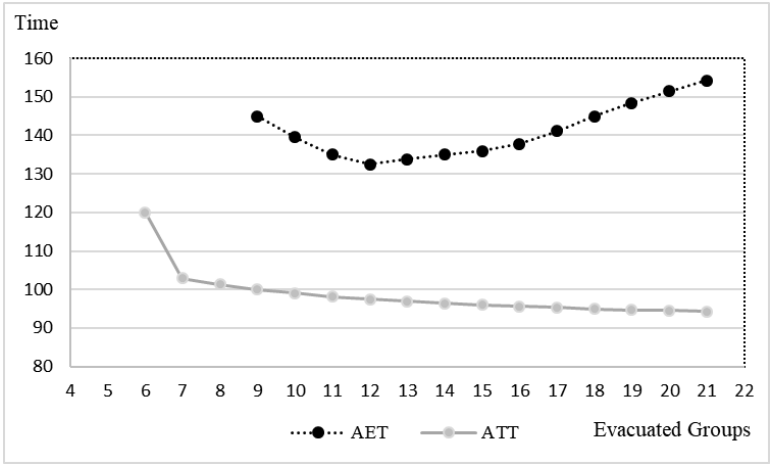

Figure 4-5: Solving the model with different number of groups to find the minimum ATT and AET

The minimum average travel time is 94.29 minutes when evacuees are grouped into 21 groups, while the minimum average evacuation time is 132.5 minutes when evacuees are grouped into 12 groups. The model is solved again minimizing the total evacuation time (TET) in the objective function (4-32). Table 4-4 summarizes the results for the 3 objectives.

$$Min\ TET = \sum_{k\in K}\sum_{r\in R}\sum_{t\in T_E} e'^{kt}_{r} \tag{4-32}$$

subject to

Constraints (4-2) - (4-26), (4-31)

Table 4-4: Summary of results of different objectives in Tampa City network

Objective (Minimize)	NCT	ATT	AET	Groups	CPU time (s)
NCT	**240**	122.50	182.50	12	27.50
ATT	240	**94.29**	154.29	21	38.72
AET	240	97.50	**132.50**	12	525.69

The number of evacuees in is random when minimizing the NCT as the objective is to evacuate the endangered zone in the shortest possible time as seen in Figure 4-6. When minimizing the ATT, the evacuees are distributed on the routes in all evacuation times to avoid congestion. Minimizing the AET pushes the evacuees towards the early evacuating times so the average evacuation time is minimized.

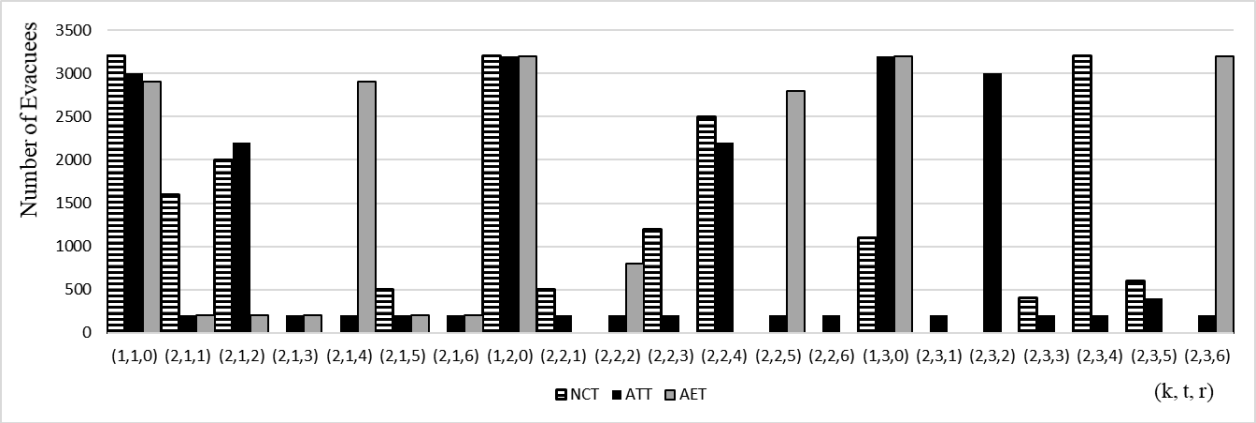

Figure 4-6: Number of evacuees for each group evacuated from community *k* at time *t* on route *r* in Tampa City network

Note that the travel time for each group of evacuees is illustrated in Figure 4-7 given that *r* is the route used and *t* is the evacuation time. Note that route 0 has a higher travel time since it is the only route that requires 120 minutes to travel, and it is most congested as it exceeds the value of 120 minutes for different groups of evacuees. Otherwise, the travel time of most of the groups of evacuees is around 90 minutes indicating that there is no congestion in most parts of the network. Note that the evacuation time for each group of evacuees in Figure 4-8 increases as the evacuees are evacuated later in time (the delay until departure time is considered).

Minimizing the ATT distributes all the evacuees on all routes in all evacuating times to minimize the overall congestion, but the AET will increase to 154.29 since the last groups evacuated will arrive late. However, minimizing the AET groups evacuees into 12 groups. Most groups are

evacuated in earlier evacuation times, and these groups will encounter congestion while the remaining groups are evacuated in later evacuation times and encounter less congestion. Minimizing ATT is excellent for non-emergency traffic assignment and minimizing AET is ideal for emergency evacuation.

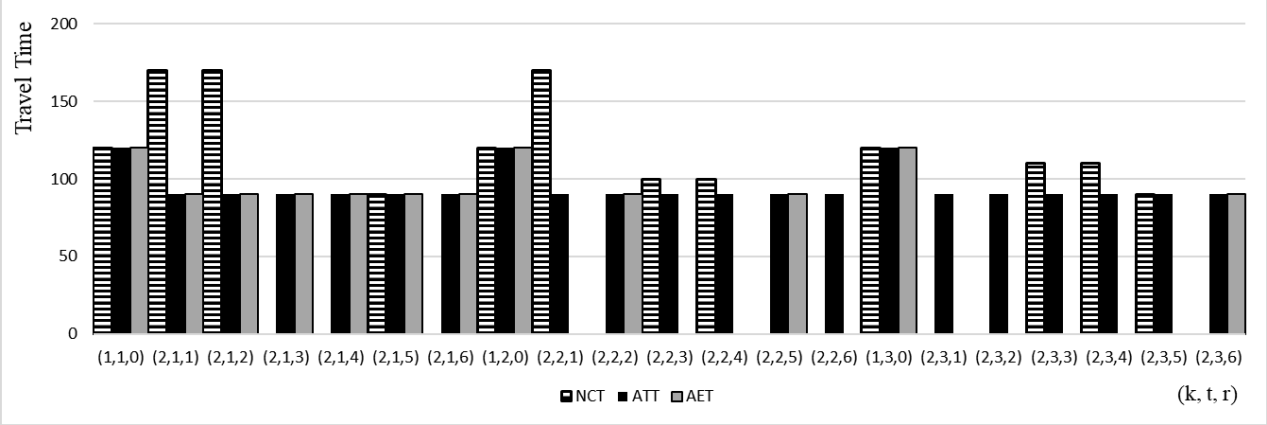

Figure 4-7: Travel time for each group of evacuees evacuated from community *k* at time *t* on route *r* in Tampa City network

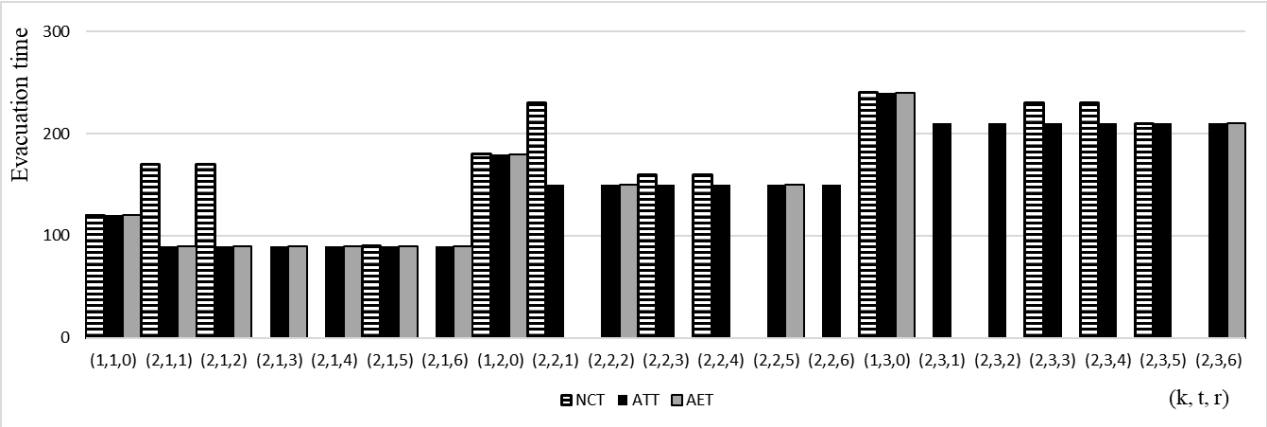

Figure 4-8: Evacuation time for each group of evacuees evacuated from community *k* at time *t* on route *r* in Tampa City network

4.4 Computational Complexity

The model is tested on the Tampa City problem using Gurobi Optimizer (2015), and the experiment was conducted on a PC with Intel quad-core 3.4 GH CPU and 32 GB memory. The model can solve small size problems with a limited number of routes. However, the

computational time can increase exponentially with the size of the problem. Note that z_{ijhg}^{ktrv} is the binary variable that indicates the time path of the evacuees. The number of variables z_{ijhg}^{ktrv} used in the model is decided by the number of hubs in a route γ, excluding the terminal hub, and the number of routes $|R|$ used in the network. The number of variables z_{ijph}^{kt} in route *r* is γ^2 at the evacuation time $t = 1$. For $t > 1$, the number of variables is $\gamma^2 + (t-1)\gamma$, and this conclusion leads us to the computational complexity of the model for multiple routes. The computational complexity of the model is $O(2^{|R|(\bar{\gamma}^2+(t-1)\bar{\gamma})})$ given that $|R|$ is the number of routes, $\bar{\gamma}$ is the average number of hubs in all routes excluding the terminal hub, and $t \in T$ is the times of evacuation. The two main factors in computational complexity are the number of routes and the average length of these routes.

Chapter 5: Reduced Complexity Latency-Based Evacuation Model

5.1 Introduction

In this chapter, we propose a reduced complexity version of the LBM in order to help decision-makers allocate demands on the available capacity resources for large-scale problems. Specifically, an LP model is developed as a DTA model. The results of the original model and the less complex version of the model are compared. The computational time for both models is included in the comparison. In addition, the results of the model are compared with the known CTM model.

The motivation of this research is to develop a model that captures the desirable properties of both static and dynamic traffic assignment models. The static traffic assignment models use the load-dependent nonlinear function but do not reflect the reality of the traffic congestion propagation effect. The DTA models consider the propagation by controlling the movement of the traffic but do not provide enough information about the evacuees. The estimated time for the evacuees, for example, to reach the destination is unknown in the CTM which, can result in very long evacuation time for some evacuees and lead to selfish behavior.

This chapter is organized as follows. In section 2, a new modeling approach is introduced and discussed. In section 5.3, toy examples are used to illustrate the model and compared with the CTM in addition to experimentation on real world network. In section 5.4, the reduced complexity LBM introduced in this chapter is compared with the original LBM presented in Chapter 4:. Next, the reduced LBM is compared with the common dynamic evacuation model the CTM is section 5.5. Finally, the computational complexity is discussed in section 5.6.

5.2 Evacuation Model

A novel approach to model the evacuation process is presented in this section. To the best of our knowledge, no similar attempts are found in the literature. Before running the model, the network is preprocessed by identifying all the hub nodes in the network and adding artificial hub nodes if necessary. Then the set of shortest routes from source nodes to terminal nodes is identified since it is unrealistic to send evacuees on the longest routes in emergencies. The hub nodes are identified or added so that the travel time in free-flow speed between each consecutive pair of hub nodes is constant. Once a group of evacuees passes through a hub node on a specific route, this group enters a new road segment with a hub increment. The system time unit is decided by the traveling time between two consecutive hub nodes in free-flow speed. However, the evacuees may be delayed by more than one time unit to travel between two hub nodes due to congestion.

Since the travel time is load dependent, the travel time function (4-1) is incorporated into the model. The travel time function, also known as BPR function, describes the relationship between the volume of traffic and the travel time used by the U.S. Department of Commerce Bureau of Public Roads (1964). The travel time $T(f)$ with traffic volume f on a road segment is described in function (4-1) where T^0 is the travel time on a road segment in free-flow speed in normal road conditions given that c is the capacity of the road segment, and α and β are turning parameters describing road characteristics with $\alpha \geq 0$ and $\beta \geq 0$. Those parameters are set to 0.15 and 4, respectively, by the U.S. Department of Commerce Bureau of Public Roads (1964). Since α and β parameters were derived based on data that may not reflect the current road conditions, they are set to 0.2745 and 5.98, respectively, based on the recent study conducted by Mtoi and Moses (2014).

Since this function is non-linear, we approximate it through a linear piecewise approximation, and each linear segment is represented by a slope and an intercept as shown in Figure 4-1. Note that f is the flow volume, and $T(f)$ is the travel time function (4-1). The accuracy of the output increases as the number of the linear segments increases.

The model complexity is significantly reduced when the evacuees follow one time path as illustrated in Figure 5-1. In section 5.4, the full model developed in chapter 4 is compared with the reduced model developed in this chapter.

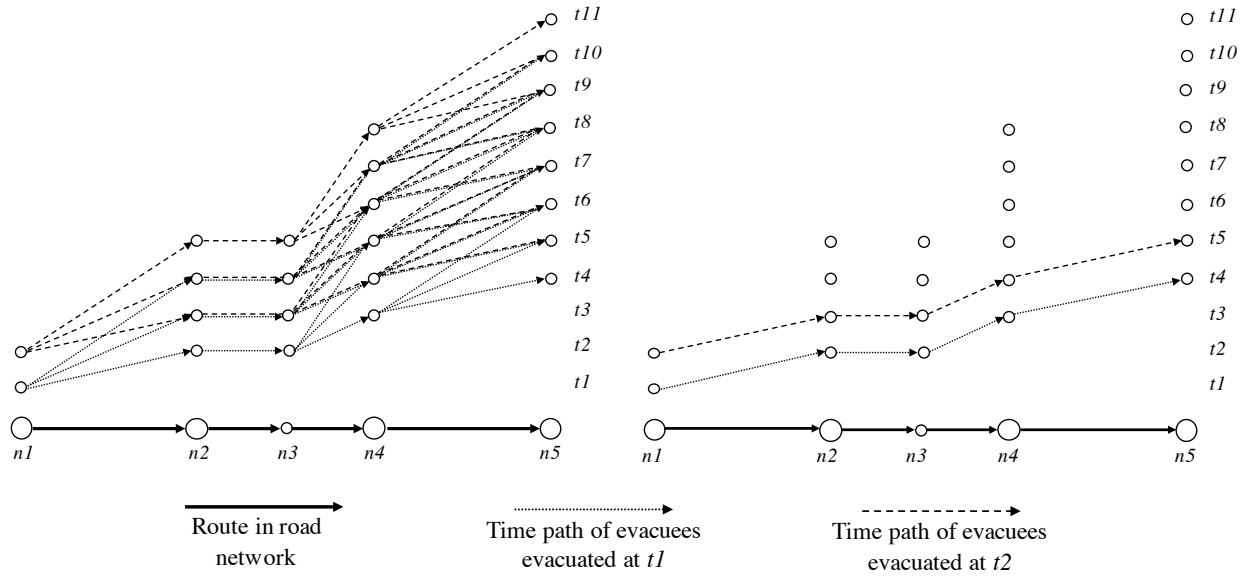

Figure 5-1 The time paths of the full model and the reduced model

5.2.1 Model Definition

Given a graph G = (N, A) with a set of nodes N and a set of directed arcs A, each arc $a \in A$ connects two nodes $i, j \in N$, where $a = (i, j)$. The nodes of the network are composed of a set of source nodes $N_S \subset N$, a set of terminal nodes $N_T \subset N$, and a set of hub nodes $N_H \subset N$ given that $N_S \subset N_H$ and $N_T \subset N_H$ since the evacuees are allowed to enter or exit through a hub node. Given a set of communities K to be evacuated, P_k is the set of the shortest routes that community k can use where P is the set of the shortest routes in the network from N_S to N_T. The evacuees can enter

and exit any route through any hub node. $T = \{1, \dots, t_e\}$ is the set of time periods when evacuees are evacuated, given that t_e is the time where the last groups are evacuated. When the time t in T equals 1, the evacuation process starts. $H = \{1, \dots, h_e\}$ is the set of hubs evacuees that are passing through the network, given that h_e is the hub where the last group of evacuees reached when they reach their destination. The link (*i, j*) on a route is linked to the time of evacuation *t* and hub *h* through the tuple S given that $(i, j, t, h) \in S$.

5.2.1.1 Parameters and Sets:

K	The set of communities
R	The set of shortest routes from the source nodes to the terminal nodes
D	The set of linear segments of the piecewise approximation to the BPR function
m^d	The slope of the linear segment $d \in D$ of the piecewise approximation
b^d	The intercept of the linear segment $d \in D$ of the piecewise approximation
u	The maximum number of evacuees on any arc
μ	The minimum number of evacuees to be evacuated in any group
ρ	The time in minutes to travel from one hub to the next hub node in free-flow speed and the system clock
c_{ij}	The time to travel from node *i* to node *j* on the link $(i, j) \in A$
C_r	The time to travel on route *r* from source to destination in free-flow speed
Q_k	The population of community *k*

5.2.1.2 Set of Variables:

x_{ijrh}^{kt}	The number of evacuees on arc (*i, j)* on route *r* at hub *h* of community *k* evacuated at time *t*
x'_{ijh}	The number of evacuees on arc (*i, j)* at hub *h*

f_r^{kt} The number of evacuees of community *k* on route *r* evacuated at time *t*

z_{ijrh}^{kt} Binary variable equals 1 if community *k* evacuated at time *t* is allowed to pass on arc (*i, j)* on route r at hub *h*, and it equals 0 otherwise

t_{ijh} The travel time on arc (*i, j*) at time *h* based on the piecewise approximated travel time function

τ_{ijh} The latency on arc (*i, j)* at hub *h* transferred to the group of evacuees that follows

$\hat{\tau}_{ijh}$ The slack latency on arc (*i, j)* at hub *h* not transferred to the group of evacuees that follows

τ'^{ktr}_{ijh} The latency of the group evacuated from community *k* at time t on route *r* on arc (*i, j)* at hub *h*

s_{ijh}^{ktr} Slack variable to remove the effect of latency of the group of evacuees from community *k* if they do not pass through the arc (*i, j*) on rote r at hub *h*

l_r^{kt} The latency of the group of evacuees on route *r* of a community *k* evacuated at time *t*

e_r^{kt} The travel time of community *k* on route *r* evacuated at time *t*

e'^{kt}_r The evacuation time of community *k* on route *r* evacuated at time *t*

E Network clearance time

5.2.2 Constraints

5.2.2.1 Flow Conservation Constraints

The hub *h* becomes *h+1* if the evacuees pass through a hub node in the flow conservation constraint (5-1). In the flow conservation constraints (5-2), evacuees hub *h* on arc (*i, j*) does not change if evacuees do not pass through a hub node. Every community to be evacuated has a population size $of\ Q_k$, as seen in constraint (5-3).

$$x_{ijr(h+1)}^{kt} - x_{jirh}^{kt} = \begin{cases} f_r^{kt} \; if \; i \in N_S \\ -f_r^{kt} \; if \; i \in N_T \\ 0, otherwise \end{cases}, if \; i \in N_H \qquad \forall r \in R, (i,j) \in r, k \in K \; t,h|(i,j,t,h) \in S \qquad (5\text{-}1)$$

$$x_{ijrh}^{kt} - x_{jirh}^{kt} = 0, if \; i \notin N_H \qquad \forall r \in R, (i,j) \in r, k \in K, \; t,h|(i,j,t,h) \in S \qquad (5\text{-}2)$$

$$\sum_{t \in T} \sum_{r \in R} f_r^{kt} = Q_k \qquad \forall k \in K \qquad (5\text{-}3)$$

5.2.2.2 Networks Link Constraints

Since all evacuees share the same road network, constraint (5-4) sums all evacuees from all communities *k* started at time *t* using all the routes *r* passing through the arc (*i, j)* at hub *h* to the variable x'_{ijh}.

$$x'_{ijh} = \sum_{r \in R} \sum_{k \in K} \sum_{t|(i,j,t,h) \in S} x_{ijrh}^{kt} \qquad \forall (i,j) \in A, h \in H \qquad (5\text{-}4)$$

5.2.2.3 Latency Constraints

Constraint (5-5) is used to find the latency τ_{ijh} on arc (*i, j)* at hub *h* transferred to the group that follows. The latency of an arc (*i, j)* at hub *h* equals the required time for evacuees to travel on the arc based on their volume subtracting the time they would spend in a free-flow speed. It can be noticed that $\hat{\tau}_{ijh}$ in (5-6) is bounded by the time evacuees spend on the arc in free-flow speed, but it can be less in the case that the delay is less than the travel time in free-flow speed, or no evacuees are passing on the arc to maintain the constraint feasibility. The initial latency of the arc (*i, j)* equals 0 in constraint (5-7).

$$\tau_{ijh} = c_{ij} t_{ijh} - \hat{\tau}_{ijh} \qquad \forall (i,j) \in A, h \in H \qquad (5\text{-}5)$$

$$\hat{\tau}_{ijh} \leq c_{ij} \qquad \forall (i,j) \in A, h \in H \qquad (5\text{-}6)$$

$$\tau_{ijh} = 0 \qquad \forall (i,j) \in A, h = 0 \qquad (5\text{-}7)$$

To find the travel time on a road segment based on the flow volume, the piecewise approximation to the BPR convex function is used. Since the function is convex, the travel time t_{ijh} on arc *(i, j)* at hub *h* can be found as seen in constraint (5-8).

$$t_{ijh} \geq m^d x'_{ijh} + b^d \qquad \forall (i,j) \in A, h \in H, d \in D \qquad (5\text{-}8)$$

5.2.2.4 Delay Propagation Constraints

Constraint (5-9) transfers the effect of congestion to the group of evacuees that follow. As the link becomes more congested, the latency increases by adding the latency of the group of evacuees that follows through the preceding link. However, the congestion effect is not fully transferred if there is a gap of time between the leading group and the group that follows. As the gap between the two groups increases, the transferred congestion effect decreases as seen in constraint (5-9).

$$\tau_{ijh} \geq \tau_{jlv} - \rho(1 + h - v)(1 - z_{ijrh}^{kt}) \qquad \forall (i,j),(j,l) \in A, k \in K, h, v \in H | h \geq v, r \in R, t \in T, (i,j,t,h) \in S \qquad (5\text{-}9)$$

5.2.2.5 Allowing to Evacuate Constraints

In constraint (5-10), all evacuees of community *k* at hub *h* evacuated at time *t* on route *r* can pass through the arc (*i, j*), meaning that no part of the group is delayed or outrun the rest of the group. In constraint (5-11), each group of evacuees is bounded by a minimum number μ decided by the decision-maker. If the variable z_{ijrh}^{kt} equals zero, no evacuees from community *k* on route *r* at hub *h* can pass through the arc (*i, j*).

$$x_{ijph}^{kt} \leq u\, z_{ijrh}^{kt} \qquad \forall\, i \in N_S, (i,j) \in A, r \in R, t, h | (i,j,t,h) \in S, k \in K \tag{5-10}$$

$$x_{ijph}^{kt} \geq \mu\, z_{ijrh}^{kt} \qquad \forall\, i \in N_S, (i,j) \in A, r \in R, t, h | (i,j,t,h) \in S, k \in K \tag{5-11}$$

5.2.2.6 Evacuees Latency Constraints

The latency on route *r* of a community *k* evacuated at time *t* in constraint (5-12) is the sum of the latencies on the specific route in addition to the slack latencies that are not transferred to the groups that follow. Since all communities evacuated in various times using different routes share the same network, the latency of a community *k* on route *r* is a subset of the latencies of the network. To prevent the latency effect to add to the latencies of non-evacuated groups due to overlapped routes, the sum of latencies is added if evacuees are using the route as seen in constraints (5-13)-(5-15). Hence, the latency of the non-evacuated group is zero.

$$l_r^{kt} = \sum_{(i,j) \in r} \sum_{h \in H} \tau'_{ijh} \qquad \forall\, t \in T, k \in K, r \in R_k \tag{5-12}$$

$$\tau'^{ktr}_{ijh} + s_{ijh}^{ktr} = \tau_{ijh} + \hat{\tau}_{ijh} \qquad \forall\, (i,j) \in A, h \in H, k \in K \tag{5-13}$$

$$\tau'^{ktr}_{ijh} \leq M z_{ijrh}^{kt} \qquad \forall\, (i,j) \in A, k \in K, t, h | (i,j,t,h) \in S \tag{5-14}$$

$$s_{ijh} \leq M(1 - z_{ijrh}^{kt}) \qquad \forall\, (i,j) \in A, k \in K, t, h | (i,j,t,h) \in S \tag{5-15}$$

5.2.2.7 Evacuation Constraints

The time required to travel for each group of evacuees evacuated at time *t* from community *k* on route *r* to reach their destination is the travel time on route *r* in free-flow speed in addition to the latency as shown in constraint (5-16). The evacuation time for each group of evacuees from

community *k* on route *r* at time *t* to reach their destination is the sum of the waiting times since the evacuation time, the travel time on route *r* in free-flow speed, and the latency on the route as seen in constraint (5-17). To minimize the network clearance time, the maximum evacuation time is minimized, as shown in constraint (5-18).

$$e_r^{kt} = C_r z_{ijrh}^{kt} + l_r^{kt} \qquad \forall i \in N_S, r \in R, (i,j) \in r, k \in K \; t,h|(i,j,t,h) \in S \tag{5-16}$$

$$e'^{kt}_r = \rho(t-1) z_{ijrh}^{kt} + C_r z_{ijrh}^{kt} + l_r^{kt} \qquad \forall i \in N_S, r \in R, (i,j) \in r, k \in K \; t,h|(i,j,t,h) \in S \tag{5-17}$$

$$e'^{kt}_r \leq E \qquad \forall\, k \in K, r \in R, t \in T \tag{5-18}$$

5.2.2.8 Non-negativity Constraints

In addition, the following non-negativity constraints (5-19) and binary variables constraints (5-20) are added.

$$x_{ijrh}^{kt}, x'_{ijh}, f_r^{kt}, \tau_{ijh}, \hat{\tau}_{ijh}, \tau'_{ijh}, s_{ijh}, l_r^{kt}, e_r^{kt}, e'^{kt}_r, E \geq 0 \quad \forall\, (i,j) \in A, k \in K, r \in R, \; t \in T, h \in H, (i,j,t,h) \in S \tag{5-19}$$

$$z_{ijh}^{kt} \in \{0,1\} \qquad \forall\, (i,j) \in A, k \in K, r \in R, \; t,h|(i,j,t,h) \in S \tag{5-20}$$

5.2.3 Objective Functions

The objective of the model is to minimize NCT that is equal to the variable *E*, where *E* is the total travel time of the last group arriving at the safe destination in addition to the waiting time since the beginning of the evacuation process, as seen in the objective function (5-21).

$$Min\ NCT = E \tag{5-21}$$

In addition, different objectives are experimented. The ATT and the AET for each group of evacuees are incorporated in the model in the objectives (5-22) and (5-23), respectively. The sum of z_{ijrh}^{kt} at the source node $i \in N_S$ is the number of groups to be evacuated, given that the minimum number of groups to be evacuated is one.

$$Min\ ATT = \frac{\sum_{k\in K}\sum_{r\in R}\sum_{t\in T} e_r^{kt}}{\sum_{k\in K}\sum_{r\in R}\sum_{(i,j)\in r}\sum_{t,h|(i,j,t,h)\in S} z_{ijrh}^{kt}} \tag{5-22}$$

$$Min\ AET = \frac{\sum_{k\in K}\sum_{r\in R}\sum_{t\in T} e'^{kt}_r}{\sum_{k\in K}\sum_{r\in R}\sum_{(i,j)\in r}\sum_{t,h|(i,j,t,h)\in S} z_{ijrh}^{kt}} \tag{5-23}$$

5.3 Illustration and Experimentation

In this section, a trivial network is used to illustrate the model. A small real-world network is also used for illustration and experimentation.

5.3.1 Illustrative Examples

5.3.1.1 Example 1

Consider the two simple networks as road segments illustrated in Figure 5-2. Assume that each road segment is composed of two lanes with a capacity of 1750 vehicles/lane/hour. The travel time in free-flow speed from one node to the next node is 60 minutes, and the travel time increases due to congestion, as illustrated in Table 5-1. The latency based on the number of vehicles is shown in Table 5-1. This information is used to approximate the nonlinear BPR flow-travel time function using a piecewise linear approximation. The lane capacity is set to 1750 vehicles/lane/hr., and each link in the network is assumed to consist of two lanes. To find the

latency on a road segment, the latency in Table 5-1 is multiplied in the travel time on the road segment in free-flow speed.

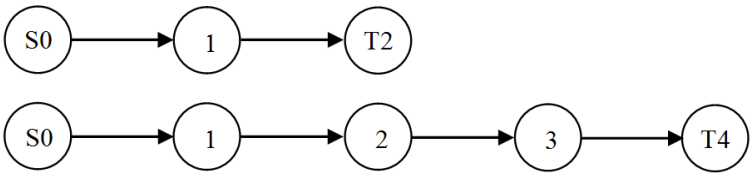

Figure 5-2: Road segment with 60 minutes travel time between each consecutive pair of nodes in free-flow speed

The number of evacuees is 4900 traveling through the three-node network in Figure 5-2 from the source node S0 to the terminal node T2 with a total travel time of 120 minutes in normal conditions. When using the CTM model we set the link capacity to 5200 vehicles, and the shockwave speed ratio is set to 0.33 as seen in Table 5-1, the NCT is 300 minutes while the LBM NCT is 360 minutes. Now we assume that the distance is doubled in the network with five nodes to become 240 minutes in normal conditions, as illustrated in Figure 5-2. Evacuating 4900 evacuees requires 420 minutes when using the CTM, and it requires 720 minutes when using the LBM. Notice that the NCT of the LBM is doubled when the distance is doubled. However, the NCT in the CTM is increased by 120 minutes, which is the distance of the added road segment. We conclude that the CTM does not capture the congestion on the added road segment. It regulates the entry of vehicles at the beginning of the road segment. Then the vehicles travel the rest of the road segment in free-flow speed, which does not reflect the reality of the real world congestion.

Table 5-1: Travel time based on the number of vehicles, using modified BPR, and the shockwave speed to the free-flow speed ratio

Number of Vehicles f	**Latency (m)*60**	**Speed Ratio δ**
0	0	1
2200	1	0.99
4350	60	0.5
4650	90	0.4
4900	120	0.33
5200	180	0.25

5.3.1.2 Example 2

Consider the network with seven nodes and seven arcs shown in Figure 5-3. The population in the node S0 is evacuated to the shelter in the node T6. Node S0 is a source node, node T6 is a terminal node, and all nodes are set as hub nodes. The time to travel from one node to the consecutive node is 60 minutes in free-flow speed. The predefined routes are S0-1-3-5-T6 and S0-2-4-5-T6. The total travel time from the source to the terminal on either route in normal conditions is 240 minutes, and the number of vehicles to be evacuated is assumed to be 15,000.

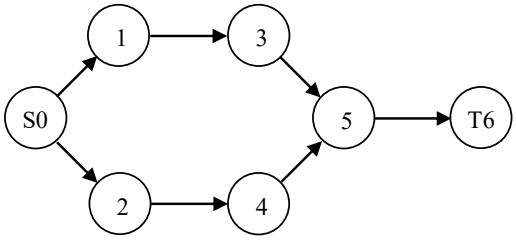

Figure 5-3: a small network for illustration. The network consists of seven nodes, and seven directed arcs.

The optimal NCT is 667.9 minutes assuming that there is no congestion at the beginning of the evacuation process, as seen in Table 5-2. Note that the first group of evacuees evacuated on both routes does not cause any congestion, which is referred to as latency τ, until they reach the bottleneck arc (5,6), but they cause delay to themselves of 1 minute on the non-bottleneck links

on route 1 and 14.72 minutes on the non-bottleneck links on route 2 which is the slack latency $\hat{\tau}$. Although the delay is 120 minutes as the total number of evacuees is 4900, the delay they transfer to the succeeding group is 60 minutes since the latter are evacuated 60 minutes later. The second group of evacuees is 60 minutes delayed on arcs (3, 5) and (4, 5) by the first group, then they cause a delay of 120 minutes on the bottleneck arc (5, 6). The third group of evacuees is delayed by the first and second groups. There is 60 minutes delay on arcs (1,3) and (2,4) due to the propagated delay from the first group, and delay 120 minutes on arcs (3, 5) and (4,5) by the second group that causes a delay of 60 minutes on the bottleneck arc.

Table 5-2: The results of the example 2 network

Number of Evacuees (f)			**Latency (τ)** Slack Latency ($\hat{\tau}$)							**Obj. NCT (m)**
Time	Route1	Route2	(0, 1)	(0, 2)	(1, 3)	(2,4)	(3,5)	(4,5)	(5,6)	
1	2200	2700	**0**	**0**						667.86
			1	14.72						
2	3000	2200	**0**	**0**	**0**	**0**				
			22.9	1	1	14.72				
3	2450	2450	**0**	**0**	**0**	**0**	**0**	**0**		
			7.86	7.86	22.95	1	1	14.72		
					60	**60**	**60**	**60**	**60**	
					0	0	0	0	60	
							120	**120**	**120**	
							0	0	60	
									60	
									60	

The summary of the travel time and evacuation time on each route and different evacuation times are presented in Table 5-3. Note that the travel time is the latency added to the travel time in free-flow speed. The evacuation time is the travel time added to the waiting time since the beginning of the evacuation process. The evacuation time for the groups evacuated in the first period equals the travel time since they are evacuated at the beginning of the evacuation process, while 60 minutes are added for every period the group of evacuees is waiting to be evacuated.

Table 5-3: Summary of the results of the second example for each group of evacuees on different route and evacuation time

Time	Route	Latency	Travel Time	Evacuation Time
1	**1**	123.00	363.00	363.00
	2	164.16	404.16	404.163
2	**1**	285.91	525.91	585.91
	2	242.00	482.00	542.00
3	**1**	307.86	547.86	667.86
	2	307.86	547.86	667.86

5.3.2 Experimentation

The network experimented in this section is Tampa City, Florida, and is obtained from Google Maps (2014). Suppose nodes 1 and 2 populations are evacuated to the uncapacitated safe zone in nodes 21 – 25, as shown in Figure 4-4. First, the nodes are identified as a hub or non-hub nodes. The non-hub nodes set is $N \backslash N_H = \{4, 6, 7, 8, 14, 17\}$, and the remainder of the nodes are hub nodes N_H. Note that nodes 11 and 15 are examples of artificial nodes that have been added to the network as hubs to give a hub increment to the evacuees passing through them, and the unit of time ρ is set to 30 minutes based on the size of the network. The number of all possible simple routes, eliminating loops, from the source node 0 to the sink node 26 is 17. All routes can be used, but in an evacuation process, the set of routes used is the set of shortest routes to minimize the travel time to reach a safe destination. The selected set of shortest routes are shown in Table 4-3.

The number of evacuees in the community in nodes 2 is assumed to be 25,000 evacuees. When minimizing the network clearance time *E*, the model requires 3-time units, which is equivalent to 1.5 hours to evacuate all the evacuees from the endangered area. Also, the minimum network clearance time is 150 minutes or 2.5 hours until the last group of evacuees reaches the destination as shown in Table 5-5.

Table 5-4: The set of shortest routes in Tampa City from the source node 0 to the destination node 26

r	Route	Length (minutes)
0	0 – 2 – 12 – 17 – 16 – 21 – 26	90
1	0 – 2 – 12 – 17 – 18 – 22 – 26	90
2	0 – 2 – 6 – 9 – 18 – 22 – 26	90
3	0 – 2 – 6 – 8 – 13 – 19 – 23 – 26	90
4	0 – 2 – 4 – 8 – 13 – 19 – 23 – 26	90
5	0 – 2 – 4 – 10 – 14 – 20 – 24 – 26	90
6	0 – 2 – 4 – 5 – 7 – 14 – 20 – 24 – 26	90
7	0 – 2 – 4 – 5 – 7 – 15 – 25 – 26	90

To find the optimal ATT and AET, $the\ \epsilon - constraint$ method is used since the range of the number of groups is known. In the Tampa City network, the evacuation time is 3-time units when the NCT is minimized. The maximum number of groups to be evacuated is 24 when fixing the evacuation time to 3 units, given that the number of routes is 8. The following model is solved to find the optimal solution of ATT:

$$Min\ TTT = \sum_{k\in K}\sum_{r\in R}\sum_{t\in T} e_r^{kt} \tag{5-24}$$

subject to

$$\sum_{k\in K}\sum_{r\in R}\sum_{h\in H}\sum_{t\in T}\sum_{(i,j)\in r|i\in N_s} z_{ijrh}^{kt} = \epsilon \tag{5-25}$$

Constraints (5-1) - (5-20)

Since the range of ϵ is known, the TTT in the objective function (5-24) is minimized while changing the total number of groups in constraint (5-25). The model is solved again, minimizing the TET in the objective function (5-26). The result is illustrated in Figure 5-4.

$$Min\ TET = \sum_{k \in K} \sum_{r \in R} \sum_{t \in T} e'^{kt}_{r} \tag{5-26}$$

subject to

Constraints (5-1) - (5-20), (5-25)

When a few groups are evacuated, the ATT and AET are high since the number of evacuees in each group is large, leading to higher congestion rates, as illustrated in Figure 5-4. As the number of groups increases, the ATT and AET decrease. Note that the AET decreases to a point, then it increases as the congestion effect fades, and the waiting time to evacuate starts delaying the evacuees. The optimum number of groups to be evacuated depends on the objective. For the NCT and AET, the number of groups is selected to avoid delay coming from congestion and waiting time, and the number of groups selected in the ATT is the maximum since the waiting time does not affect travel time.

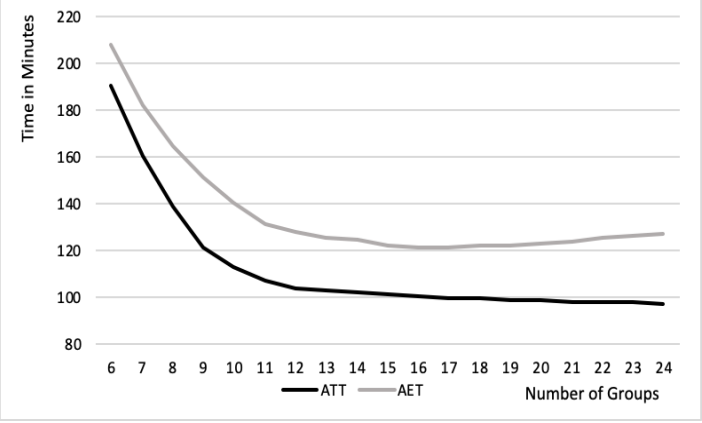

Figure 5-4: The ATT and AET behavior of 25,000 evacuees when changing the number of groups of evacuees

The minimum average travel time is 97.25 when evacuees are grouped into 24 groups, while the minimum average evacuation time is 121.13 when evacuees are grouped into 17 groups.

Table 5-5: Summary of results in minutes for different objectives

Objective (Minimize)	NCT	ATT	AET	Groups	CPU time (s)
NCT	**150.02**	123.32	147.32	15	5.65
ATT	182.00	**97.25**	127.25	24	16.4
AET	153.00	99.95	**121.13**	17	6.30

Assume that the demand to evacuate in the Tampa City network is 45,000 evacuees. Note that the ATT is around 350 minutes compared to 120 minutes when 25,000 people are evacuated, and the number of groups is set to 9, as seen in Figure 5-5. The ATT and AET for the 45,000 evacuees are significantly higher than the 25,000 evacuees since the congestion is higher. Also, the AET for the 45,000 is not considerably affected by the waiting time when the number of groups is set to 24, as shown in Figure 5-5. From this information, we conclude that all routes can be used for all evacuating times when the demand to evacuate is high in case of emergencies. When all routes are used for all evacuating times, the model becomes LP, and the complexity is greatly reduced.

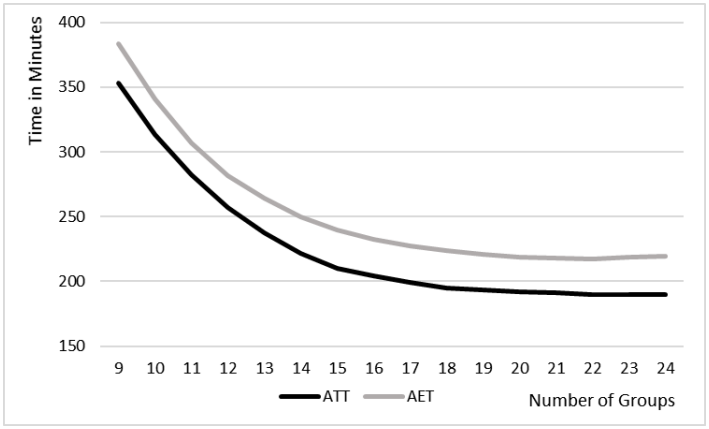

Figure 5-5: The ATT and AET behavior of 45,000 evacuees when ranging the number of groups

The number of evacuees in each group is illustrated in Figure 5-6. Note that the number of evacuees on the routes that cause bottleneck congestion is minimal. The variability in the number of evacuees for the objective NCT is high since the objective is to clear the network in the

shortest time. Minimizing the ATT distributes all evacuees on all routes with minimum congestion since the waiting time to be evacuated does not affect the ATT. Note that the number of evacuees does not exceed 2000 vehicles since the delay time for this number of evacuees is insignificant, as seen in Table 5-1. After 2000, the function becomes steeper, leading to more congestion and delay. Minimizing the AET pushes most evacuees to be evacuated in the early periods to avoid waiting time, as seen in Figure 5-6.

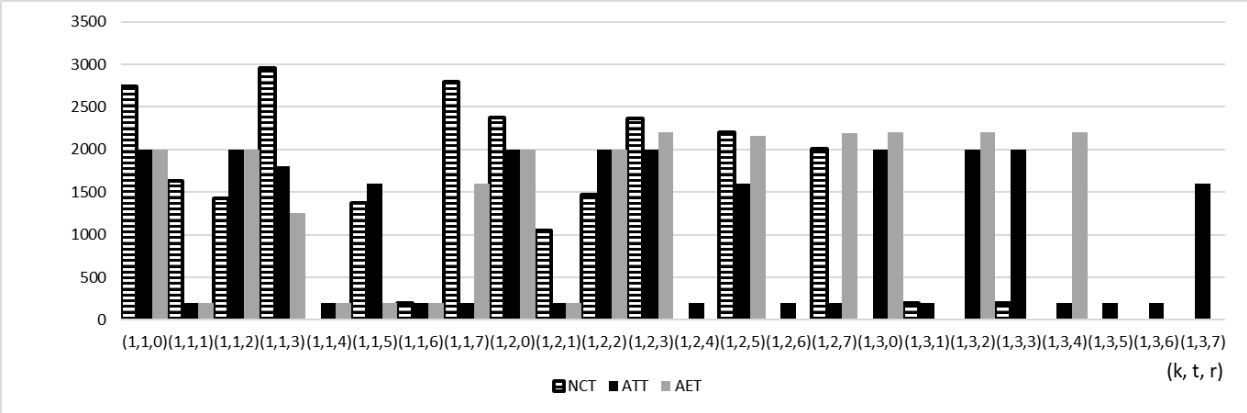

Figure 5-6: The number of evacuees in each group from community *k*, on route *r*, and evacuated at time *t*

The travel and evacuation time for each group of evacuees on each route *r* evacuated at time *t* for the three objectives is illustrated in Figure 5-7. Note that the travel time for groups evacuated early is higher due to congestion in the NCT, and the evacuation time is 150 for most groups. The early groups are delayed because of the congestion, while the later groups are delayed waiting to be evacuated. Hence, the model minimized the congestion for the later groups since they are delayed by waiting to evacuate. The variability in the travel time for the ATT is low since all evacuees are distributed on all routes and evacuating times, minimizing the overall congestion in the network. The overall travel and evacuation times are minimized for most groups for the AET objective by minimizing the congestion overall the network but avoiding waiting time to evacuate.

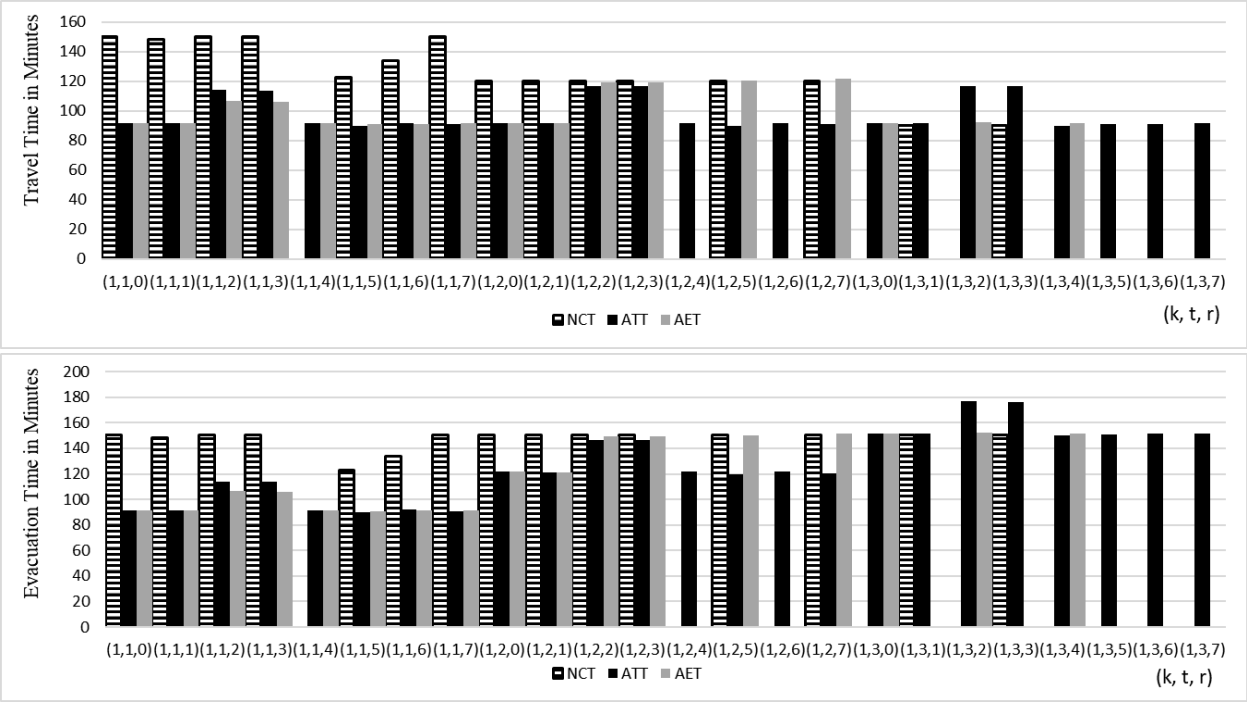

Figure 5-7: The travel and evacuation time in minutes for each group of evacuees evacuated on route r at time t

5.4 Comparing the Original LBM Model with the Reduced Complexity Model

The original LBM developed in chapter 4 (LBM I) results are compared with the reduced complexity version of the LBM developed in chapter 5 (LBM II). The network used is Tampa City with the set of routes R = {0, 1, 2, 3, 5, 7}. The NCT for LBM I and LBM II is shown in Figure 5-8 when ranging the demand from 10,000 to 40,000 evacuees.

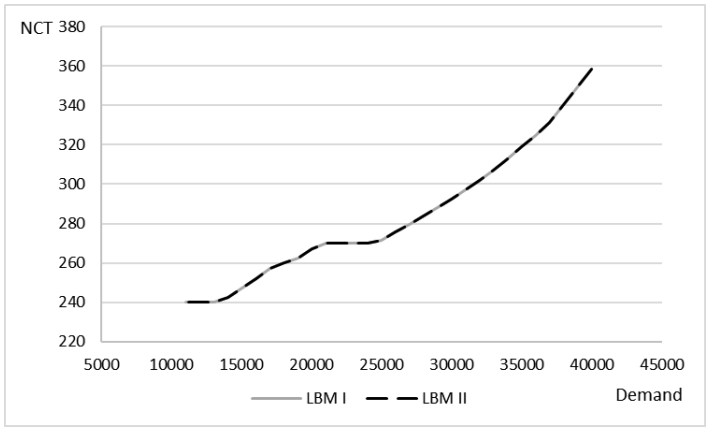

Figure 5-8: The NCT for the LBM I and LBM II models for the demand range from 10,000 to 40,000 evacuees

Note that the NCT is identical in both models. However, the reduction in computational time is significant. The computational time for the LBM I and LBM II is illustrated in Figure 5-9.

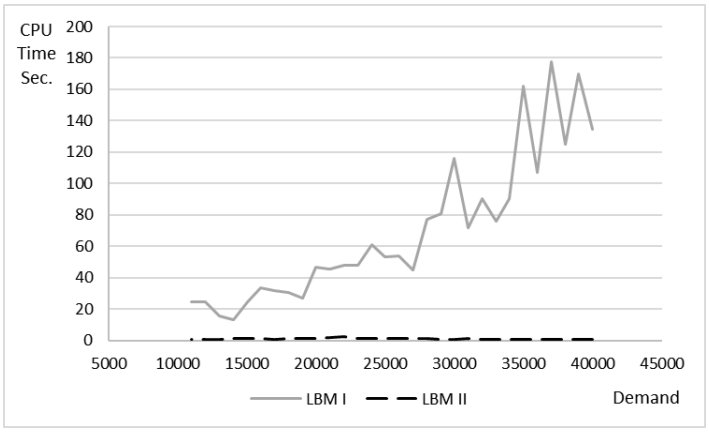

Figure 5-9: The computational time for the LBM I and LBM II models in seconds when ranging the demand from 10,000 to 40,000 evacuees

Notice that the computational time of the LBM I increases with the demand to evacuate while the computational time for the LBM II is not affected by the demand. The average computational time is of the LBM II is 1.25 seconds. We conclude that the computational time can be reduced by more than 99% while maintaining an identical output.

5.5 Comparing the LBM with the CTM Model

After comparing the reduced complexity LBM with the original LBM, the LBM is compared with the CTM. The network used for comparison is network illustrated in Figure 5-3. Although the number of groups to be evacuated cannot be decided in the CTM, we assume that the total evacuees are divided into 6 groups evacuated in 3 periods on two routes. From this assumption, the shockwave speed ratio can be decided based on the travel time, as seen in Table 5-1. Note that the demand is ranging from 500 up to 15500. When the demand is 500, the NCT is 240 for both models since there is no congestion, and all evacuees can be evacuated in the first period with no delays, as seen in Figure 5-10. As the demand increases, the NCT increases nonlinearly following the behavior of the BPR function, given that the shockwave speed parameter δ_i is updated for every node $i \in N_R$ for each demand scenario.

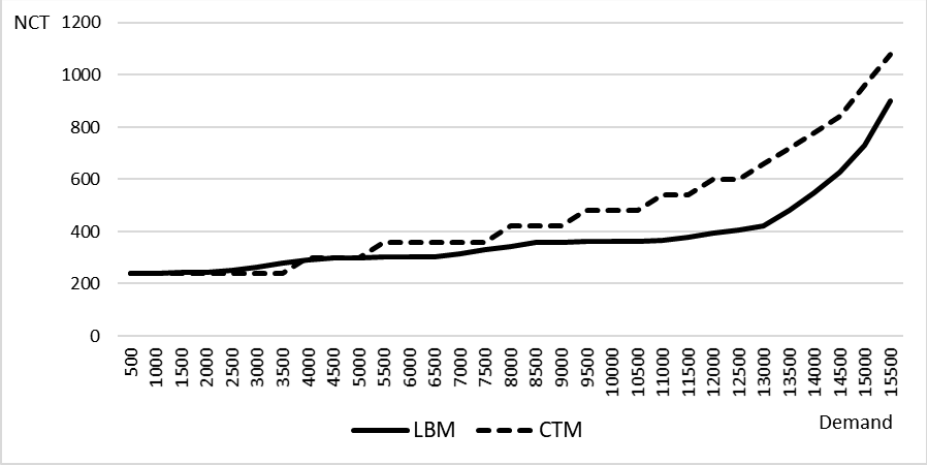

Figure 5-10: The NCT in minutes for the LBM is compared with the CTM output

5.6 Computational Complexity

The model is tested on the Tampa city problem using Gurobi Optimizer (2015), and the experiment was conducted on a PC with Intel quad-core 3.4 GH CPU and 32 GB memory. The model can solve small to medium size problems with a limited number of routes. However, the

computational time can increase exponentially with the size of the problem. Note that z_{ijrh}^{kt} is the binary variable that indicates whether the evacuees of community *k* are evacuated at time *t* . The number of variables z_{ijrh}^{kt} used in the model is decided by the number of routes $|R|$ used in the network and the number of evacuating times $|T|$. The number of hubs does not contribute to the size of the network. The number of variables z_{ijrh}^{kt} in the model is the number of routes *r* and the number of evacuating times $|T|$. The computational complexity of the model is reduced from $O\left(2^{|R|\left(\bar{\gamma}^2+(t-1)\bar{\gamma}\right)}\right)$ to $O(2^{|R|\cdot|T|})$ given that $|R|$ is the number of routes, $\bar{\gamma}$ is the average number of hubs in all paths excluding the terminal hub. The two main factors in computational complexity are the number of routes and evacuating times.

Chapter 6: Min-Max Fairness in the Non-Convex Latency-Based Evacuation Model

6.1 Introduction

The motivation of the work in this chapter is to find the optimal MMF evacuation time using the LBM model. The proposed algorithm in this chapter follows a similar approach to the *water-filling* algorithm. However, the proposed algorithm does not rely on the complementary slackness condition to identify the groups whose evacuation time cannot be improved any further. Hence, the algorithm is capable of finding the MMF resources allocation for nonconvex problem structures. On the other hand, the LBM model captures the desirable properties of the static and the dynamic models and fills the gap between them. The static models use the load-dependent functions but do not consider the congestion propagation. The dynamic models propagate the congestion effect by regulating the entry of traffic to a road segment but do not compute the estimated time each group of evacuees spends in the network. The output of the algorithm is compared with other objectives to show the effectiveness of the developed approach. The two measures used to compare the outputs from different objectives are efficiency and fairness. The AET is considered as a measure of efficiency, and the SAD is used to measure fairness.

The organization of this chapter is as follows. In section 6.2, the fair evacuation model is introduced, including the set of variables, constraints, and objective functions. In section 6.3, the model is illustrated on a small example and experimented on a real-world network. Fairness is in the evacuation is experimented in section 6.4, using θ*-progressive-filling* algorithm approach. The chapter is summed up with computational complexity discussion in sections 6.5.

6.2 Evacuation Model

A novel approach to model the evacuation process is presented in this section. To the best of our knowledge, there is no attempt found in the literature to model fairness in evacuation, similar to the one proposed in this chapter. The network is preprocessed by identifying all the hub nodes and adding artificial hub nodes before running the model if necessary. Then the set of shortest routes from the endangered nodes to the safe zone nodes are identified since it is unrealistic to send evacuees on longer routes in emergencies. The hub nodes are added, so the travel time in free-flow speed between each pair of consecutive nodes is constant. Once a group of evacuees pass through a hub node, they enter a new road segment with a hub increment. The constant travel time between each pair of consecutive hub nodes is the system time unit. However, the evacuees may spend a longer time on a road segment if the network is congested.

The travel time function (4-1) used in the model, also known by BPR, is used by the U.S. Department of Commerce Bureau of Public Roads (1964). This function is incorporated in the model to simulate the effect of congestion since the travel time is load-dependent. The travel time function describes the non-linear relationship between traffic volume and travel time. T^0 is the travel time in free-flow speed on a road segment in normal road conditions given the capacity c of the road segment. The tuning parameters α and β describe the road characteristics with $\alpha \geq 0$ and $\beta \geq 0$. Those parameters are set to 0.15 and 4, respectively, by the U.S. Department of Commerce Bureau of Public Roads. Since α and β parameters were derived based on data that may not reflect the current road conditions, they are set to 0.2745 and 5.98, respectively, based on the recent study conducted by Mtoi and Moses (2014). To avoid non-linear constraints in the model, the travel time function is linearized using a piecewise approximation. Every linear

segment is represented by a slope and intercept parameters. The accuracy of the output of the function increases as the number of the linear segments increase.

6.2.1 Model Definition

Given a graph G = (N, A) with a set of nodes N and a set of directed arcs A, each arc $a \epsilon A$ connects two nodes $i, j \in N$ where $a = (i, j)$. The nodes of the network are composed of a set of source nodes $N_S \subset N$, a set of terminal nodes $N_T \subset N$, and a set of hub nodes $N_H \subset N$ given that $N_S \subset N_H$ and $N_T \subset N_H$ since the evacuees are allowed to enter or exit through a hub node. Given a set of communities K to be evacuated, P_k is the set of the shortest routes that community k can use where R is the set of the shortest routes in the networks from N_S to N_T. The evacuees can enter and exit any route through any hub node. $T = \{1, \dots, t_e\}$ is the set of time periods when evacuees are evacuated, given that t_e is the time where the last groups are evacuated, and the evacuation process starts when the time t in T equals 1. The set of hubs nodes $H = \{1, \dots, h_e\}$ is considered as marking points to identify the evacuees' location in time, given that h_e is the hub where the last group of evacuees reached their destination. The link (i, j) on a route is linked to the time t of evacuation and hub h through the tuple S given that $(i, j, t, h) \in S$.

6.2.1.1 Parameters and Sets:

K	The set of communities
R	The set of shortest routes from the source nodes to the terminal nodes
Q_k	The population of community k
D	The set of linear segments of the piecewise approximation to the BPR function
m^l	The slope of the linear segment $l \in L$ of the piecewise approximation
b^l	The intercept of the linear segment $l \in L$ of the piecewise approximation

u The maximum number of evacuees on any arc

μ The minimum number of evacuees to be evacuated in any group

ρ The time in minutes to travel from one hub to the next hub node in free-flow speed and the system clock

c_{ij} The time to travel from node *i* to node *j* on the link $(i, j) \in A$

C_r The time to travel on route *r* from source to destination in free-flow speed

6.2.1.2 Set of Variables:

x_{ijrh}^{kt} The number of evacuees on arc *(i, j)* on route *r* at hub *h* of community *k* evacuated at time *t*

x'_{ijh} The number of evacuees on arc *(i, j)* at hub *h*

f_r^{kt} The number of evacuees of community *k* on route *r* evacuated at time *t*

z_{ijrh}^{kt} Binary variable equals 1 if community *k* evacuated at time *t* is allowed to pass on arc *(i, j)* on route r at hub *h*

t_{ijh} The travel time on arc (*i, j*) at time *h* based on the piecewise approximated travel time function

τ_{ijh} The latency on arc *(i, j)* at hub *h* transferred to the group of evacuees that follows

$\hat{\tau}_{ijh}$ The slack latency on arc *(i, j)* at hub *h* not transferred to the group of evacuees that follows

τ'^{ktr}_{ijh} The latency on arc *(i, j)* at hub *h* equals to the latency added to slack latency if the group is evacuated, and zero otherwise

s_{ijh}^{ktr} Slack variable to remove the effect of latency of the group of evacuees from community *k* if they do not pass through the arc (*i, j*) at hub *h*

l_r^{kt} The latency of the group of evacuees on route *r* of a community *k* evacuated at time *t*

e_r^{kt} The travel time of community *k* on route *r* evacuated at time *t*

e'^{kt}_r The evacuation time of community *k* on route *r* evacuated at time *t*

E Network clearance time

d^{tv}_{rq} The positive difference of the route *r* of time *t* compared with the route *q* at time *v*

6.2.2 The Evacuation Model

$$Min\ NCT\ =\ E \tag{6-1}$$

subject to

$$x^{kt}_{ijr(h+1)} - x^{kt}_{jirh} = \begin{cases} f^{kt}_r\ if\ i\ \in N_S \\ -f^{kt}_r\ if\ i \in N_T\ ,if\ i\ \in N_H \\ 0, otherwise \end{cases} \quad \forall\, r \in R, (i,j) \in r, k \in K \quad t,h|(i,j,t,h) \in S \tag{6-2}$$

$$x^{kt}_{ijrh} - x^{kt}_{jirh} = 0, if\ i\ \notin N_H \quad \forall\, r \in R, (i,j) \in r, k \in K, \quad t,h|(i,j,t,h) \in S \tag{6-3}$$

$$\sum_{t\in T}\sum_{r\in R} f^{kt}_r = Q_k \quad \forall\, k\ \in K \tag{6-4}$$

$$x'_{ijh} = \sum_{r\in R}\sum_{k\in K}\sum_{t|(i,j,t,h)\in S} x^{kt}_{ijrh} \quad \forall\, (i,j) \in A, h \in H \tag{6-5}$$

$$\tau_{ijh} = c_{ij}t_{ijh} - \hat{\tau}_{ijh} \quad \forall\, (i,j) \in A, h \in H \tag{6-6}$$

$$\hat{\tau}_{ijh} \le c_{ij} \quad \forall\, (i,j) \in A, h \in H \tag{6-7}$$

$$\tau_{ijh} = 0 \quad \forall\, (i,j) \in A, h = 0 \tag{6-8}$$

$$t_{ijh} \ge m^d x'_{ijh} + b^d \quad \forall\, (i,j) \in A, h \in H, d \in D \tag{6-9}$$

$$\tau_{ijh} \ge \tau_{jlv} - \rho(1 + h - v)(1 - z^{kt}_{ijrh}) \quad \forall\, (i,j),(j,l) \in A, k \in K, \quad h,v \in H|h \ge v, r \in R, t \in T \quad (i,j,t,h) \in S \tag{6-10}$$

$$x^{kt}_{ijph} \le u\, z^{kt}_{ijrh} \quad \forall\, i \in N_S, (i,j) \in A, r \in R, \quad t,h|(i,j,t,h) \in S, k \in K \tag{6-11}$$

$$x^{kt}_{ijph} \ge \mu\, z^{kt}_{ijrh} \quad \forall\, i \in N_S, (i,j) \in A, r \in R, \quad t,h|(i,j,t,h) \in S, k \in K \tag{6-12}$$

$$l_r^{kt} = \sum_{(i,j)\in r} \sum_{h\in H} \tau'_{ijh} \qquad \forall\, t \in T, k \in K, r \in R_k \tag{6-13}$$

$$\tau'^{ktr}_{ijh} + s^{ktr}_{ijh} = \tau_{ijh} + \hat{\tau}_{ijh} \qquad \forall\, (i,j) \in A, h \in H, k \in K \tag{6-14}$$

$$\tau'_{ijh} \le M z^{kt}_{ijrh} \qquad \forall\, (i,j) \in A, k \in K, t, h|(i,j,t,h) \in S \tag{6-15}$$

$$s_{ijh} \le M(1 - z^{kt}_{ijrh}) \qquad \forall\, (i,j) \in A, k \in K, t, h|(i,j,t,h) \in S \tag{6-16}$$

$$e_p^{kt} = C_p z^{kt}_{ijph} + l_p^{kt} \qquad \forall i \in N_S, r \in R, (i,j) \in r, t, h|(i,j,t,h) \in S \tag{6-17}$$

$$e'^{kt}_r = \rho(t-1) z^{kt}_{ijrh} + C_r z^{kt}_{ijrh} + l_r^{kt} \qquad \forall i \in N_S, r \in R, (i,j) \in r, t, h|(i,j,t,h) \in S \tag{6-18}$$

$$e'^{kt}_r \le E \qquad \forall\, k \in K, r \in R, t \in T \tag{6-19}$$

$$x^{kt}_{ijrh}, x'_{ijh}, f_r^{kt}, \tau_{ijh}, \hat{\tau}_{ijh}, \tau'_{ijh}, s_{ijh}, l_r^{kt}, e_r^{kt}, e'^{kt}_r, E \ge 0 \qquad \forall\, (i,j) \in A, k \in K, r \in R, t \in T, h \in H, (i,j,t,h) \in S \tag{6-20}$$

$$z^{kt}_{ijh} \in \{0,1\} \qquad \forall\, (i,j) \in A, k \in K, r \in R, t, h|(i,j,t,h) \in S \tag{6-21}$$

Note that the flow conservation constraints (6-2) and (6-3) are slightly modified compared to the original flow conservation constraints. These constraints allow evacuees to follow one time path along the predefined route. Constraint (6-4) sums all evacuees evacuated at all times on all routes to equal the community population. Evacuees from different communities evacuated at different times from different routes meet on a road segment (i,j) at hub h in constraint (6-5). The latency τ_{ijh} is the travel time based on the volume of the evacuees subtracting their travel time in free-flow speed as seen in constraint (6-6). Note that $\hat{\tau}_{ijh}$ can be less than the free-flow speed in case that no evacuees pass to maintain the constraint feasibility as shown in constraint (6-7) given that the initial latency is 0, as seen in constraint (6-8). The travel time based on the volume is illustrated in constraint (6-9) since the travel time is a convex function. Constraint (6-10)

transfers the delay to the group of evacuees that follow to propagate the congestion to the upstream road segments. Constraints (6-11) and (6-12) use the binary variable z_{ijrh}^{kt} to whether it allows the evacuees from community *k* evacuated at time *t* to pass through the arc *(i, j)* on route r at hub *h* given that *u* is the capacity of the road segment and μ is the minimum number of evacuees in a group. The latency of group from community *k* evacuated at time *t* on route *r* is the sum of latencies along that route as seen in constraint (6-13). Since the routes overlap, Constraints (6-14), (6-15), (6-16) extracts the latencies from the network with the help of the indicator variable z_{ijrh}^{kt}. The travel time of a group is the travel time in free-flow speed in addition to the latency as seen in constraint (6-17), and the evacuation time is the waiting time since the beginning of the evacuation process in addition to the travel time as seen in constraint (6-18). The network clearance time *E* is the maximum evacuation time among all evacuated groups as shown in constraint (6-19). Finally, constraints (6-20) and (6-21) are the nonnegativity constraints.

6.2.3 Objective Functions

The objective of the model is to minimize NCT variable *E* where *E* is the total travel time of the last group arriving at the safe destination in addition to the waiting time since the beginning of the evacuation process, as seen in the objective (6-22).

$$Min\ NCT = E \tag{6-22}$$

The other objective used in the MMF allocation algorithm is minimizing the sum of the positive deviation (SPD), as seen in the objective (6-23). The objective is to minimize the positive difference between the evacuation time e'^{t}_{r} of the group evacuated on route *r* at time *t* and the preset threshold parameter θ to identify the improvable evacuation times. More details in section 6.3.

$$Min\ SPD = \sum_{r\in R}\sum_{t\in T} \omega_r^{kt} d_{krt}^{+} \tag{6-23}$$

subject to

$$e'^{kt}_r - \theta + d_{krt}^{-} - d_{krt}^{+} = 0 \qquad \forall k \in K, r \in R, t \in T \tag{6-24}$$

$$e'^{kt}_r \le \gamma_r^{kt} \qquad \forall k \in K, r \in R, t \in T \tag{6-25}$$

Constraints (6-2) - (6-21)

In addition, different objectives are experimented. The AET for each group of evacuees is incorporated in the model in the objectives (6-26). The sum of z_{ijrh}^{kt} at the source node $i \in N_S$ is the number of groups to be evacuated given that the minimum number of groups to be evacuated is one.

$$Min\ AET = \frac{\sum_{k\in K}\sum_{p\in P}\sum_{t\in T} e'^{kt}_r}{\sum_{k\in K}\sum_{r\in R}\sum_{(i,j)\in r}\sum_{t,h|(i,j,t,h)\in S} z_{ijrh}^{kt}} \tag{6-26}$$

6.3 Fairness in Evacuation

In this section, a new algorithm called *θ-progressive-filling* algorithm is introduced to find the optimal MMF evacuation time for the LBM model. This algorithm guarantees convergence and finds the optimal MMF evacuation time. The algorithm starts by setting initial values to the parameters $\omega_r^{kt}, \gamma_r^{kt}$, and θ for the road segment *r* and time of evacuation *t*. The parameter ω_r^{kt} equals 1 if the objective of minimizing the evacuation time considers the group evacuated on route r at time *t* in the minimization process, and it equals 0 otherwise. The parameter γ_r^{kt} is the upper bound of the evacuation time. The parameter θ is used as a threshold to identify the improvable evacuation times by minimizing the SPD, as illustrated in (6-23). In the first step, the evacuation time for all groups is considered by setting the parameter ω_r^{kt} to 1 for the groups

evacuated on all routes *r* and time of evacuation *t*. The upper bound parameter γ_r^{kt} of evacuation time is set to M, given that M is a sufficiently large number. The initial value of the threshold parameter θ is set to 0 since it has no effect on the first iteration of the algorithm. In step 2, the algorithm stops if all groups evacuation times are excluded from the objective to be minimized. Otherwise, the model is solved to minimize the evacuation time of the groups that are considered for improvement. In the first iteration, the evacuation time for all groups is considered in the objective. In step 3, an upper bound is set for the evacuation times considered in the objective by setting the evacuation time upper bound parameter γ_r^{kt} for the group evacuated on route *r* at time *t* equal to the minimum E, and setting the threshold parameter θ equal to $E - \varepsilon$ given that ε is a small value. In step 4, the model is solved again with the objective SPD, as seen in (6-23), to identify the groups of evacuees whose evacuation time can be improved by ε. If the evacuation time e'^t_r, in step 5, for the group evacuated on route *r* at time *t* is greater than or equal to the minimum *E* from step 2, it indicates that the evacuation time for that specific group of evacuees cannot be improved any further. Hence, its parameter ω_{rt} is set to 0 to be excluded from the minimization objective in step 2.

Table 6-1: *θ-progressive-filling* algorithm

Algorithm:	**Finds MMF resource allocation for general problems**
Step 1	Set $\omega_r^{kt} = 1$, $\gamma_r^{kt} = M$, and $\theta = 0 \ \forall r \in R, t \in T$
Step 2	If $\sum_{r\in R}\sum_{t\in T}\omega_r^{kt} = 0$, stop. Otherwise find the minimum E by solving the problem $P_{NCT}(\omega, \gamma, \theta)$
Step 3	If $\omega_r^{kt} = 1$, set $\gamma_r^{kt} = E$, and $\theta = E - \varepsilon \ \forall r \in R, t \in T$
Step 4	solve the problem $P_{\mathrm{SPD}}(\omega, \gamma, \theta)$
Step 5	if $e'^{kt}_r \geq E$, set $\omega_r^{kt} = 0 \ \forall r \in R, t \in T$
Step 6	Go to step 2

The computational time of the *θ-progressive-filling* algorithm is very similar to the water filling algorithm, if not faster. The water filling algorithm may encounter degeneracy since not all binding constraints are identified due to the unnecessary condition of the complementary slackness. Since this algorithm does not rely on complementary slackness in identifying the blocking constraints, it is capable of finding the optimal MMF resource allocation in convex or nonconvex structure problems, and it may require fewer iterations to reach the optimal MMF solution.

Fairness is measured using the SAD, as seen in the equation (6-27), to achieve an approximation to the MMF solution, as illustrated by Bin Obaid and Trafalis (2018).

$$SAD = \sum_{r,q \in R | r>q} \sum_{t,v \in T |\ t \geq v} \sum_{k,l \in K} \left| e'^{kt}_{r} - e'^{lv}_{q} \right| \tag{6-27}$$

Assuming that all evacuees are evacuated from one community, d_{rq}^{tv} is the positive difference in evacuation time between every pair of groups evacuated on different routes at various times. The SAD function (6-27) is converted to the linear constraints shown in (6-28) and (6-29).

$$SAD = \sum_{r,q \in R | r>q} \sum_{t,v \in T | t \geq v} d_{rq}^{tv} + d_{qr}^{vt} \tag{6-28}$$

$$e'^{t}_{r} - e'^{v}_{q} + d_{rq}^{tv} - d_{qr}^{vt} = 0 \qquad \forall r, q \in R, t, v \in T, \; r > q, t \geq v \tag{6-29}$$

6.4 Illustration and Experimentation

In this section, an example network is used to illustrate the model. In addition, a small real-world network is used for illustration and experimentation.

6.4.1 Illustrative Example

Consider the network used in chapter 5 with seven nodes and seven arcs as seen in Figure 6-1. Suppose that the population in the endangered zone in node S0 is to be evacuated to the safe zone in node T6 given that S0 is the source node and node T6 is the terminal node. All nodes are considered as hub nodes, and the travel time in free-flow speed from each pair of consecutive hub nodes is 60 minutes. The total travel time from node S0 to node T6 in free-flow speed is 240 minutes on either route. Due to the limited capacity of roads, evacuees spend more time in the network as a result of congestion.

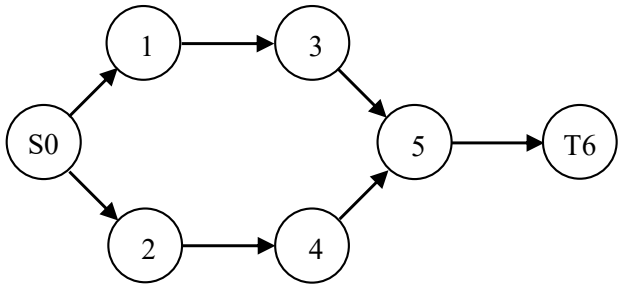

Figure 6-1 Small network with 7 nodes and 7 arcs

As shown in Table 6-2, the travel time is based on the traffic volume on any road segment. If the traffic volume is 0, the latency is 0 indicating that no evacuees are evacuated. This information is used to find the slope and intercept of each linear segment of the piecewise linear approximation of the BPR function. The lane capacity is set to 1750 vehicles/lane/hr., and each road segment in the network is assumed to consist of two lanes in each direction.

Table 6-2: Latency based on the traffic volume

Number of Vehicles	Latency (m)*60
0	0
2200	1
4350	60
4650	90
4900	120
5200	180

The MMF algorithm is tested on the example network in Figure 6-1 to find the MMF evacuation time. The output of the algorithm is illustrated in Table 6-3. Note that the groups of evacuees evacuated at the first time period are delayed by 11.97 minutes on either route, but not causing any delay to the groups following them until they reach the bottleneck road segment (5, 6). At the bottleneck, they are delayed by 180 minutes, transferring 120 minutes delay to the groups that follow. The groups evacuated at time 2 are delayed by 7.86 minutes until they are delayed by 120 minutes on the road segments (3, 5) and (4, 5) caused by the groups evacuated at time t additional to the 120 minutes delay on the bottleneck. The group of evacuees evacuated at time 3 are delayed by 7.86 minutes on (0, 1) and (0, 2) road segments, 120 minutes caused by the groups evacuated at time 1, and 60 minutes caused by the groups evacuated at time 2 in addition to the 120 minutes delay at the bottleneck.

Table 6-3: The results of the illustrative example network

Number of Evacuees (f)			**Latency (τ)** Slack Latency ($\hat{t}$)							**Obj. NCT (m)**
Time	Route1	Route2	(0, 1)	(0, 2)	(1, 3)	(2,4)	(3,5)	(4,5)	(5,6)	
1	2600	2600	0 11.97	0 11.97						667.86
2	2450	2450	0 7.86	0 7.86	0 11.97	0 11.97				
3	2450	2450	0 7.86	0 7.86	0 7.86	0 7.86	0 11.97	0 11.97		
					120 0	120 0	120 0	120 0	120 60	
							60 0	60 0	60 60	
									60 60	

The network in Figure 6-1 is tested using other objectives, as illustrated in Table 6-4. Note that the objective of minimizing the NCT achieves the minimum NCT of 667.86 minutes, but it distributes the evacuees randomly, resulting in a relatively high AET and SAD. The objective of minimizing the AET results in a higher NCT of 671.98 minutes and minimum AET of 517.09

minutes among all the tested objectives. Fixing the minimum NCT to its minimum, then minimizing the AET in the $\mathrm{AET_{NCT}}$ results in the worst SAD of 769.51 minutes among the tested objectives. Note that the evacuation time of the groups evacuated at time 1 in the MMF is higher compared with the AET_{NCT} objective. The reason for increasing the evacuation time of the groups evacuated at time 1 in MMF compared with $\mathrm{AET_{NCT}}$ is to decrease the evacuation time of the groups evacuated at time 2 from 563.95 to 555.72 minutes. In objective $\mathrm{AET_{ED}}$, the AET is minimized with an equal number of evacuees in each group to compare with the other objectives.

Table 6-4: The evacuation time for each group of evacuees of different objectives tested on the network of example 1 is illustrated in addition to the AET, SAD, and NCT for each objective

	Time	**Route**	**NCT**	**AET**	**$\mathrm{AET_{NCT}}$**	**MMF**	**$\mathrm{AET_{ED}}$**
Evacuation Time	1	**1**	363.00	404.16	404.16	455.93	407.69
		2	404.16	363.00	363.00	455.93	407.69
	2	**1**	585.91	509.44	563.95	555.72	538.46
		2	542.00	482.00	563.95	555.72	538.46
	3	**1**	667.86	671.98	667.87	667.86	669.23
		2	667.86	671.98	667.87	667.86	669.23
	AET		538.47	517.09	538.47	559.84	538.47
	SAD		793.09	699.42	769.51	523.81	653.84
	NCT		667.86	671.98	667.86	667.86	669.23

6.4.2 Experimentation

The model is tested on the Fort Worth Dallas network studied in the literature by Sbayti and Mahmassani (2006) and Murray-Tuite (2007). The network is composed of 179 nodes and 459 arcs. Some of the existing nodes are set as hub nodes, and artificial nodes are added as hub nodes, as seen in Figure 6-2. After adding the artificial nodes, the network consists of 195 nodes and 475 arcs. The population of the community is to be evacuated from the set of source nodes $N_S = \{108, 155, 178, 194\}$ to the set of terminal nodes $N_T = \{116, 117\}$ assuming the terminal

nodes do not have capacities. It is assumed that the population to be evacuated consists of 2,000 vehicles. The population is pushed to evacuate in 3 time units to simulate the high demand to evacuate, leading to higher congestion.

Table 6-5: Set of routes of the Fort Worth experiment network

r	Route	Travel Time (minutes)
0	108-107-106-105-104-103-102-101-100-190-116	6
1	108-107-106-105-104-103-98-116	4
2	155-99-176-96-151-97-89-4-22-2-116	4
3	155-99-152-146-145-140-91-90-6-26-25-21-116	4
4	155-153-147-141-92-8-7-85-84-83-82-81-116	6
5	178-177-93-10-9-86-72-71-70-69-68-67-130-81-116	7
6	178-177-93-10-9-86-72-73-74-75-76-77-78-79-117	8
7	178-177-93-10-9-40-11-43-46-13-50-15-56-57-17-61-117	7
8	194-154-95-149-94-12-11-43-44-45-49-180-55-58-62-117	5
9	110-195-111-112-192-113-114-173-115-117	5

The summary of the results and the computational time of different objectives are listed in Table 6-6. When minimizing the NCT, the resulting objective is 62.38 minutes. Minimizing the AET results in the minimum AET among all tested objectives, but it results in significantly higher NCT and SAD. Minimizing the AET subject to minimum NCT results in a similar output to the MMF. However, MMF results in the lowest fairness measure SAD of 3329.25 minutes among the tested objectives.

Table 6-6: Summary of the results when testing different objectives

Objective (Minimize)	**NCT**	**AET**	**SAD**	**CPU time (s)**
NCT	62.38	49.51	3475.41	0.47
AET	96.78	46.65	5577.94	1.55
AET_{NCT}	62.38	49.34	3389.22	1.37
MMF	62.38	49.33	3329.25	14.71

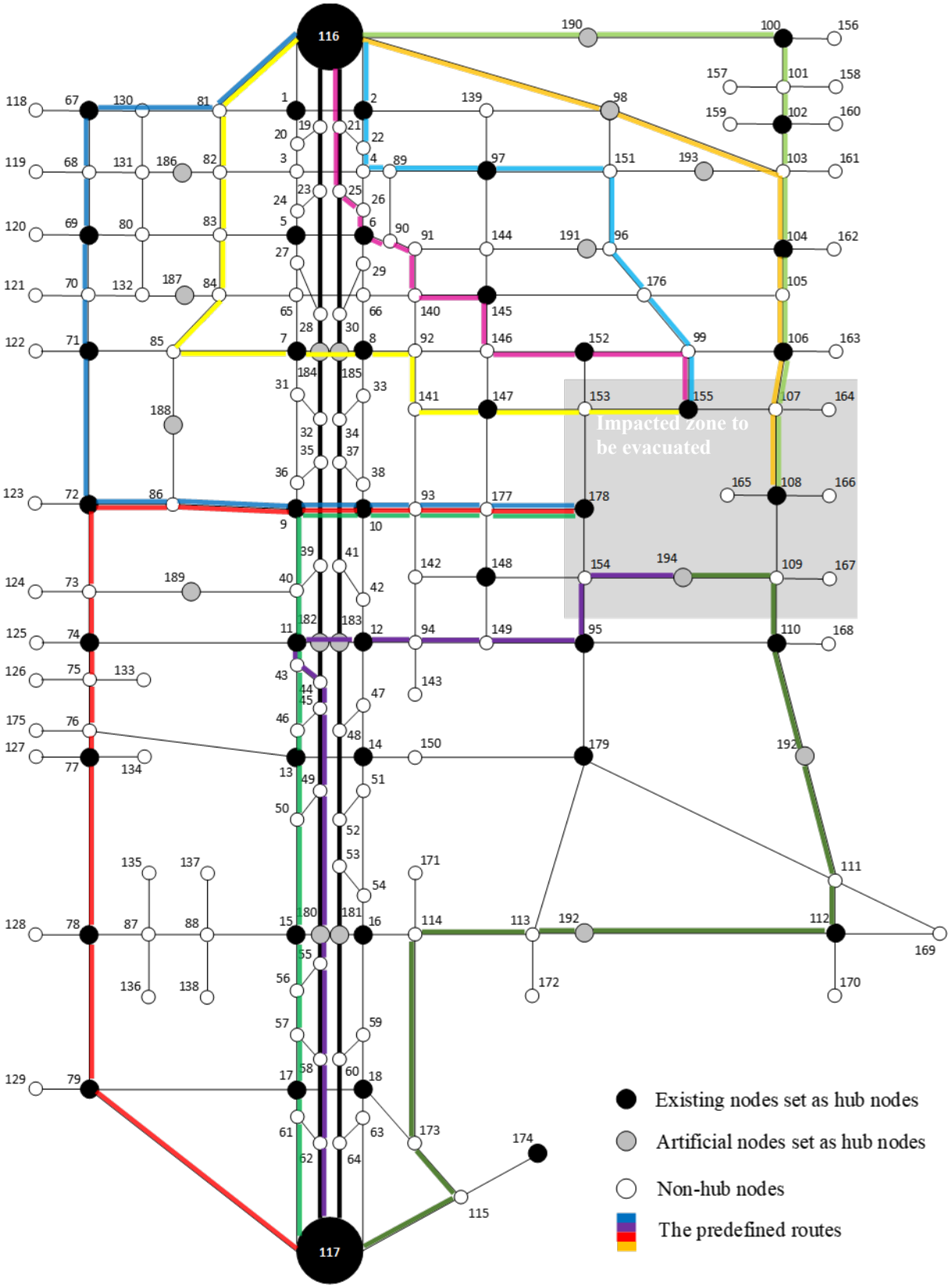

Figure 6-2: Fort Worth Experiment Network. The affected area is highlighted in grey.

The algorithm is tested on convex and non-convex structure problems for comparison purposes. For the convex problem, the number of groups of evacuees is fixed, assuming that the evacuees use all routes and all times of evacuation. The problem becomes LP as the binary variables are fixed to equal one. Hence, the computational complexity is reduced significantly. For the nonconvex problem, the problem is MILP, as there is no restriction on the binary variable. In this section, the difference between these problems is illustrated. The NCT behavior for the convex and nonconvex case when ranging the number of evacuees from 200 to 2,000 is illustrated in Figure 6-3. Note that the NCT is identical when the number of evacuees is greater than 1,000. The evacuation time is higher when the number of evacuees is less than 1,000 since that the evacuees are forced to evacuate later in time while they have enough space to evacuate earlier, or they are forced to travel on longer routes while the shorter routes are not congested.

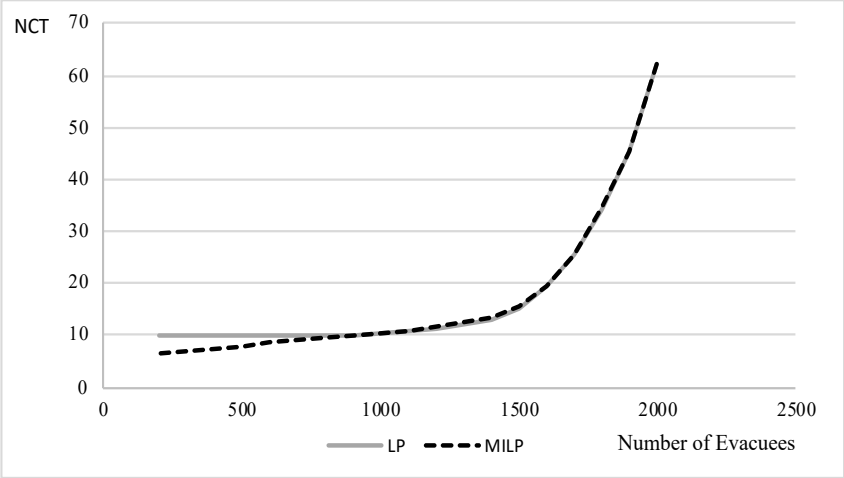

Figure 6-3: The NCT in minutes in Fort Worth for the range of number of evacuees from 200 to 2,000 for the LP and MILP

The AET behavior for the convex and nonconvex problems when ranging the number of evacuees from 200 to 2,000 is illustrated in Figure 6-4. Note that the AET of the convex case is almost identical to the nonconvex one as the number of evacuees increases. It indicates that the

evacuees are evacuated on all routes and all times of evacuation is ideal for higher demands to evacuate in emergency evacuations.

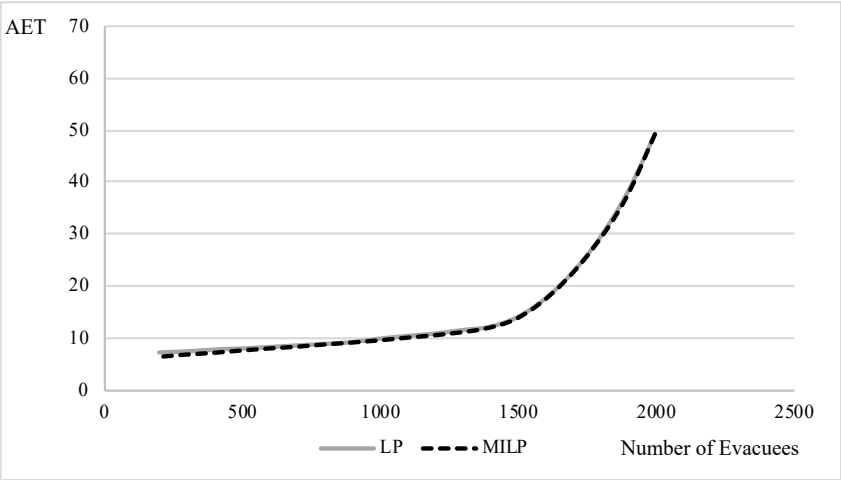

Figure 6-4: The AET in minutes in Fort Worth for the range of number of evacuees from 200 to 2,000 for the LP and MILP

The evacuation time for the convex and nonconvex structure problems for each group of evacuees is illustrated in Figure 6-5. The evacuation time is illustrated in Figure 6-5 is for the number of evacuees ranging from 200 to 2,000 evacuees. Darker lines indicate higher demand. Note that the evacuation time decreases as the number of evacuees decreases. In the convex problem, all routes are used in all times of evacuation. However, in the nonconvex problem, the number of routes decrease as the number of evacuees decreases. The number of groups is 30 when the number of evacuees is 2,000 while the number of groups is 7 when the number of evacuees is 200.

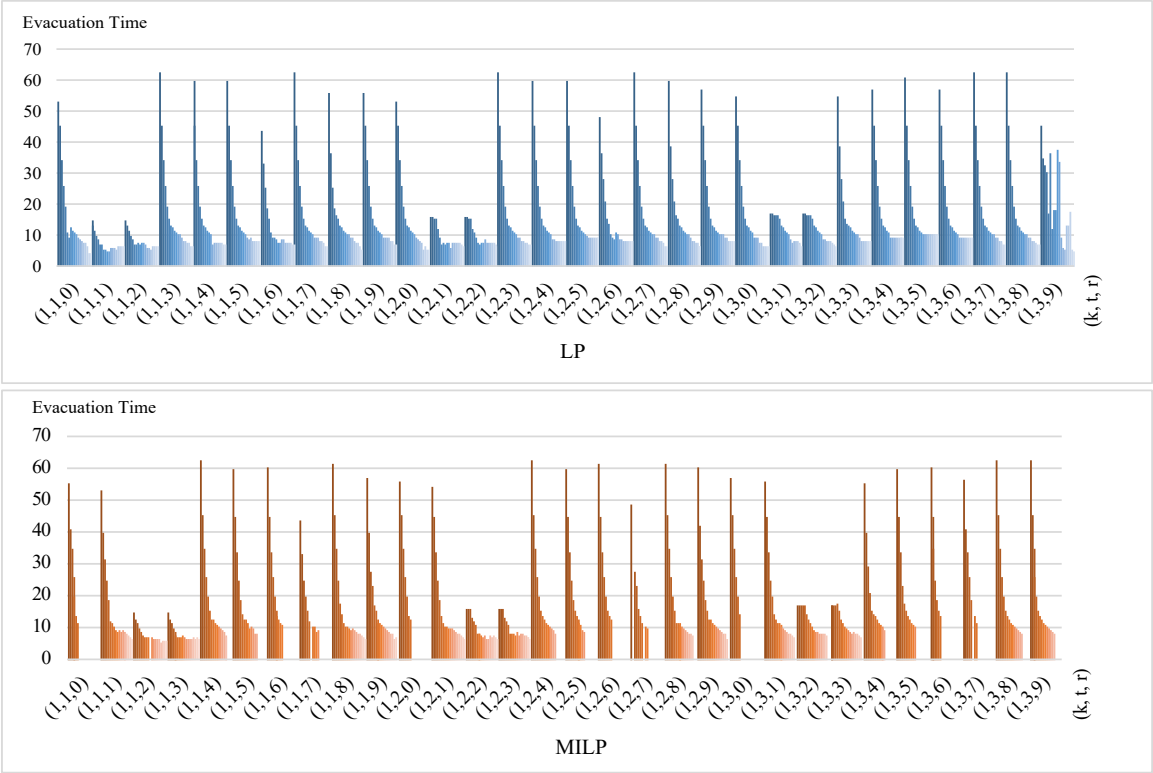

Figure 6-5: The evacuation time for the convex and nonconvex problems for each group of evacuees. Darker lines indicate higher demands

6.5 Computational Complexity

The model is tested on the Tampa City problem used for experimentation in chapter 5 using Gurobi Optimizer (2015), and the experiment was conducted on a PC with Intel quad-core 3.4 GH CPU and 32 GB memory. The model can solve small to medium size problems with a limited number of routes. However, the computational time can increase exponentially with the number of routes and evacuating times. Note that z_{ijrh}^{kt} is the binary variable indicates that community k evacuated at time t is allowed to pass on arc (i, j) on route r at hub h. The number of the binary variables z_{ijrh}^{kt} used in the model is decided by the number of routes $|R|$ used in the network and the planning time horizon. The number of the binary variables z_{ijrh}^{kt} is not affected by the number of hubs on the route r because when the group of evacuees is not allowed to enter the first hub, they will not be able to pass through the rest of the hubs along that route, and the

opposite is true. This conclusion leads us to the computational complexity of the model for multiple routes. The computational complexity of the model is $O(2^{|R|\cdot|T|})$ multiplied by the number of iterations in the θ-*progressive-filling* algorithm, given that $|R|$ is the number of routes of all communities, and $|T|$ is the number of evacuating times. The upper bound of the number of iterations in the θ-*progressive-filling* algorithm is the number of groups evacuated. The number of groups is $|T| \cdot |R|$, given that $|T|$ is the times of evacuation, and $|R|$ is the number of routes for all communities.

However, the computational complexity can be reduced from exponential to polynomial by assuming that all routes are used in all times of evacuations, as illustrated in section 5.3.2. This assumption is valid in the case of emergencies to utilize all routes since the high demand needs to be evacuated in a short time period.

Chapter 7: Robust Fair Latency-Based Evacuation Model Under Demand Uncertainty

7.1 Introduction

Evacuation modeling has been receiving tremendous attention due to the increasing number of natural and manmade disasters that require evacuation. Various modeling approaches and algorithms have been proposed over the past few decades to help allocate resources efficiently in the evacuation process and alleviate the impact of these disasters by reducing the risk of loss in lives and properties. Among the critical decisions is the routing of evacuees to reduce the congestion effect given the limited roads' capacity. However, the limited availability of data can lead to unreliable estimates of the number of evacuees and their demand rates. Using deterministic information, such as the expected demand, may not reflect the actual problem and produce invalid nominal solutions, or even infeasible solutions, as uncertainty is inherent in such problems. For example, the expected number of evacuees to evacuate Galveston and Harris counties in Hurricane Rita was 686,000, while an estimated 1.8 million evacuated (Lindell and Prater (2007)). Hence, there is a need to develop robust optimization models to consider the uncertainty in the evacuation problem.

This chapter presents a robust optimization approach using the LBM to help the decision-makers improve the evacuation process, given the uncertain nature of the evacuation problem. The tested model is the latency-based dynamic traffic assignment model (LB DTA), which is developed as an MILP model. In addition, the iterative θ-*progressive-filling* algorithm is tested to achieve a robust fair and efficient distribution of evacuees by finding the MMF evacuation times on the given set of used routes. The other objective tested is the average evacuation time (AET), which

finds the most efficient evacuation plan. The travel time on any road segment is a function of the number of evacuees. The function used is a modified version of the BPR function proposed in a recent study by Mtoi and Moses (2014), and the delay that takes place downstream the network is propagated to the road segments upstream the network.

This chapter is organized as follows. In the next section, the evacuation model is presented. The robust modeling approach is introduced in section 7.3. The experimentation is implemented in section 7.4, including the discussion. In section 7.5, the computational complexity is discussed.

7.2 Evacuation Model

In this section, the evacuation model is defined, including its parameters, in addition to the constraints and objective functions.

7.2.1 Model Definition

Given a graph G = (N, A) with a set of nodes N and a set of directed arcs A, where each arc $a \in A$ represents a road segment that connects two nodes $i, j \in N$ with a number of lanes $l \in L$ where $a = (i, j, l)$. The nodes of the network are composed of a set of source nodes $N_S \subset N$, and a set of terminal nodes $N_T \subset N$. The network is preprocessed by identifying a set of hub nodes $N_H \subset N$ given that $N_S \subset N_H$ and $N_T \subset N_H$, and the travel time in free-flow speed between each pair of consecutive hub nodes is constant and equal to the system clock. R is the set of routes in the networks from N_S to N_T, and R_k is the set of routes that community k can use where K is the set of communities in the network. $T = \{1, \dots, t_e\}$ is the set of clock times when evacuees are evacuated, given that t_e is the time where the last group of evacuees is evacuated, and $H = \{1, \dots, h_e\}$ is the set of clock times of evacuees while traveling in the network given that t_h is the time when the last group of evacuees reached the safe destination. The evacuation process starts

when the time *t* in T equals 1 given that evacuees can enter and exit any route through any hub node. The link (*i, j*) on a route is linked to the time *t* of evacuation and hub *h* through the tuple (i, j, t, h) that belong to S.

7.2.1.1 Parameters and Sets:

K	The set of communities
R	The set of shortest routes from the source nodes to the terminal nodes
L	The set of number of lanes
D	The set of linear segments of the piecewise approximation to the BPR function
m^{dl}	The slope of the linear segment *d* with number of lanes *l*
b^{dl}	The intercept of the linear segment *d* with number of lanes *l*
u^{l}	The maximum capacity of a road segment (vehicle/time unit) with number of lanes *l*
μ	The minimum number of evacuees to be evacuated in a group
ρ	The time in minutes to travel from one hub to the next hub node in free-flow speed and the system clock
c_{ij}	The percentage of time to reach the next hub node from node *i* to node *j* on the link $(i, j) \in A$
C_r	The time to travel on route *r* from source to destination in free-flow speed
Q_k	The population of community *k*

7.2.1.2 Set of Variables:

x_{ijrh}^{kt}	The number of evacuees on arc (*i, j)* on route *r* at time *h* of community *k* evacuated at time *t*.
x'_{ijh}	The number of evacuees on arc (*i, j)* at time *h*
f_r^{kt}	The number of evacuees of community *k* on route *r* evacuated at time *t* arriving at time *h*

z_{ijrh}^{kt} Binary variable equals 1 if community *k* evacuated at time *t* is allowed to pass on arc (*i, j)* on route r at time *h*

t_{ijh} The travel time on arc (*i, j*) at time *h* based on the piecewise approximated travel time function

τ_{ijh} The latency on arc (*i, j)* at time *h*

$\hat{\tau}_{ijh}$ The residual latency of the preceding group to remove the effect of latency on the following group

τ'^{ktr}_{ijh} The latency of the group evacuated from community *k* at time *t* on route *r* on arc (*i, j)* at hub *h*

s_{ijh}^{ktr} A slack variable to complement the latency of the group evacuated from community *k* at time *t* on route *r* on arc (*i, j)* at time *h*

l_r^{kt} The latency of a full route *r* of a community *k* evacuated at time *t*

e_r^{kt} The travel time of community *k* on route *r* evacuated at time *t*

e'^{kt}_r The evacuation time of community *k* on route *r* evacuated at time *t*

E Network clearance time

7.2.2 The Evacuation Model

$$Min\ NCT\ =\ E \tag{7-1}$$

subject to

$$x_{ijr(h+1)}^{kt} - x_{jirh}^{kt} = \begin{cases} f_r^{kt}\ if\ i\ \in N_S \\ -f_r^{kt}\ if\ i \in N_T\ \ ,if\ i\ \in N_H \\ 0, otherwise \end{cases} \qquad \forall\ r \in R, (i,j) \in r, k \in K,\ t, h|(i,j,t,h) \in S \tag{7-2}$$

$$x_{ijrh}^{kt} - x_{jirh}^{kt} = 0, if\ i\ \notin N_H \qquad \forall\ r \in R, (i,j) \in r, k \in K,\ t, h|(i,j,t,h) \in S \tag{7-3}$$

$$\sum_{t\in T}\sum_{r\in R} f_r^{kt} = Q_k \qquad \forall\ k\ \in K \tag{7-4}$$

$$x'_{ijh} = \sum_{r\in R}\sum_{k\in K}\sum_{t|(i,j,t,h)\in S} x_{ijrh}^{kt} \qquad \forall\,(i,j)\in A, h\in H \qquad (7\text{-}5)$$

$$\tau_{ijh} = c_{ij}t_{ijh} - \hat{\tau}_{ijh} \qquad \forall\,(i,j)\in A, h\in H \qquad (7\text{-}6)$$

$$\hat{\tau}_{ijh} \le c_{ij} \qquad \forall\,(i,j)\in A, h\in H \qquad (7\text{-}7)$$

$$\tau_{ijh} = 0 \qquad \forall\,(i,j)\in A, h = 0 \qquad (7\text{-}8)$$

$$t_{ijh} \ge m^{dl}x'_{ijh} + b^{dl} \qquad \forall\,(i,j,l)\in A, h\in H, d\in D \qquad (7\text{-}9)$$

$$\tau_{ijh} \ge \tau_{jlv} - \rho(1+h-v)(1-z_{ijrh}^{kt}) \qquad \forall\,(i,j),(j,l)\in A, k\in K, h,v\in H|h\ge v, r\in R, t\in T, (i,j,t,h)\in S \qquad (7\text{-}10)$$

$$x_{ijrh}^{kt} \le u^{l}z_{ijrh}^{kt} \qquad \forall\, i\in N_S, (i,j)\in A, r\in R, t,h|(i,j,t,h)\in S, k\in K \qquad (7\text{-}11)$$

$$x_{ijph}^{kt} \ge \mu\, z_{ijrh}^{kt} \qquad \forall\, i\in N_S, (i,j)\in A, r\in R, t,h|(i,j,t,h)\in S, k\in K \qquad (7\text{-}12)$$

$$l_r^{kt} = \sum_{(i,j)\in r}\sum_{h\in H}\tau'_{ijh} \qquad \forall\, t\in T, k\in K, r\in R_k \qquad (7\text{-}13)$$

$$\tau'^{ktr}_{ijh} + s_{ijh}^{ktr} = \tau_{ijh} + \hat{\tau}_{ijh} \qquad \forall\,(i,j)\in A, h\in H, k\in K \qquad (7\text{-}14)$$

$$\tau'_{ijh} \le Mz_{ijrh}^{kt} \qquad \forall\,(i,j)\in A, k\in K, t,h|(i,j,t,h)\in S \qquad (7\text{-}15)$$

$$s_{ijh} \le M(1-z_{ijrh}^{kt}) \qquad \forall\,(i,j)\in A, k\in K, t,h|(i,j,t,h)\in S \qquad (7\text{-}16)$$

$$e_p^{kt} = C_p z_{ijph}^{kt} + l_p^{kt} \qquad \forall i\in N_S, r\in R, (i,j)\in r, t,h|(i,j,t,h)\in S \qquad (7\text{-}17)$$

$$e'^{kt}_r = \rho(t-1)z_{ijrh}^{kt} + C_r z_{ijrh}^{kt} + l_r^{kt} \qquad \forall i\in N_S, r\in R, (i,j)\in r, t,h|(i,j,t,h)\in S \qquad (7\text{-}18)$$

$$e'^{kt}_r \le E \qquad \forall\, k\in K, r\in R, t\in T \qquad (7\text{-}19)$$

$$x_{ijrh}^{kt}, x'_{ijh}, f_r^{kt}, \tau_{ijh}, \hat{\tau}_{ijh}, \tau'_{ijh}, s_{ijh}, l_r^{kt}, e_r^{kt}, e'^{kt}_r, E \ge 0 \qquad \forall\,(i,j)\in A, k\in K, r\in R, t\in T, h\in H, (i,j,t,h)\in S \qquad (7\text{-}20)$$

$$z_{ijh}^{kt} \in \{0,1\} \qquad \forall (i,j) \in A, k \in K, r \in R, t, h | (i,j,t,h) \in S \tag{7-21}$$

The constraints (7-2) and (7-3) are the flow conservation constraints for *i* as a hub or non-hub node, respectively. These constraints allow evacuees to follow one time path along the predefined route. All evacuees evacuated at all times on all routes are summed to equal the community population in constraint (7-4). As seen in constraint (7-5), evacuees from different communities evacuated at different times from different routes meet on a road segment (i,j) at hub h. In constraint (7-6), the latency τ_{ijh} is the travel time based on the volume of the evacuees subtracting their travel time in free-flow speed. Note that, in constraint (7-7), $\hat{\tau}_{ijh}$ can be less than the free-flow speed in case that no evacuees pass to maintain the constraint feasibility, and the initial latency is 0, as shown in constraint (7-8). Since the travel time is a convex function, the travel time based on the volume and the number of lanes *l* is illustrated in the inequality constraint (7-9). The delay is transferred, in constraint (7-10), to the group of evacuees that follow to propagate the congestion to the upstream road segments. The binary variable z_{ijrh}^{kt} is used in Constraints (7-11) and (7-12) to either allow the evacuees from community *k* evacuated at time *t* to pass through the arc *(i, j)* on route r at hub *h* given that *u* is the capacity of the road segment and μ is the minimum number of evacuees in a group. In constraint (7-13), the latency of group from community *k* evacuated at time *t* on route *r* is the sum of latencies along that route. Since the routes overlap, the latencies are extracted from the network with the help of the indicator variable z_{ijrh}^{kt} in the set of constraints (7-14), (7-15), and (7-16). The travel time of a group is the travel time in free-flow speed in addition to the latency as seen in constraint (7-17), and the evacuation time is the waiting time since the beginning of the evacuation process in addition to the travel time as seen in constraint (7-18). The network clearance time *E* is the

maximum evacuation time among all evacuated groups as shown in constraint (7-19). Finally, constraints (7-20) and (7-21) are the nonnegativity constraints.

7.2.3 Objective Functions

The other objective experimented is the AET as shown in (7-22) where the number of evacuated groups is the sum of z_{ijph}^{kt} given that the minimum number of evacuated groups is one.

$$Min\ AET = \frac{\sum_{k\in K}\sum_{r\in R}\sum_{t\in T} e'^{kt}_{r}}{\sum_{k\in K}\sum_{r\in R}\sum_{(i,j)\in r}\sum_{t,h|(i,j,t,h)\in S} z_{ijrh}^{kt}} \tag{7-22}$$

Min-max fairness is achieved through the θ-*progressive-filling* algorithm illustrated in (6-1). The algorithm follows a similar approach to the *progressive-filling* algorithm. However, the θ-*progressive-filling* algorithm does not rely on the complementary slackness condition. Thus, it uses a threshold θ to identify the blocking evacuation times through the SPD as illustrated in the following model:

$$Min\ SPD = \sum_{r\in R}\sum_{t\in T} \omega_r^{kt} d_{rt}^{+} \tag{7-23}$$

subject to

$$e'^{t}_{r} - \theta + d_{rt}^{-} - d_{rt}^{+} = 0 \qquad \forall r \in R, t \in T \tag{7-24}$$

$$e'^{kt}_{r} \le \gamma_r^{kt} \qquad \forall k \in K, r \in R, t \in T \tag{7-25}$$

Constraints (7-2) - (7-21)

7.3 The Robust Counterpart of the Latency-Based Evacuation Model

The demand in most evacuation models is assumed to be deterministic. However, the demand in real case scenarios is uncertain, which can lead to an invalid evacuation plan. In this section, the model robustness is tested using a box uncertainty set. The assumption is that the demand is

higher than the anticipated demand to test the model adaptation to higher demands as seen in (7-26).

$$\sum_{t\in T}\sum_{r\in R} f_r^{kt} \geq Q_k \qquad \forall\, k \in K \qquad (7\text{-}26)$$

In box uncertainty set, the demand belongs to uncertain set with upper and lower bounds as shown in (7-27) and (7-28).

$$U_{Q_k} = \left[\hat{Q}_k(1-\theta_k), \hat{Q}_k(1+\theta_k)\right], \qquad \forall\, k \in K \qquad (7\text{-}27)$$

$$\sum_{t\in T}\sum_{r\in R} f_p^{kt} \geq Q_k, \quad Q_k \in U_{Q_k}, \qquad \forall\, k \in K \qquad (7\text{-}28)$$

where $\hat{Q}_k$ is the expected nominal value of Q_k. For a robust model, the demand is maximized to the point that the constraint is not violated, and the model is feasible as seen in (7-29).

$$\sum_{t\in T}\sum_{r\in R} f_r^{kt} \geq \max_{Q_k\in U_{Q_k}} Q_k \qquad \forall\, k \in K \qquad (7\text{-}29)$$

7.4 Experimentation and Discussion

The robustness of the model is tested in this section using a network similar to the Nguyen and Dupuis (1984) test network as shown in Figure 7-1. The network is composed of 13 nodes and 20 arcs. The evacuees are evacuated from the source nodes $N_s = \{1, 4\}$ to the terminal node $N_T = \{2\}$, and the total number of routes they can use is 24. The road capacity is 1800 vehicle/lane/hr. and 30 mile/hr. speed limit.

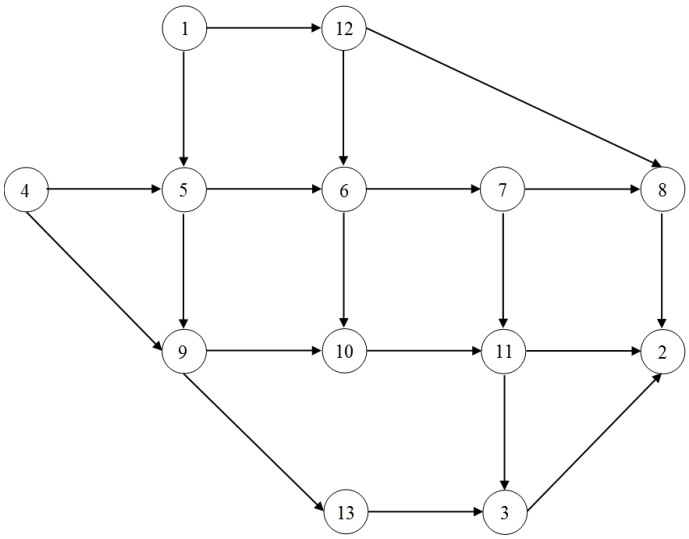

Figure 7-1: Nguyen and Dupuis experiment network

The network is preprocessed by adding hub nodes. After adding the hub nodes, the network consists of 55 nodes and 62 links, as illustrated in Figure 7-2. The source nodes in areas to be evacuated are $N_s = \{1, 12\}$, and the set of terminal nodes in the safe area is $N_T = \{11\}$. The system clock and the travel time in free-flow speed between each consecutive pair of hub nodes is 10 seconds.

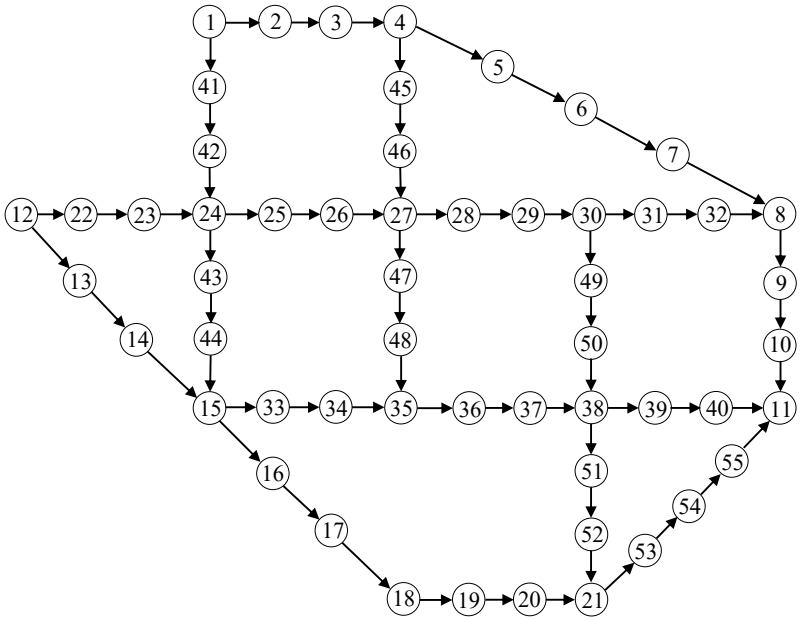

Figure 7-2: Nguyen and Dupuis experiment network after adding the hub nodes

The set of shortest routes that evacuees can use are illustrated in Table 7-1. Since the demand is assumed to be uncertain, the demand used in this model is within the set (7-27), and θ_k ranges between 0 and 0.3. The number of generated demands within the defined set is 100 using beta distribution $B(\hat{\alpha}, \hat{\beta})$ with its parameters $\hat{\alpha}$ and $\hat{\beta}$ set to 3 and 1, respectively. The beta distribution is the most suitable since it is a bounded distribution. One of the objectives of robust optimization is to maintain model feasibility. The model is guaranteed to be feasible when θ_k is less than or equal to 0.3.

Table 7-1: Set of routes of the Nguyen and Dupuis experiment network

r	**Route**	**Travel Time (seconds)**
0	1-2-3-4-5-6-7-8-9-10-11	120
1	1-2-3-4-45-46-27-28-29-30-31-32-8-9-10-11	170
2	1-2-3-4-45-46-27-28-29-30-49-50-38-39-40-11	170
3	1-2-3-4-45-46-27-47-48-35-36-37-38-39-40-11	170
4	1-41-42-24-25-26-27-28-29-30-31-32-8-9-10-11	170
5	1-41-42-24-25-26-27-28-29-30-49-50-38-39-40-11	170
6	1-41-42-24-25-26-27-47-48-35-36-37-38-39-40-11	170
7	1-41-42-24-43-44-15-33-34-35-36-37-38-39-40-11	170
8	1-41-42-24-43-44-15-16-17-18-19-20-21-53-54-55-11	180
9	12-22-23-24-25-26-27-28-29-30-31-32-8-9-10-11	170
10	12-22-23-24-25-26-27-28-29-30-49-50-38-39-40-11	170
11	12-22-23-24-25-26-27-47-48-35-36-37-38-39-40-11	170
12	12-22-23-24-43-44-15-33-34-35-36-37-38-39-40-11	170
13	12-13-14-15-33-34-35-36-37-38-39-40-11	140
14	12-13-14-15-33-34-35-36-37-38-51-52-21-53-54-55-11	180
15	12-13-14-15-16-17-18-19-20-21-53-54-55-11	150

In addition, the networks Tampa and Fort Worth networks are used to test the robustness model. The information of the networks tested is listed in Table 7-2, including the system unit in minutes, a number of scenarios for each uncertainty level, and the expected demand. The model is solved with two main objectives. The first objective is to find an efficient solution by minimizing the AET, and the other objective is to find the fair-efficient solution by finding the

MMF solution using the algorithm. It is important to mention that the system time unit of the Nguyen and Dupuis network is in seconds while the system time unit of the Tampa City and Fort Worth networks is in minutes.

Table 7-2: Network information and computational time in seconds

Network	Nodes	Links	Routes	System unit (m)	Scenarios	demand
Nguyen and Dupuis	55	62	16	1/6	100	127
Tampa City	26	33	9	30	1000	37000
Fort Worth	195	475	10	1	500	1540

7.4.1 Worst Case Analysis

The relative improvement of the robust model output from their corresponding deterministic model output under the worst-case scenario is investigated for the tested networks. The relative improvement is defined in equation (7-30), where the E_D^θ is the NCT of the deterministic model of MMF objective, and E_R^θ is the NCT of the robust model of the MMF objective.

$$RI(\theta) = \frac{(E_D^\theta - E_R^\theta)}{E_D^\theta} \tag{7-30}$$

The average relative improvement of the robust model output over the nominal model output is calculated against the θ ranging between 0 to 0.3 in intervals of 0.02 as seen in Table 7-3.

Table 7-3: The improvement of robust NCT relative to the nominal NCT

	Relative Improvement (%)		
$\boldsymbol{\theta}$	**Nguyen and Dupuis**	**Tampa City**	**Fort Worth**
0	0	0	0
0.02	0.83	0.6	2.69
0.04	1.43	1.23	7.74
0.06	2.4	2.02	13.97
0.08	3.16	2.82	15.52
0.1	4.34	3.67	16.49
0.12	5.2	4.49	18.73
0.14	6.4	5.46	21.22
0.16	7.64	6.45	22.96
0.18	10.36	7.37	25.61
0.2	14.45	8.79	26.22
0.22	22.26	10.1	29.46
0.24	26.93	11.86	30.7
0.26	32.79	13.55	33.24
0.28	42.83	15.85	35.05
0.3	50.18	19.81	38.67

The relative improvement is plotted against the given uncertainty levels. Note that the robust model output outperforms the deterministic model for all networks. The improvement in the Nguyen and Dupuis network is significant when the uncertainty level is higher than 0.2, as seen in Figure 7-3. The average relative improvement for Nguyen and Dupuis network is 15.4%, with a maximum improvement of 50.18% on the maximum given uncertainty level.

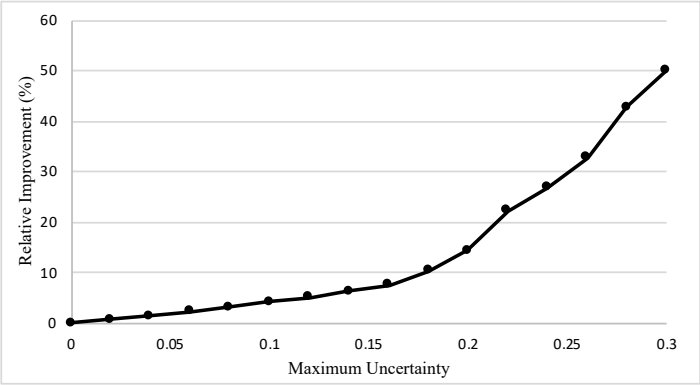

Figure 7-3: The relative improvement of the robust model output of Nguyen and Dupuis network

The relative improvement of the Tampa City network is plotted in Figure 7-4. The average improvement of the robust model output over its corresponding deterministic model is 7.6%, and the maximum improvement is 19.81% for the maximum given uncertainty set.

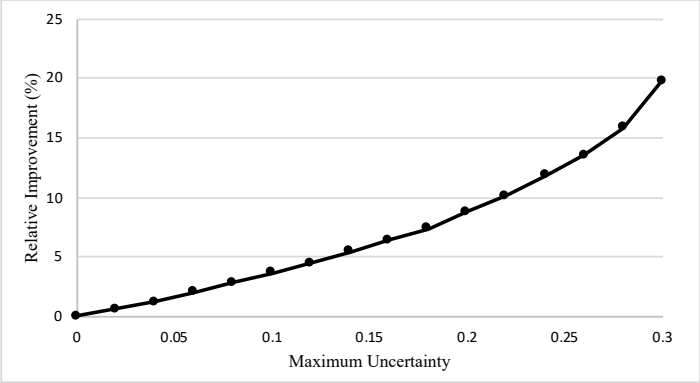

Figure 7-4: The relative improvement of the robust model output of Tampa City network

The relative improvement of the Fort Worth network is plotted against the given uncertainty set in Figure 7-5. The average relative improvement over the given uncertainty set is 22.55 %, while the maximum improvement is 38.67%. In all tested networks, the robust solution significantly improves the deterministic solution as the uncertainty level increases. Note that the relative improvement is non-monotone, similar to the observation by Yao et al. (2009). However, the robust model outperforms the deterministic model under the worst-case scenario.

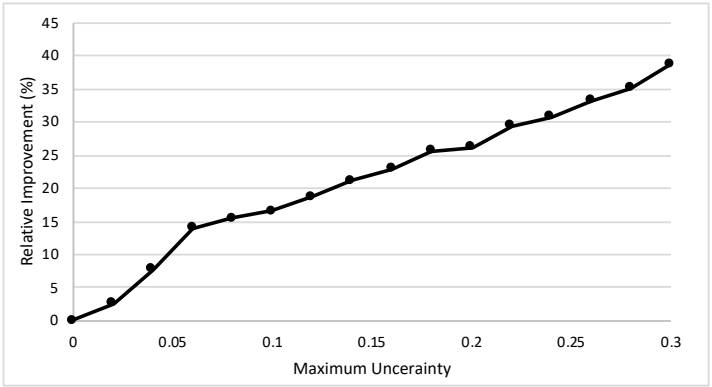

Figure 7-5: The relative improvement of the robust model output of Fort Worth network

7.4.2 Robustness of the MMF model

The robustness of the LBM model with MMF objective is tested and compared with the AET objective that finds the most efficient solution. The mean, standard deviation, and maximum NCT of the three networks found for the robust efficient evacuation (REE) model and the robust fair-efficient evacuation (RFEE) model is reported in Table 7-4. Notice that the mean NCT of RFEE is lower than the mean NCT of the REE in all networks and uncertainty levels. The standard deviation in RFEE is lower, and the maximum NCT in RFEE is lower in all given networks and uncertainty levels. We conclude that the NCT of the MMF model is more robust against uncertainties than the efficient model with the AET objective.

Table 7-4: The NCT mean, standard deviation, and maximum NCT for the three networks with different values of θ

		NCT					
Network	θ	**Mean**		**Standard deviation**		**Maximum**	
		REE	**RFEE**	**REE**	**RFEE**	**REE**	**RFEE**
Nguyen and Dupuis	0.1	261.66	231.28	14.38	7.94	275.35	242.09
	0.2	269.69	243.87	26.70	20.35	366.11	290.08
	0.3	370.95	314.93	126.50	94.79	753.80	588.86
Tampa City	0.1	357.82	259.29	11.39	7.4	381.9	296.8
	0.2	388.59	273.28	35.65	17.95	419.64	303.34
	0.3	395.02	296.24	40.11	38.18	419.88	379.91
Fort Worth	0.1	41.77	20.55	11.29	3.26	49.78	25.13
	0.2	51.20	26.57	16.94	7.51	72.55	38.83
	0.3	63.43	35.31	24.31	14.03	96.78	62.37

The next step is to find the mean, standard deviation, and maximum AET and SAD of the REE and RFEE, as illustrated in Table 7-5. The AET is located at the top of each cell while the SAD is located at the bottom of the cell. Note that the AET is slightly compromised to reduce the SAD

significantly. Up to 10 percent increase in the AET can result in up to 95 percent decrease in the SAD, leading to a fair-efficient solution with a slight compromise in the AET.

Table 7-5: The mean, standard deviation, and maximum AET and SAD for robust efficient evacuation and robust fair-efficient evacuation in all networks

		AET					
		SAD					
Network	θ	**Mean**		**Standard deviation**		**Maximum**	
		REE	**RFEE**	**REE**	**RFEE**	**REE**	**RFEE**
Nguyen and Dupuis	0.1	212.88	217.13	7.21	6.80	222.52	226.02
		14224.5	9830.72	1692.81	720.34	16183.5	10965.00
	0.2	222.54	226.46	16.44	15.89	250.63	254.34
		14264.8	11904.20	2550.92	2732.22	22952.6	19050.00
	0.3	249.69	254.81	34.91	36.03	327.18	333.96
		26303.10	23988.20	15011.60	16072.90	96852.30	70013.30
Tampa City	0.1	243.58	250.34	6.38	5.29	252.09	257.29
		4243.02	1189.64	117.52	242.41	4512.68	1568.94
	0.2	252.56	258.42	12.96	11.44	270.93	275.49
		4258.08	1713.06	230.76	659.36	4615.46	2865.3
	0.3	262.9	268.35	21.72	19.85	296.42	298.89
		4531.82	2675.46	611.31	1549.56	6068.45	5836.76
Fort Worth	0.1	17.16	18.54	2.26	2.63	20.42	22.20
		1880.60	731.27	593.33	183.22	2640.37	1001.22
	0.2	21.31	23.27	5.28	5.99	30.03	32.97
		2367.84	112.17	768.28	443.07	3320.64	1851.52
	0.3	27.64	30.09	10.12	10.99	46.65	49.33
		3200.05	1637.42	1394.37	846.44	5639.03	3342.32

The evacuation time and the number of evacuees in each group are plotted for all networks for different uncertainty levels. The number of evacuees for different uncertainty levels is plotted to help the decision-maker visualize the distribution of evacuees on different routes and times of evacuation.

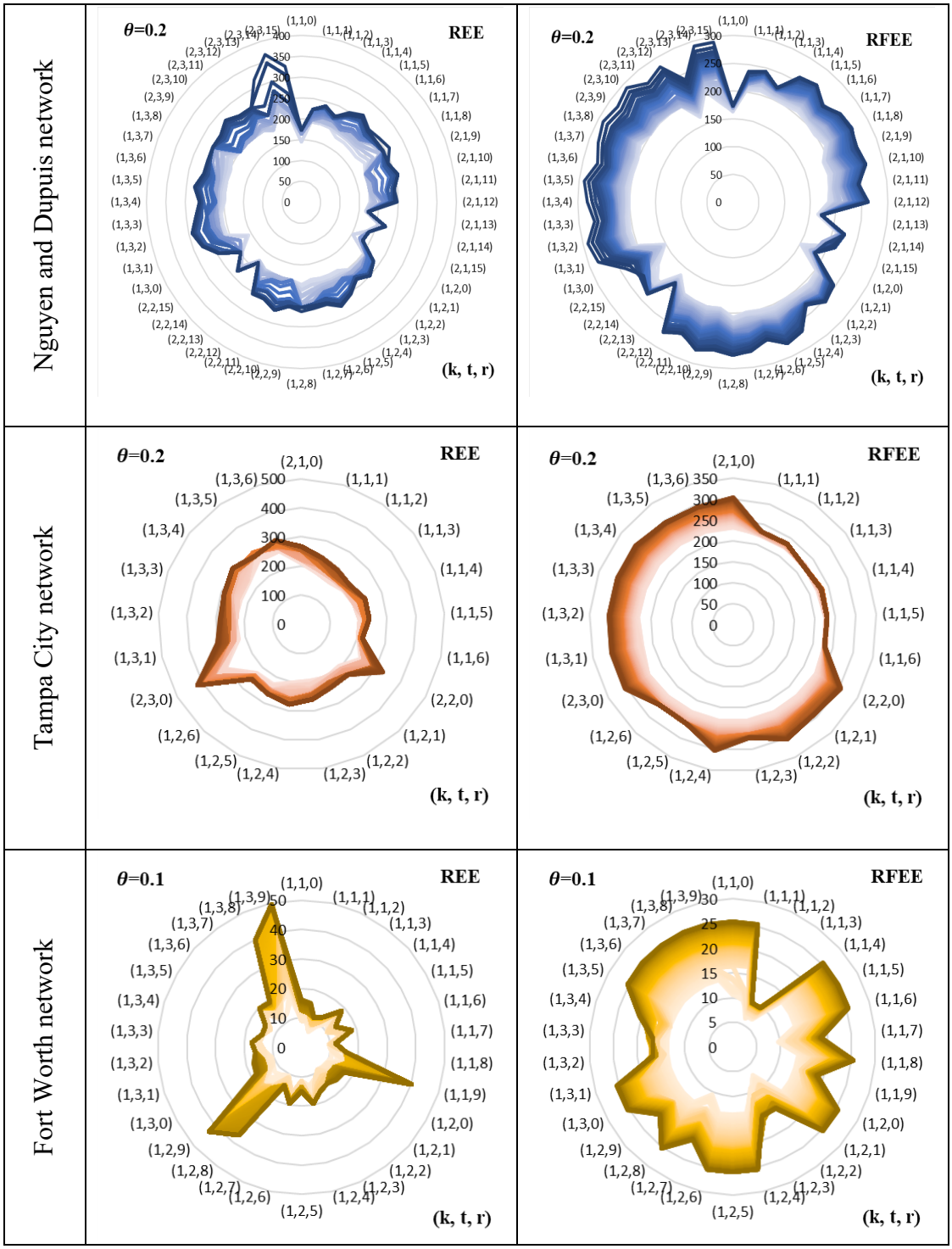

Figure 7-6: The evacuation time of the groups evacuated from community *k* at time *t* on route *r* of all networks for the robust efficient evacuation and robust fair-efficient evacuation

The evacuation time for each group of evacuees for Nguyen and Dupuis network when $\theta = 0.2$ is illustrated in Figure 7-6. Note that darker color indicates higher demand. The evacuation time of the group evacuated on route 14 at time 3 can be more than 350 minutes when the demand is high while other groups evacuation time is around 250 minutes in the REE. In the RFEE, the evacuation time is less than 300 minutes for all evacuees when the demand is high, and the uncertainty level is 0.2

The evacuation time for each group of evacuees for the Tampa City network when $\theta = 0.2$. The evacuation time for all groups is uniform for evacuees of RFEE, given that when the line is a perfect circle, the evacuation time for all groups of evacuees is equal. Note that in RFEE, the evacuation time for all groups of evacuees in different times of evacuation is equal when the demand is low, as illustrated in Figure 7-6.

The evacuation time of most groups in Fort Worth network for the REE is below 20 minutes at the cost of increasing the evacuation time of groups 8 and 9, which experience an evacuation time more than 40 minutes. On the other hand, the evacuation time for the evacuees on routes 2 and 3 in RFEE is minimized without affecting the rest of the groups' evacuation time, which is below 27 minutes.

The distribution of evacuees evacuated from community *k* at time *t* on route *r* is illustrated in Figure 7-7. Note that not all routes are fully utilized in Nguyen and Dupuis network, and the minimum is sent given than the darker color indicates higher demand. In the Tampa City network, the maximum number of evacuees in the REE is 4000 vehicles, while the maximum number of evacuees in RFEE is 3500 vehicles.

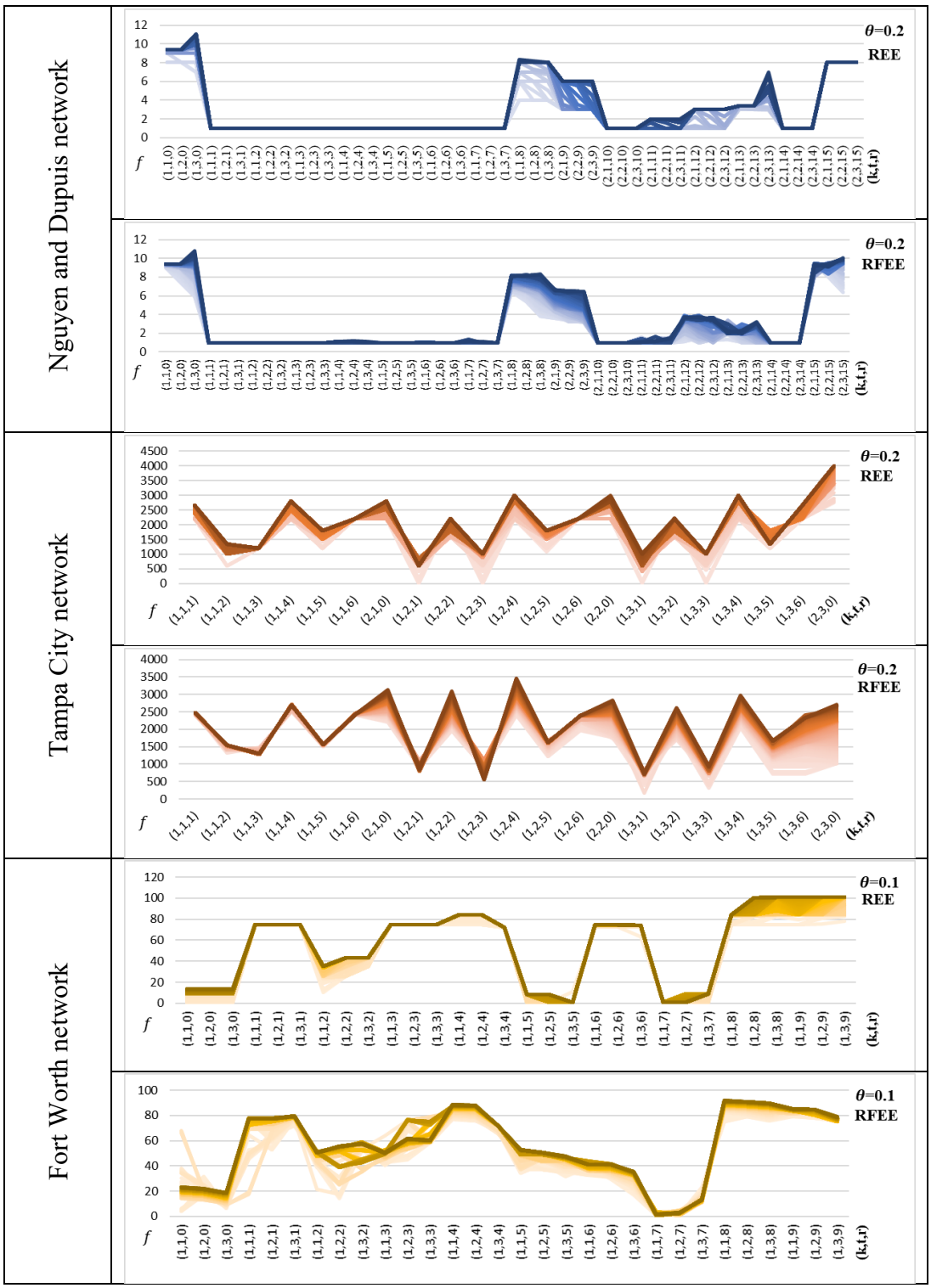

Figure 7-7: The number of evacuees f in the groups evacuated from community k at time t on route r of all networks for robust efficient evacuation and robust fair-efficient evacuation

7.4.3 Route Selection

The routes used for the Nguyen and Dupuis network is not fully utilized. The θ-progressive-filling algorithm can be used for route selection to identify the set of the optimal routes that can be used in the network. The set of optimal routes selected by the θ-progressive-filling algorithm is $R^* = \{0, 1, 6, 7, 8, 10, 12, 14\}$. The mean, standard deviation, and maximum of the NCT, AET, and SAD are reported in Table 7-6. Note that the NCT and AET have been significantly reduced when compared with Nguyen and Dupuis network with all routes.

Table 7-6: The mean, standard deviation, and maximum NCT, AET, and SAD for robust efficient evacuation and robust fair-efficient evacuation of Nguyen and Dupuis with optimal routes

Network	$\boldsymbol{\theta}$	Mean		Standard deviation		Maximum	
		REE	**RFEE**	**REE**	**RFEE**	**REE**	**RFEE**
NCT	0.1	225.58	215.93	4.12	6.49	229.83	224.74
	0.2	245.38	226.40	26.53	16.28	315.42	266.99
	0.3	333.98	295.34	112.24	92.71	584.69	560.29
AET	0.1	202.03	207.10	6.18	5.20	210.20	213.52
	0.2	210.18	214.38	14.13	12.59	236.71	239.36
	0.3	237.42	241.29	34.35	33.68	311.97	317.61
SAD	0.1	3397.53	1508.21	324.87	237.54	4005.11	1902.35
	0.2	3512.20	2077.00	430.68	719.86	5042.92	4109.36
	0.3	6499.84	5253.02	3721.40	4095.86	16612.2	16111.40

The evacuation time for each group evacuated from community *k* at time *t* on route *r* in Nguyen and Dupuis network with optimal routes is illustrated in Figure 7-8. Note that the evacuation time under the highest demand of the uncertainty level is more than 300 in REE and less than 270 in RFEE.

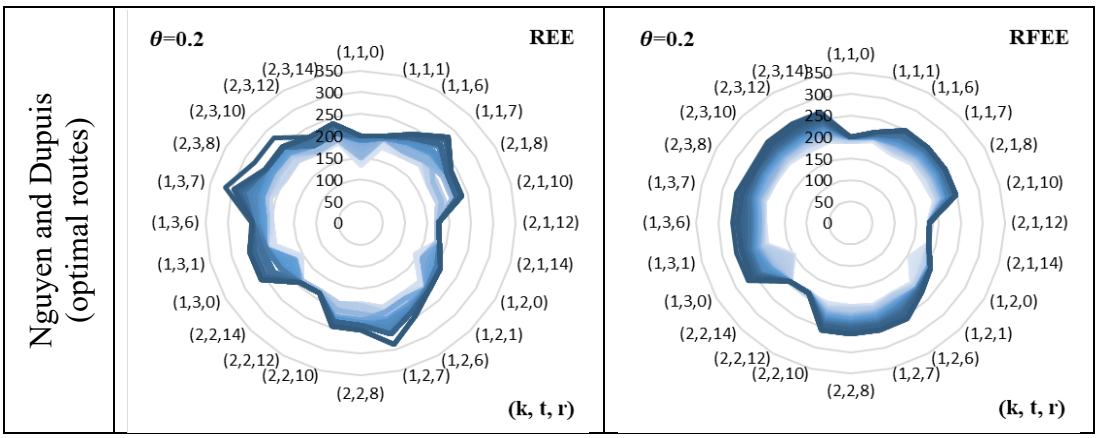

Figure 7-8: The evacuation time of all groups of evacuees evacuated on route r at time t of Nguyen and Dupuis network with optimal routes for REE and RFEE

The number of evacuees in each group evacuated from community *k* at time *t* on route *r* is illustrated in Figure 7-9 for Nguyen and Dupuis network with all routes. When compared with the original network, note that the routes are more utilized.

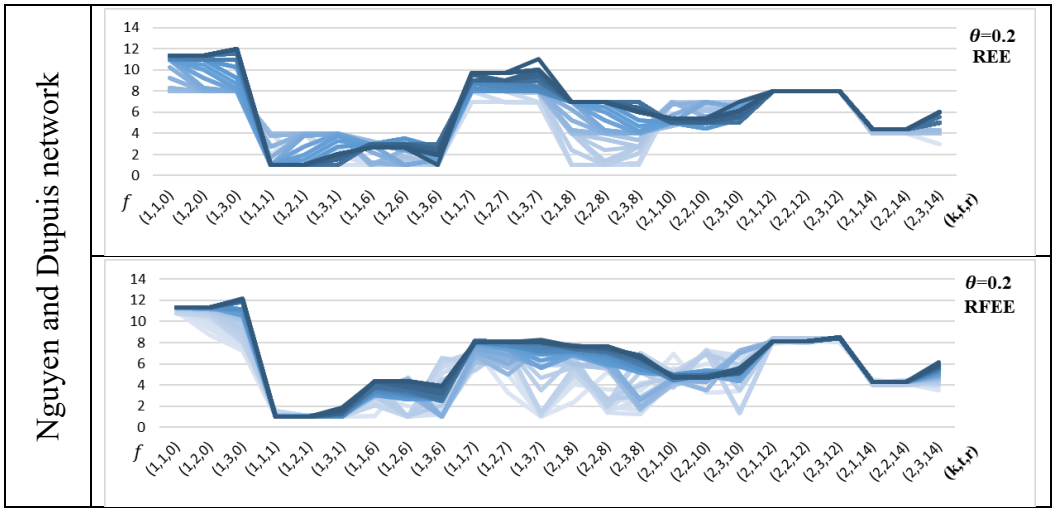

Figure 7-9: The number of evacuees evacuated at all time periods on all routes of Nguyen and Dupuis network for REE and RFEE

7.4.4 Uncontrolled Traffic Flow

The demand in the LBM is controlled by assigning evacuees on predefined routes and time of evacuation, as seen in constraint (4-4). This might not be the case. The evacuees, in reality, make their own decision on the departure time in the evacuation process. Hence, the model's only decision would be to allocate evacuees on routes. Constraint (4-4) now becomes (7-31).

$$\sum_{r \in R} f_r^{kt} = Q_{kt} \qquad \forall\, k \in K, t \in T \qquad (7\text{-}31)$$

The mean, standard deviation, and maximum of the NCT when the traffic flow is uncontrolled is reported in Table 7-7. Notice that, on average, the NCT is worsened by around 35 – 55% in both Nguyen and Dupuis networks when the traffic flow is uncontrolled. The difference in mean NCT between the controlled and uncontrolled is around 1 – 3% in the networks Tampa City and Fort Worth for REE, and the uncontrolled flow has lower NCT in some cases. The NCT of the networks Tampa City and Fort Worth of the uncontrolled flow is higher by around 5 – 30% than the controlled flow in the RFEE.

Table 7-7: The mean, standard deviation, and maximum NCT for REE and RFEE for all networks when the traffic flow is uncontrolled

		NCT					
Network	θ	**Mean**		**Standard deviation**		**Maximum**	
		REE	**RFEE**	**REE**	**RFEE**	**REE**	**RFEE**
Nguyen and Dupuis	0.1	377.82	312.57	48.46	22.31	418.96	351.52
	0.2	411.92	353.60	63.94	51.41	483.62	439.15
	0.3	501.79	425.33	161.32	128.86	754.45	703.98
Tampa City	0.1	353.42	273.39	12.51	4.96	359.50	282.28
	0.2	381.84	286.41	33.42	12.12	419.10	315.03
	0.3	399.44	331.63	31.14	38.77	419.83	409.20
Fort Worth	0.1	40.57	21.06	7.74	1.84	51.98	24.45
	0.2	50.03	30.33	8.75	5.09	72.32	39.52
	0.3	68.71	45.36	18.69	14.93	96.58	92.49
Nguyen and Dupuis (Optimal Routes)	0.1	349.99	289.79	32.67	22.46	378.37	327.95
	0.2	376.63	330.32	50.86	51.62	493.23	424.94
	0.3	459.84	400.96	142.64	124.59	724.61	653.88

The mean, standard deviation, and maximum AET and SAD is illustrated in Table 7-8. The AET of the uncontrolled flow worsened by around 6 – 10% for both Nguyen and Dupuis networks for REE and RFEE. The difference in AET between the controlled and uncontrolled flow for Tampa City and Fort Worth networks is around 0 – 3% given that the uncontrolled flow has lower AET in some cases. The increase in the mean SAD from the controlled to the uncontrolled flow can reach up to 1300% as seen in Fort Worth for RFEE and 0.2 uncertainty level.

Table 7-8: The mean, standard deviation, and maximum AET and SAD for REE and RFEE for all networks when the traffic flow is uncontrolled

		AET					
		SAD					
Network	θ	**Mean**		**Standard deviation**		**Maximum**	
		REE	**RFEE**	**REE**	**RFEE**	**REE**	**RFEE**
Nguyen and Dupuis	0.1	224.71	230.39	6.44	7.60	236.97	244.15
		30604.28	27229.05	6310.03	4362.09	38963.53	35127.06
	0.2	241.36	247.73	15.67	17.21	273.95	280.94
		35937.50	34073.82	8895.88	9750.96	52857.90	52452.43
	0.3	265.38	271.51	33.97	34.93	343.97	348.79
		46986.16	45892.15	21682.12	22403.97	98718.81	98569.14
Tampa City	0.1	244.28	251.10	3.58	3.30	252.12	258.08
		4274.08	2555.20	278.37	293.84	5260.76	3216.93
	0.2	253.69	259.37	7.47	6.47	270.94	274.50
		4535.94	2682.09	465.93	486.23	5957.74	4100.03
	0.3	264.70	269.16	12.59	11.35	296.90	298.63
		4936.77	3511.16	630.12	815.57	6427.89	5859.70
Fort Worth	0.1	16.61	17.97	1.19	1.43	19.25	20.97
		1614.74	839.24	335.08	161.03	2462.94	1351.87
	0.2	21.17	23.27	2.94	3.43	27.55	29.92
		2546.99	1546.19	477.06	434.85	3831.37	2833.18
	0.3	27.73	30.41	6.14	6.79	43.11	45.55
		3763.05	2619.76	1059.85	1038.15	6576.79	5639.74
Nguyen and Dupuis (optimal routes)	0.1	216.49	220.91	7.38	7.76	230.19	235.20
		7587.50	5966.55	1910.22	1131.11	10906.06	8413.98
	0.2	233.17	237.87	16.61	16.76	265.86	269.39
		9482.91	7424.27	2571.32	2422.99	13137.40	12746.43
	0.3	254.96	259.57	32.77	33.68	323.65	330.29
		11571.70	10122.74	4927.09	5098.16	22248.70	21416.76

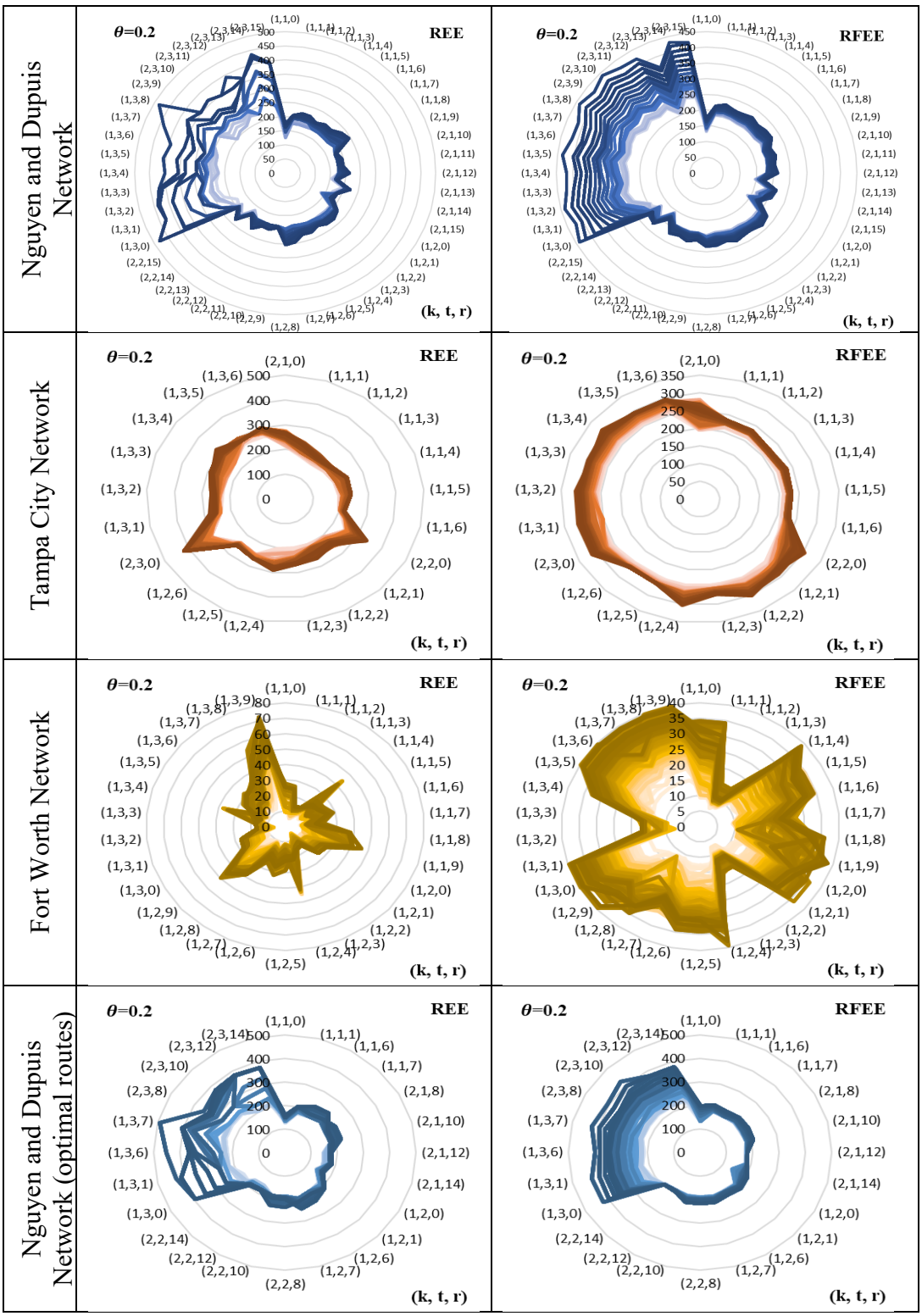

Figure 7-10: The evacuation time of the groups evacuated from community k at time t on route r of all networks for REE and RFEE when the traffic is uncontrolled

The evacuation time for all groups is in all networks is illustrated in Figure 7-10. Note that the evacuation time when the flow is uncontrolled is very similar to the evacuation time of the evacuees with controlled flow except for the Nguyen and Dupuis network. Since the travel time in free-flow speed in Nguyen and Dupuis network and the system unit is 10 seconds, the travel time is very sensitive to the change in the number of evacuees.

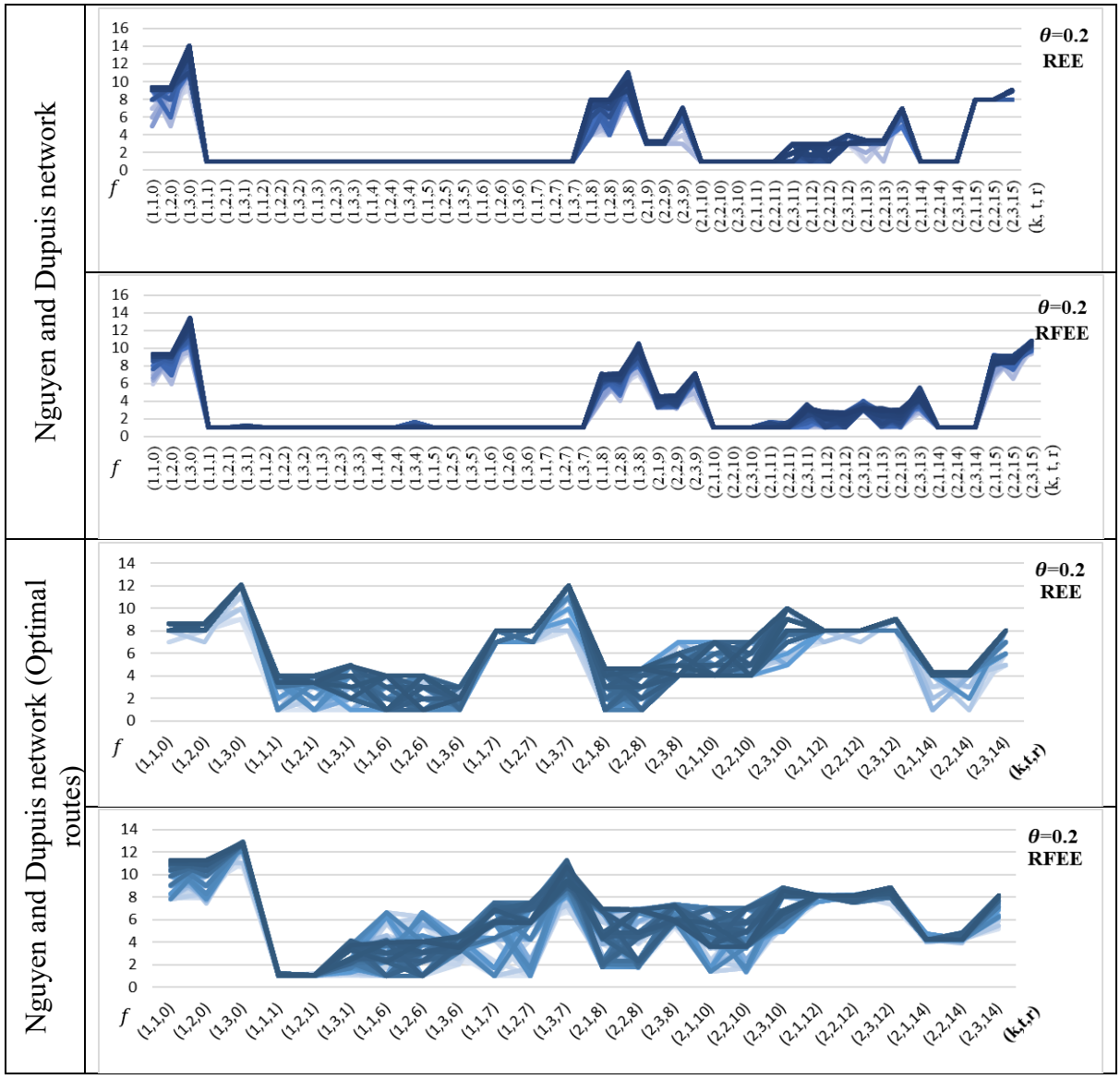

Figure 7-11: The number of evacuees f in the groups evacuated from community k at time t on route r of Nguyen and Dupuis network (regular and optimal routes) for REE and RFEE

The number of evacuees for the Nguyen and Dupuis network is illustrated in Figure 7-11, and the number of evacuees of the Tampa City and Fort Worth networks is illustrated in Figure 7-12. Although there are similarities in the number of evacuees for the controlled and uncontrolled flow, the controlled flow yields a more robust distribution of the evacuees on different demand levels.

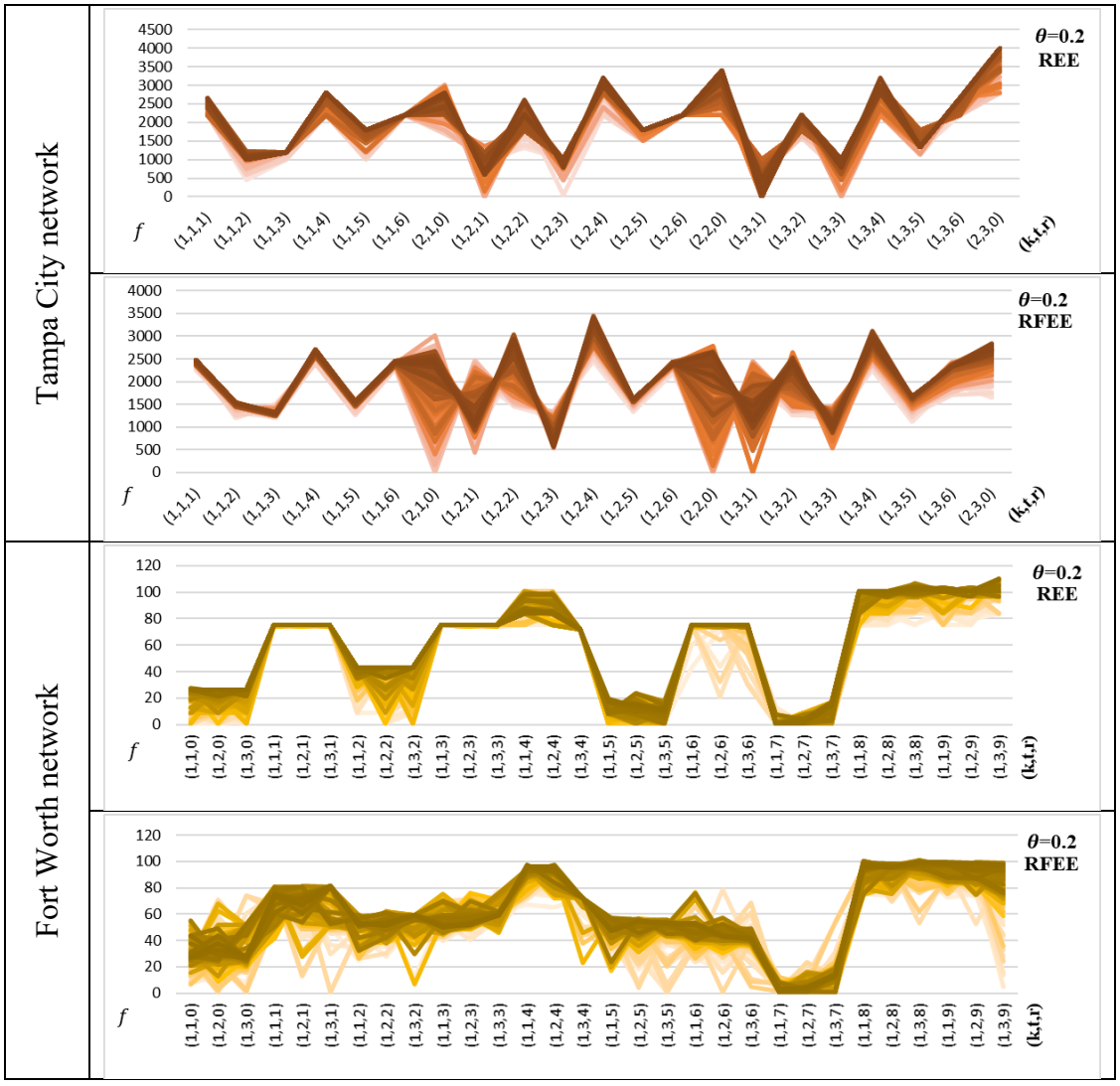

Figure 7-12: The number of evacuees f in the groups evacuated from community k at time t on route r of Tampa City and Fort Worth networks for REE and RFEE

7.5 Computational Complexity

The model is tested on Nguyen and Dupuis, Tampa City, and Fort Worth networks using Python and Gurobi Optimizer (2015). The experiment was conducted on a PC with Intel quad-core 3.4 GH CPU and 32 GB memory. The model is capable of solving large-size problems since it can be reduced to an LP model. Note that z_{ijrh}^{kt} is the only binary variable which indicates whether the group of evacuees from community *k* is allowed to evacuate on that specific link (*i, j*) at time *t* on route *r*. The number of variables z_{ijrh}^{kt} used in the model is decided by the number of routes $|P|$ used in the network and the number of evacuating times $|T|$. The z_{ijrh}^{kt} of all links on a specific route evacuated from community *k* at time *t* are equal because if a group is allowed to use one link on the route, they are allowed to use all the links along the route. Hence, the length of the route has no effect on the number of z_{ijrh}^{kt} variables. The assumption in this model is that all routes in all time periods are utilized, so z_{ijph}^{kt} has no effect on the complexity of the model. The computational complexity of the model is reduced from exponential to polynomial.

Chapter 8: Conclusion

This chapter sums up the dissertations by discussing the concluding remarks and future research.

8.1 Concluding Remarks

In this section, the contributions in this research are presented.

8.1.1 Approximation to MMF Using Multicriteria Optimization

A multicriteria optimization approach to find MMF bandwidth allocation approximation using goal programming is proposed. The resulting linear model was described as a bi-objective model where we maximize the flow as the first objective and minimize the difference among the commodities flow as the second objective. A small example from communication networks was used to illustrate the approach. The model is applied to real and random network topologies. Two approaches to select the ϵ value are proposed since the selection of the ϵ value is critical in utilizing the resource capacity of the network while putting fairness into consideration. The first approach to select ϵ value is to identify a clear elbow shape in the Pareto front, as illustrated in Figure 3-2. The second approach is to add utilization to the Pareto front to help to decide the ϵ value. The Pareto front and utilization plot can give a deep insight into the network structure, as seen in the experimentation section 3.4.1. France and Nobel-US are ideal examples of network topologies that do not have many shared links as opposed to the network topologies Net70 and Net26. Although the random networks' sources and terminals are selected in a way that commodities share links to reach their destinations, they are excellent examples of networks that have many shared links. In addition, the demand can be incorporated in the model, and the flow variable becomes a ratio indicating demand satisfaction if the variable is greater than or equal 1. Moreover, the model is more general since adjusting the ϵ is more subjective, depending on the

decision-maker selection. Finally, adding weight to the deviation decision variable can put more emphasis on selected commodity flows.

8.1.2 Evacuation Modeling

The LBM reports very detailed information about each group of evacuees, such as their departure time, travel time, evacuation time, the route used, latency, and the number of evacuees in each group. However, this information comes at a cost. The computational time increases exponentially with the size of the problem. The model has the ability to distribute evacuees on the available routes when setting different objectives. ATT and AET objectives result in a different distribution of evacuees on the available routes and departure times. Minimizing AET is ideal for emergency evacuation and ATT for non-emergencies. Minimizing the NCT distributes the evacuees on routes randomly as the main objective is to send the evacuees from the endangered zone to the safe destination in the shortest possible time. Since the model complexity increase with large-size networks, we develop a reduced model with lower complexity and exact results.

The evacuees in the LBM follow predefined routes. However, the time path they follow is based on their volume. The problem becomes UFP so the evacuees remain in one group to reflect their delay based on the travel time function and their location in time through the time path they follow based on their volume. The model complexity is reduced by reducing the time paths to one path, as illustrated in Figure 5-1. The model is tested on the Tampa City network and reported the exact output of the original LBM model. In addition, the output of the model is compared to the CTM output showing similar behavior, although their basic concept of the evacuees' movement is very different.

8.1.3 Fairness in Evacuation

The nonlinear BPR function is a travel time convex function of the traffic volume linearized through the piecewise approximation. Since the function is convex, the travel time of any traffic volume is found through the constraint (4-12). The multicriteria model is not suitable to find the approximate MMF travel time of the evacuees because it may overestimate the travel time of some groups for fairer evacuation and not reflect the actual travel time for each group. As a result, a new algorithm, we called it θ-*progressive-filling* algorithm, that finds the MMF for general problems is developed. The new algorithm does not rely on complementary slackness to identify saturated commodities. Hence, it is capable of finding the MMF resource allocation for problems with the nonconvex structure. The new algorithm is tested on the LBM model. Then the output is compared to other objectives such as NCT and AET.

8.1.4 Robustness of the LBM model

The model is tested on a variety of real and random networks with different sizes resulting in quality solutions and low computational time. To test the model robustness under demand uncertainty, a set-based approach is used, given that the demand belongs to a bounded set. The mean, standard deviation, and maximum NCT, AET, and SAD are reported to compare the REE and RFEE. Moreover, the evacuation time and the number of evacuees in each group are plotted to analyze the behavior of REE and RFEE. In reality, the evacuees select their departure time. Hence, the flow over time is not controlled, and the only decision the model makes is distributing the flow of evacuees on the predefined routes. We simulate the uncontrolled flow using beta distribution since it is suitable as bounded distribution, then compare the output with the controlled flow model output. We concluded that the results of the uncontrolled flow are very similar to the controlled flow results.

8.2 Future Research

In this section, a few recommendations and possible extensions of the research in this dissertation is presented.

8.2.1 Contraflow

The capacity of any road network is limited based on the number of lanes and the speed limit. One approach to expand the road capacity to accommodate more vehicles and reduce congestion is to implement the contraflow strategy. Contraflow lane is a road segment where the traffic flows in the opposite direction or a two directions road where all flow travels in one direction. This strategy is an effective method to double the road capacity at almost no cost. However, the drawback of contraflow is that emergency supplies such as medical and food supplies may not be able to reach the disaster location since that contraflow is implemented in the outbound direction. To allow supplies to reach the center of the disaster, partial contraflow can be implemented by allowing a few lanes to go inbound towards the disaster center.

8.2.2 Uncertainty in the Road Capacity

In mass evacuations, road capacities become highly uncertain due to the panic and need to evacuate. Accidents such as car crashes, building collapses, or medical conditions can add to the delay experienced because of congestion. These uncertainties can be incorporated in the model by modifying the deterministic travel time parameters, i.e., slope and intercept, to uncertain parameters.

8.2.3 Capacitated Terminals

In this dissertation, the assumption is that the terminal nodes are uncapacitated. However, some disasters require immediate shelter, such as hurricanes and tornados, which is usually

capacitated. If the assumption is that shelter is capacitated, the evacuation plan and the evacuees' distribution on routes become different. Also, the evacuees can be labeled based on their destination. Some evacuees prefer to seek shelters while others prefer to travel to a different city or state, so the latter is assigned to uncapacitated dummy terminals.

8.2.4 Evacuating Communities Based on the Threat Level

The threat level might be different from one area to another based on the disaster type. The threat level can be included in the fairness process to give the community with higher threat level the priority to evacuate. Giving higher priority to the communities with higher threat level can increase the number of evacuees who reach shelters safely. In future research, the communities will be given different priorities based on the threat level and find the percentage of evacuees who arrive at the shelter safely.

8.2.5 Following the Route Guidance System (RGS)

The assumption is this research is that all evacuees follow the directions from the RGS. However, in reality, evacuees may follow the routes they know and ignore the RGS directions. The model can tolerate a percentage of evacuees not following the RGS and still achieve the optimal solution. In future research, the model robustness will be tested when a percentage of evacuees do not follow the RGS.

References

Abdi, H. (2010). Coefficient of variation. *Encyclopedia of research design*, *1*, 169-171.

Amaldi, E., Coniglio, S., & Taccari, L. (2014, March). Maximum throughput network routing subject to fair flow allocation. In *International Symposium on Combinatorial Optimization* (pp. 1-12). Springer, Cham.

Anshelevich, E., & Ukkusuri, S. (2009, October). Equilibria in dynamic selfish routing. In *International Symposium on Algorithmic Game Theory* (pp. 171-182). Springer, Berlin, Heidelberg.

Bashllari, A., Nace, D., Gourdin, E., & Klopfenstein, O. (2007). The MMF rerouting computation problem. In *Proceedings of the 3rd International Network Optimization Conference (INOC 2007), Spa, Belgium*.

Bayram, V. (2016). Optimization models for large scale network evacuation planning and management: A literature review. *Surveys in Operations Research and Management Science*, *21*(2), 63-84.

Bayram, V., Tansel, B. Ç., & Yaman, H. (2015). Compromising system and user interests in shelter location and evacuation planning. *Transportation research part B: methodological*, *72*, 146-163.

Beheshtifar, S., & Alimoahmmadi, A. (2015). A multiobjective optimization approach for location-allocation of clinics. *International Transactions in Operational Research*, *22*(2), 313-328.

Ben-Tal, A., & Nemirovski, A. (1998). Robust convex optimization. Mathematics of operations research, 23(4), 769-805.

Ben-Tal, A., Do Chung, B., Mandala, S. R., & Yao, T. (2011). Robust optimization for emergency logistics planning: Risk mitigation in humanitarian relief supply chains. Transportation research part B: methodological, 45(8), 1177-1189.

Bertsekas, D., & Gallager, R. (1987). Data Networks, *Prentice-Hall*.

Bertsekas, D. P., Gallager, R. G., & Humblet, P. (1992). *Data networks* (Vol. 2). New Jersey: Prentice-Hall International.

Bertsimas, D., Farias, V. F., & Trichakis, N. (2011). The price of fairness. *Operations research*, *59*(1), 17-31.

Bertsimas, D., & Sim, M. (2004). The price of robustness. Operations research, 52(1), 35-53.

Bin-Obaid, H. S., & Trafalis, T. B. (2018, May). Fairness in Resource Allocation: Foundation and Applications. In *International Conference on Network Analysis* (pp. 3-18). Springer, Cham.

Bish, D. R., Sherali, H. D., & Hobeika, A. G. (2014). Optimal evacuation planning using staging and routing. *Journal of the Operational Research Society*, *65*(1), 124-140.

Boche, H., Wiczanowski, M., & Stanczak, S. (2007). Unifying view on min-max fairness, max-min fairness, and utility optimization in cellular networks. *EURASIP Journal on Wireless Communications and Networking*, *2007*(1), 034869.

Bonald, T., Massoulié, L., Proutiere, A., & Virtamo, J. (2006). A queueing analysis of max-min fairness, proportional fairness and balanced fairness. *Queueing systems*, *53*(1-2), 65-84.

Brams, S. J., & Taylor, A. D. (1996). Fair division: From cake-cutting to dispute resolution.

BUREAU, O. P. R. (1964). Traffic assignment manual. *US Department of Commerce*.

Buzna, Ľ., Kohání, M., & Janáček, J. (2014). An approximation algorithm for the facility location problem with lexicographic minimax objective. *Journal of Applied Mathematics*, *2014*.

Carey, M. (1986). A constraint qualification for a dynamic traffic assignment model. *Transportation Science*, *20*(1), 55-58.

Carey, M. (1992). Nonconvexity of the dynamic traffic assignment problem. *Transportation Research Part B: Methodological*, *26*(2), 127-133.

Carey, M., & McCartney, M. (2002). Behaviour of a whole-link travel time model used in dynamic traffic assignment. *Transportation Research Part B: Methodological*, *36*(1), 83-95.

Carey, M., & Subrahmanian, E. (2000). An approach to modelling time-varying flows on congested networks. *Transportation Research Part B: Methodological*, *34*(3), 157-183.

Carvalho, R., Buzna, L., Just, W., Helbing, D., & Arrowsmith, D. K. (2012). Fair sharing of resources in a supply network with constraints. *Physical Review E*, *85*(4), 046101.

Ceylan, H., & Bell, M. G. (2005). Genetic algorithm solution for the stochastic equilibrium transportation networks under congestion. *Transportation Research Part B: Methodological*, *39*(2), 169-185.

Charnes, A., & Cooper, W. W. (1961). Multicopy traffic network models. *Theory of traffic flow*, *85*, 85-96.

Chen, M. A. (2000). Individual monotonicity and the leximin solution. *Economic Theory*, *15*(2), 353-365.

Cohen, E., & Megiddo, N. (1994). Algorithms and complexity analysis for some flow problems. *Algorithmica*, *11*(3), 320-340.

Cong, Z., De Schutter, B., & Babuška, R. (2013). Ant colony routing algorithm for freeway networks. *Transportation Research Part C: Emerging Technologies*, *37*, 1-19.

Correa, J. R., Schulz, A. S., & Stier-Moses, N. E. (2007). Fast, fair, and efficient flows in networks. *Operations Research*, *55*(2), 215-225.

Correa, J. R., & Stier-Moses, N. E. (2011). Wardrop equilibria. *Encyclopedia of Operations Research and Management Science. Wiley*.

Daganzo, C. (1993). The cell transmission model Part I: a simple dynamic representation of highway traffic. *PATH Report, 93-0409*, *3*.

Daganzo, C. F. (1995). The cell transmission model, part II: network traffic. *Transportation Research Part B: Methodological*, *29*(2), 79-93.

Danna, E., Mandal, S., & Singh, A. (2012, March). A practical algorithm for balancing the max-min fairness and throughput objectives in traffic engineering. In *2012 Proceedings IEEE INFOCOM* (pp. 846-854). IEEE.

Di Gangi, M. (2011). Modeling evacuation of a transport system: application of a multimodal mesoscopic dynamic traffic assignment model. *IEEE Transactions on Intelligent Transportation Systems*, *12*(4), 1157-1166.

Do Chung, B., Yao, T., Xie, C., & Thorsen, A. (2011). Robust optimization model for a dynamic network design problem under demand uncertainty. Networks and Spatial Economics, 11(2), 371-389.

Do Chung, B., Yao, T., & Zhang, B. (2012). Dynamic traffic assignment under uncertainty: a distributional robust chance-constrained approach. *Networks and Spatial Economics*, *12*(1), 167-181.

Drissi-Kaïtouni, O., & Hameda-Benchekroun, A. (1992). A dynamic traffic assignment model and a solution algorithm. *Transportation Science*, *26*(2), 119-128.

Erkut, E., Karagiannidis, A., Perkoulidis, G., & Tjandra, S. A. (2008). A multicriteria facility location model for municipal solid waste management in North Greece. *European Journal of Operational Research*, *187*(3), 1402-1421.

Feitelson, D. G., & Rudolph, L. (1995, April). Parallel job scheduling: Issues and approaches. In *Workshop on Job Scheduling Strategies for Parallel Processing* (pp. 1-18). Springer, Berlin, Heidelberg.

Florian, M., Constantin, I., & Florian, D. (2009). A new look at projected gradient method for equilibrium assignment. *Transportation Research Record*, *2090*(1), 10-16.

Friesz, T. L., Bernstein, D., Smith, T. E., Tobin, R. L., & Wie, B. W. (1993). A variational inequality formulation of the dynamic network user equilibrium problem. *Operations research*, *41*(1), 179-191.

Gastwirth, J. L. (1972). The estimation of the Lorenz curve and Gini index. *The review of economics and statistics*, 306-316.

Gini, C. (1912). Variabilità e mutabilità. *Reprinted in Memorie di metodologica statistica (Ed. Pizetti E, Salvemini, T). Rome: Libreria Eredi Virgilio Veschi*.

Gini, C. (1914). Sulla misura della concentrazione e della variabilità dei caratteri. *Atti del Reale Istituto veneto di scienze, lettere ed arti*, *73*, 1203-1248.

Goldberg, J. B. (2004). Operations research models for the deployment of emergency services vehicles. *EMS management Journal*, *1*(1), 20-39.

Golovin, D. (2005). Max-min fair allocation of indivisible goods.

Google Maps. (2014). *Tampa City, Florida, USA*. Retrieved from https://www.google.com/maps/ @28.5315991,-82.5746581,8.92z

Gurobi Optimizer, 2015, http://www.gurobi.com.

Haurie, A., & Marcotte, P. (1985). On the relationship between Nash—Cournot and Wardrop equilibria. *Networks*, *15*(3), 295-308.

Hayrapetyan, A., Tardos, É., & Wexler, T. (2007). A network pricing game for selfish traffic. *Distributed Computing*, *19*(4), 255-266.

Hsu, C. C., Lin, K. C. J., Lai, Y. R., & Chou, C. F. (2010). On exploiting spatial-temporal uncertainty in max-min fairness in underwater sensor networks. *IEEE Communications Letters*, *14*(12), 1098-1100.

Hulme, D., & Mosley, P. (1996). *Finance against poverty: Effective institutions for lending to small farmers and microenterprises in developing countries*. London. Routledge, 1, 106.

Jahn, O., Möhring, R. H., Schulz, A. S., & Stier-Moses, N. E. (2005). System-optimal routing of traffic flows with user constraints in networks with congestion. *Operations research*, *53*(4), 600-616.

Jain, R., Durresi, A., & Babic, G. (1999). *Throughput fairness index: An explanation* (pp. 99-0045). Tech. rep., Department of CIS, The Ohio State University.

Janson, B. N. (1991). Dynamic traffic assignment for urban road networks. *Transportation Research Part B: Methodological*, *25*(2-3), 143-161.

Jayakrishnan, R., Tsai, W. K., & Chen, A. (1995). A dynamic traffic assignment model with traffic-flow relationships. Transportation Research Part C: Emerging Technologies, 3(1), 51-72.

Jonker, G. M., Meyer, J. J., & Dignum, F. P. M. (2005). Efficiency and fairness in air traffic control. In *Proceedings 7th Belgium-Netherlands Conference on Artificial Intelligence* (pp. 151-157). KVAB.

Kachroo, P., & Sastry, S. (2016). Traffic assignment using a density-based travel-time function for intelligent transportation systems. *IEEE Transactions on Intelligent Transportation Systems*, *17*(5), 1438-1447.

Kagaris, D., Pantziou, G. E., Tragoudas, S., & Zaroliagis, C. D. (1999). Transmissions in a network with capacities and delays. *Networks*, *33*(3), 167-174.

Kaufman, D. E., Nonis, J., & Smith, R. L. (1998). A mixed integer linear programming model for dynamic route guidance. *Transportation Research Part B: Methodological*, *32*(6), 431-440.

Kelly, F. (1997). Charging and rate control for elastic traffic. *European transactions on Telecommunications*, *8*(1), 33-37.

Kelly, F. P., Maulloo, A. K., & Tan, D. K. (1998). Rate control for communication networks: shadow prices, proportional fairness and stability. *Journal of the Operational Research society*, *49*(3), 237-252.

Kimms, A., & Maiwald, M. (2018). Bi-objective safe and resilient urban evacuation planning. *European Journal of Operational Research*, *269*(3), 1122-1136.

Kisko, T. M., & Francis, R. L. (1985). EVACNET+: a computer program to determine optimal building evacuation plans. *Fire Safety Journal*, *9*(2), 211-220.

LeBlanc, L. J., Morlok, E. K., & Pierskalla, W. P. (1975). An efficient approach to solving the road network equilibrium traffic assignment problem. *Transportation research*, *9*(5), 309-318.

Leclerc, P. D., McLay, L. A., & Mayorga, M. E. (2012). Modeling equity for allocating public resources. In *Community-based operations research* (pp. 97-118). Springer, New York, NY.

Li, J., Fujiwara, O., & Kawakami, S. (2000). A reactive dynamic user equilibrium model in network with queues. *Transportation Research Part B: Methodological*, *34*(8), 605-624.

Lighthill, M. J., & Whitham, G. B. (1955a). On kinematic waves I. Flood movement in long rivers. *Proceedings of the Royal Society of London. Series A. Mathematical and Physical Sciences*, *229*(1178), 281-316.

Lighthill, M. J., & Whitham, G. B. (1955b). On kinematic waves II. A theory of traffic flow on long crowded roads. *Proc. R. Soc. Lond. A*, *229*(1178), 317-345.

Lim, G. J., Rungta, M., & Baharnemati, M. R. (2015). Reliability analysis of evacuation routes under capacity uncertainty of road links. *Iie Transactions*, *47*(1), 50-63.

Lim, G. J., Rungta, M., & Davishan, A. (2019). A robust chance constraint programming approach for evacuation planning under uncertain demand distribution. *IISE Transactions*, *51*(6), 589-604.

Lindell, M. K., & Prater, C. S. (2007). Critical behavioral assumptions in evacuation time estimate analysis for private vehicles: Examples from hurricane research and planning. *Journal of Urban Planning and Development*, *133*(1), 18-29.

Litman, T. (2006). Lessons from Katrina and Rita: What major disasters can teach transportation planners. *Journal of transportation engineering*, *132*(1), 11-18. Lujak, M., Giordani, S., & Ossowski, S. (2015). Route guidance: Bridging system and user optimization in traffic assignment. *Neurocomputing*, *151*, 449-460.

Mahajan, R., Floyd, S., & Wetherall, D. (2001, November). Controlling high-bandwidth flows at the congested router. In *Network Protocols, 2001. Ninth International Conference on*(pp. 192-201). IEEE.

Mahmassani, H. S. (2001). Dynamic network traffic assignment and simulation methodology for advanced system management applications. Networks and spatial economics, 1(3-4), 267-292.

Margulis, L., Charosky, P., Fernandez, J., & Centeno, M. A. (2006, June). Hurricane evacuation decision-support model for bus dispatch. In *Fourth LACCEI International Latin American and Caribbean Conference for Engineering and Technology (LACCET '2006),"Breaking Frontiers and Barriers in Engineering: Education, Research, and Practice* (pp. 21-23).Mas-Colell, A. (1995). Microeconomic theory/Andreu Mas-Colell, Michael D. Whinston and Jerry R. Green.

Max, R. (2016). Natural catastrophes. *Our World in Data*.

Megiddo, N. (1974). Optimal flows in networks with multiple sources and sinks. *Mathematical Programming*, *7*(1), 97-107.

Merchant, D. K., & Nemhauser, G. L. (1978a). A model and an algorithm for the dynamic traffic assignment problems. *Transportation science*, *12*(3), 183-199.

Merchant, D. K., & Nemhauser, G. L. (1978b). Optimality conditions for a dynamic traffic assignment model. *Transportation Science*, *12*(3), 200-207.

Mitradjieva, M., & Lindberg, P. O. (2013). The stiff is moving—conjugate direction Frank-Wolfe Methods with applications to traffic assignment. *Transportation Science*, *47*(2), 280-293.

Mo, J., & Walrand, J. (2000). Fair end-to-end window-based congestion control. *IEEE/ACM Transactions on networking*, *8*(5), 556-567.

Mtoi, E. T., & Moses, R. (2014). Calibration and evaluation of link congestion functions. *Journal of Transportation Technologies*, *4*(2).

Murray-Tuite, P. (2007). Perspectives for network management in response to unplanned disruptions. *Journal of urban planning and development*, *133*(1), 9-17.

Nace, D., Doan, L. N., Klopfenstein, O., & Bashllari, A. (2008). Max–min fairness in multi-commodity flows. *Computers & Operations Research*, *35*(2), 557-573.

Nace, D., & Pióro, M. (2008). Max-min fairness and its applications to routing and load-balancing in communication networks: a tutorial. *IEEE Communications Surveys & Tutorials*, *10*(4), 5-17.

Nash, J. (1951). Non-cooperative games. *Annals of mathematics*, 286-295.

Ng, M., & Waller, S. T. (2010). Reliable evacuation planning via demand inflation and supply deflation. *Transportation Research Part E: Logistics and Transportation Review*, *46*(6), 1086-1094.

Nguyen, S., & Dupuis, C. (1984). An efficient method for computing traffic equilibria in networks with asymmetric transportation costs. *Transportation Science*, *18*(2), 185-202.

Nie, X., & Zhang, H. M. (2005). A comparative study of some macroscopic link models used in dynamic traffic assignment. *Networks and Spatial Economics*, *5*(1), 89-115.

Nie, Y. M. (2011). A cell-based Merchant–Nemhauser model for the system optimum dynamic traffic assignment problem. *Transportation Research Part B: Methodological*, *45*(2), 329-342.

Nikolova, E., & Stier-Moses, N. E. (2011, October). Stochastic selfish routing. In *International Symposium on Algorithmic Game Theory* (pp. 314-325). Springer, Berlin, Heidelberg.

Obaid, H. B., & Trafalis, T. B. (2016, May). Linear Max-Min Fairness in Multi-commodity Flow Networks. In *International Conference on Network Analysis* (pp. 3-10). Springer, Cham.

Obaid, H. S. B., & Trafalis, T. B. (2018). An approximation to max min fairness in multi commodity networks. *Computational Management Science*, 1-13.

Orlowski, S., Wessäly, R., Pióro, M., & Tomaszewski, A. (2010). SNDlib 1.0—Survivable network design library. *Networks: An International Journal*, *55*(3), 276-286.

Parisi, D. R., & Dorso, C. O. (2005). Microscopic dynamics of pedestrian evacuation. *Physica A: Statistical Mechanics and its Applications*, *354*, 606-618.

Pan, D., & Yang, Y. (2007, March). Max-min fair bandwidth allocation algorithms for packet switches. In *2007 IEEE International Parallel and Distributed Processing Symposium*(p. 52). IEEE.

Radunović, B., & Boudec, J. Y. L. (2007). A unified framework for max-min and min-max fairness with applications. *IEEE/ACM Transactions on Networking (TON)*, *15*(5), 1073-1083.

Rawls, J. (1971). *A theory of justice*. Harvard university press.

Re, M. (2018). NatCatSERVICE Natural catastrophes in 2017. *Munich: Münchener Rückversicherungs-Gesellschaft, Geo Risks Research*.

Ren, G., Huang, Z., Cheng, Y., Zhao, X., & Zhang, Y. (2013). An integrated model for evacuation routing and traffic signal optimization with background demand uncertainty. Journal of advanced transportation, 47(1), 4-27.

Rétvári, G., Bíró, J. J., & Cinkler, T. (2007, May). Fairness in capacitated networks: A polyhedral approach. In *IEEE INFOCOM 2007-26th IEEE International Conference on Computer Communications* (pp. 1604-1612). IEEE.

Rhodes, D. L. (2016). Efficient multistate route computation. *IEEE Transactions on Network Science and Engineering*, *3*(3), 171-182.

Richards, P. I. (1956). Shock waves on the highway. *Operations research*, *4*(1), 42-51.

Rosen, J. B. (1960). The gradient projection method for nonlinear programming. Part I. Linear constraints. *Journal of the society for industrial and applied mathematics*, *8*(1), 181-217.

Sbayti, H., & Mahmassani, H. (2006). Optimal scheduling of evacuation operations. *Transportation Research Record: Journal of the Transportation Research Board*, (1964), 238-246.

Schwiegelshohn, U., & Yahyapour, R. (1998, January). Analysis of first-come-first-serve parallel job scheduling. In *SODA* (Vol. 98, pp. 629-638).

Siu, K. Y., & Tzeng, H. Y. (1995, November). Congestion control for multicast service in ATM networks. In *Global Telecommunications Conference, 1995. GLOBECOM'95., IEEE* (Vol. 1, pp. 310-314). IEEE.

Smith, J. H. (1882). Exit from theaters. No. 254,717. Patented Mar. 7,1882.

Smith, M. J. (1993). A new dynamic traffic model and the existence and calculation of dynamic user equilibria on congested capacity-constrained road networks. *Transportation Research Part B: Methodological*, *27*(1), 49-63.

Southworth, F. (1991). *Regional Evacuation Modeling: A State of the Art Reviewing* (No. ORNL/TM-11740). ORNL Oak Ridge National Laboratory (US).

Soyster, A. L. (1973). Convex programming with set-inclusive constraints and applications to inexact linear programming. *Operations research*, *21*(5), 1154-1157.

Sridharan, A., & Krishnamachari, B. (2009). Maximizing network utilization with max–min fairness in wireless sensor networks. *Wireless Networks*, *15*(5), 585-600.

Steinhaus, H. (1948). The problem of fair division. *Econometrica*, *16* (1).

Tang, J., Xue, G., & Zhang, W. (2006, April). Maximum throughput and fair bandwidth allocation in multi-channel wireless mesh networks. In *INFOCOM 2006. 25th IEEE International Conference on Computer Communications. Proceedings* (pp. 1-10). IEEE.

Thawari, V. W., Babar, S. D., & Dhawas, N. A. (2012). An efficient data locality driven task scheduling algorithm for cloud computing. *International Journal in Multidisciplinary and Academic Research (SSIJMAR)*, *1*(3).

Thulasiraman, P., Chen, J., & Shen, X. (2011). Multipath routing and max-min fair QoS provisioning under interference constraints in wireless multihop networks. *IEEE Transactions on Parallel & Distributed Systems*, (5), 716-728.

Tuydes-Yaman, H., & Ziliaskopoulos, A. (2014). Modeling demand management strategies for evacuations. *Annals of Operations Research*, *217*(1), 491-512.

Ukkusuri, S. V., & Waller, S. T. (2008). Linear programming models for the user and system optimal dynamic network design problem: formulations, comparisons and extensions. *Networks and Spatial Economics*, *8*(4), 383-406.

van Essen, M., Thomas, T., van Berkum, E., & Chorus, C. (2016). From user equilibrium to system optimum: a literature review on the role of travel information, bounded rationality and non-selfish behaviour at the network and individual levels. *Transport reviews*, *36*(4), 527-548.

Vira, C., & Haimes, Y. Y. (1983). Multiobjective decision making: theory and methodology. In *North Holland series in system science and engineering* (No. 8). North-Holland.

Waller, S. T., & Ziliaskopoulos, A. K. (2006). A chance-constrained based stochastic dynamic traffic assignment model: Analysis, formulation and solution algorithms. *Transportation Research Part C: Emerging Technologies*, *14*(6), 418-427.

Wang, L., Yang, L., Gao, Z., Li, S., & Zhou, X. (2016). Evacuation planning for disaster responses: A stochastic programming framework. *Transportation research part C: emerging technologies*, *69*, 150-172.

Wang, Y., Tan, J., Yu, W., Zhang, L., Meng, X., & Li, X. (2013, June). Preemptive ReduceTask Scheduling for Fair and Fast Job Completion. In *ICAC* (pp. 279-289).

Wardrop, J. G. (1952, June). Some theoretical aspects of road traffic research. In *Inst Civil Engineers Proc London/UK/*.

Wie, B. W., Friesz, T. L., & Tobin, R. L. (1990). Dynamic user optimal traffic assignment on congested multidestination networks. *Transportation Research Part B: Methodological*, *24*(6), 431-442.

Wie, B. W., Tobin, R. L., Friesz, T. L., & Bernstein, D. (1995). A discrete time, nested cost operator approach to the dynamic network user equilibrium problem. *Transportation Science*, *29*(1), 79-92.

Xu, S., Jiang, W., Deng, X., & Shou, Y. (2018). A modified Physarum-inspired model for the user equilibrium traffic assignment problem. *Applied Mathematical Modelling*, *55*, 340-353.

Yagar, S. (1971). DYNAMIC TRAFFIC ASSIGNMENT BY INDIVIDUAL PATH MINIMIZATION AND QUEUEING. Transportation Research/UK/, 5(3).

Yao, T., Mandala, S. R., & Do Chung, B. (2009). Evacuation transportation planning under uncertainty: a robust optimization approach. *Networks and Spatial Economics*, *9*(2), 171.

Yazici, A., & Ozbay, K. (2010). Evacuation network modeling via dynamic traffic assignment with probabilistic demand and capacity constraints. *Transportation Research Record: Journal of the Transportation Research Board*, (2196), 11-20.

Yusoff, M., Ariffin, J., & Mohamed, A. (2008, August). Optimization approaches for macroscopic emergency evacuation planning: a survey. In *Information Technology, 2008. ITSim 2008. International Symposium on* (Vol. 3, pp. 1-7). IEEE.

Zaharia, M., Borthakur, D., Sen Sarma, J., Elmeleegy, K., Shenker, S., & Stoica, I. (2010, April). Delay scheduling: a simple technique for achieving locality and fairness in cluster scheduling. In *Proceedings of the 5th European conference on Computer systems* (pp. 265-278). ACM.

Zhang, Y., Xiong, K., An, F., Di, X., & Su, J. (2016). Mobile-service based max-min fairness resource scheduling for heterogeneous vehicular networks. *arXiv preprint arXiv:1603.03645*.

Ziliaskopoulos, A. K. (2000). A linear programming model for the single destination system optimum dynamic traffic assignment problem. *Transportation science*, *34*(1), 37-49.

APPENDIX A: Additional Figures

A.1 Chapter 3 Additional Figures

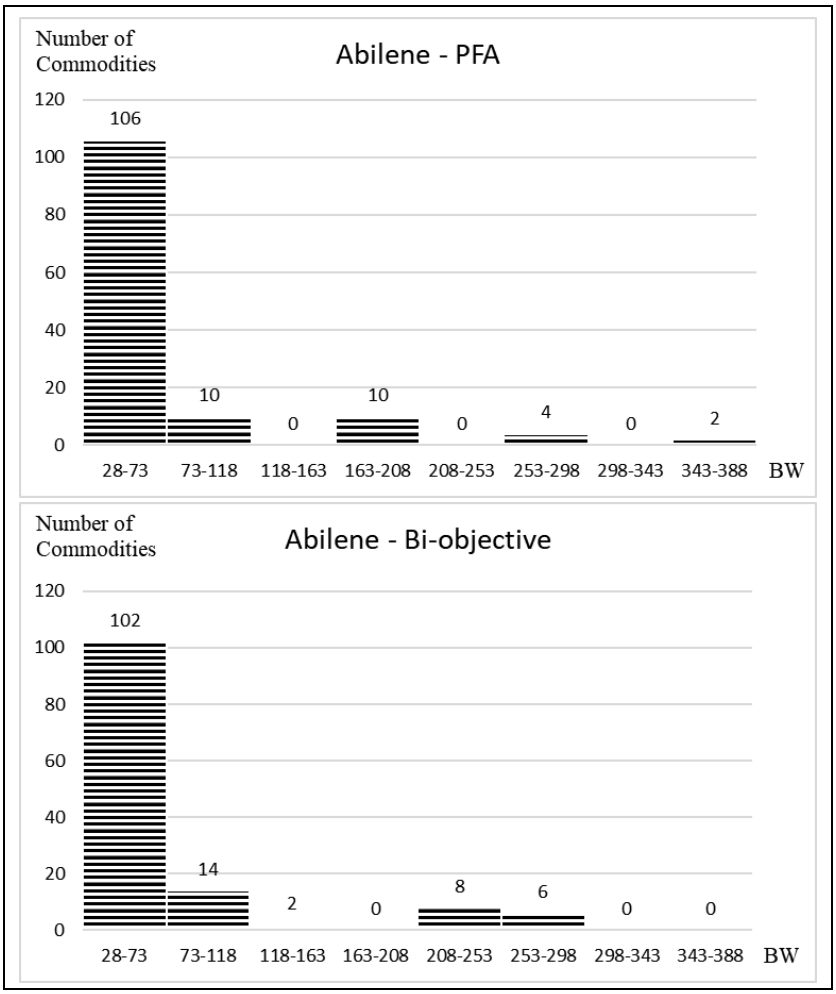

Figure A-0-1: The number of commodities in each bandwidth period using the progressive-filling algorithm and the bi-objective model for Abilene network

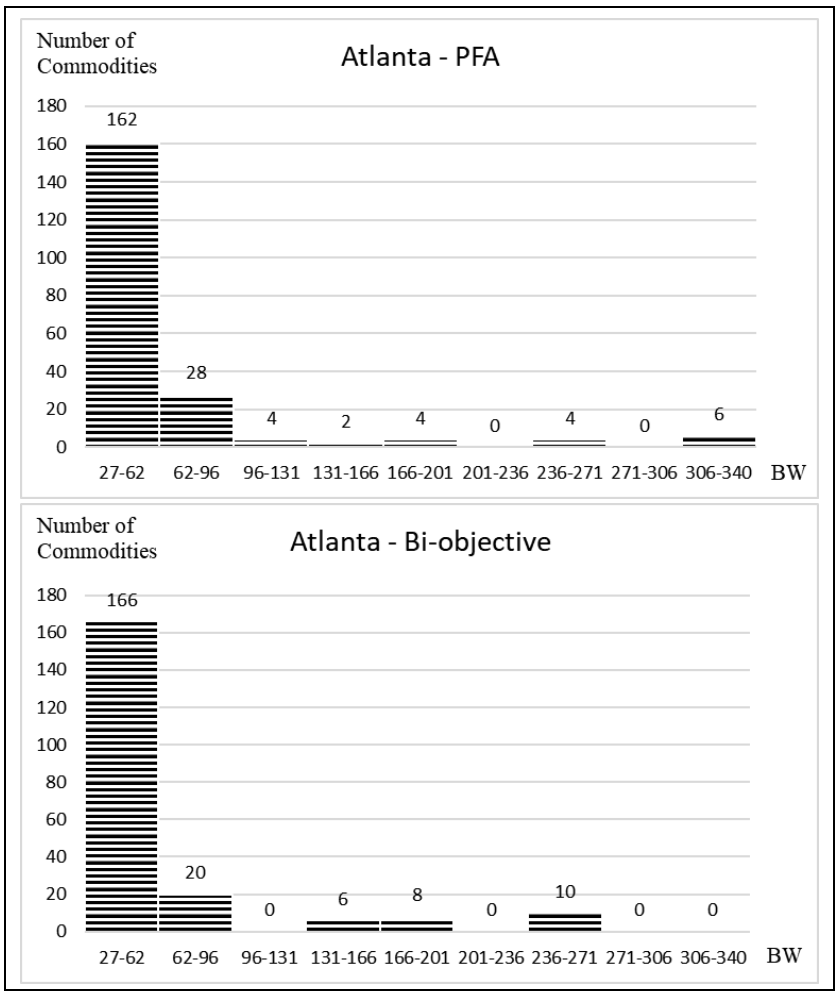

Figure A-0-2: The number of commodities in each bandwidth period using the progressive-filling algorithm and the bi-objective model for Atlanta network

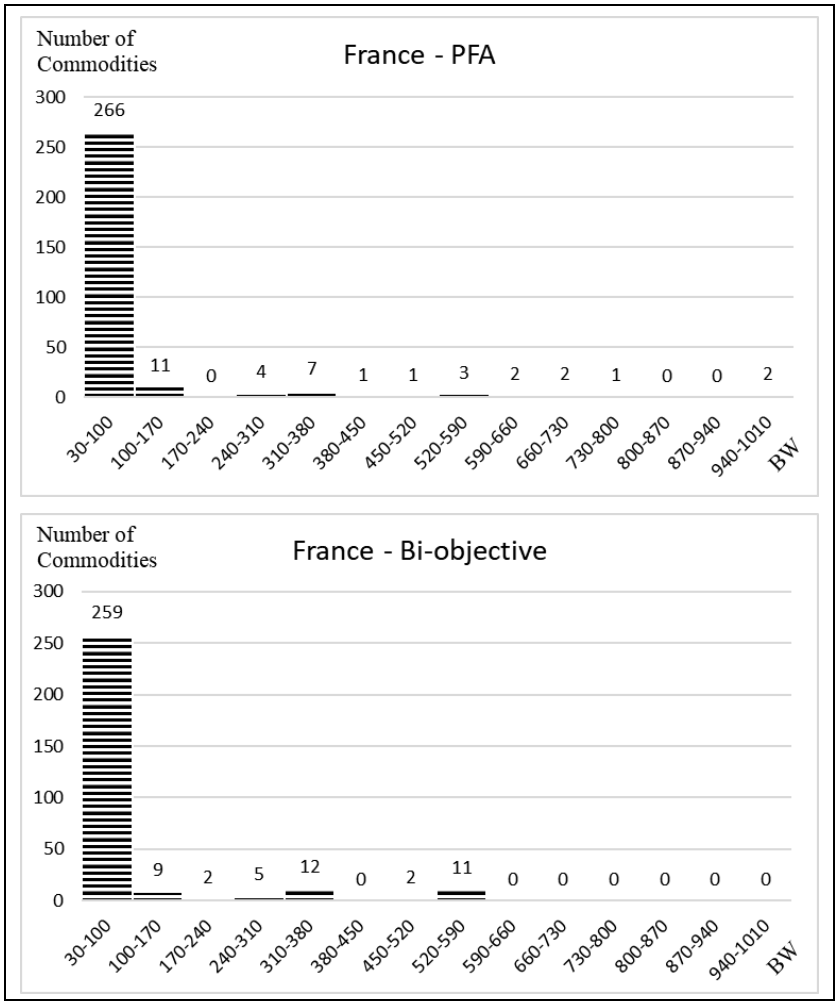

Figure A-0-3: The number of commodities in each bandwidth period using the progressive-filling algorithm and the bi-objective model for France network

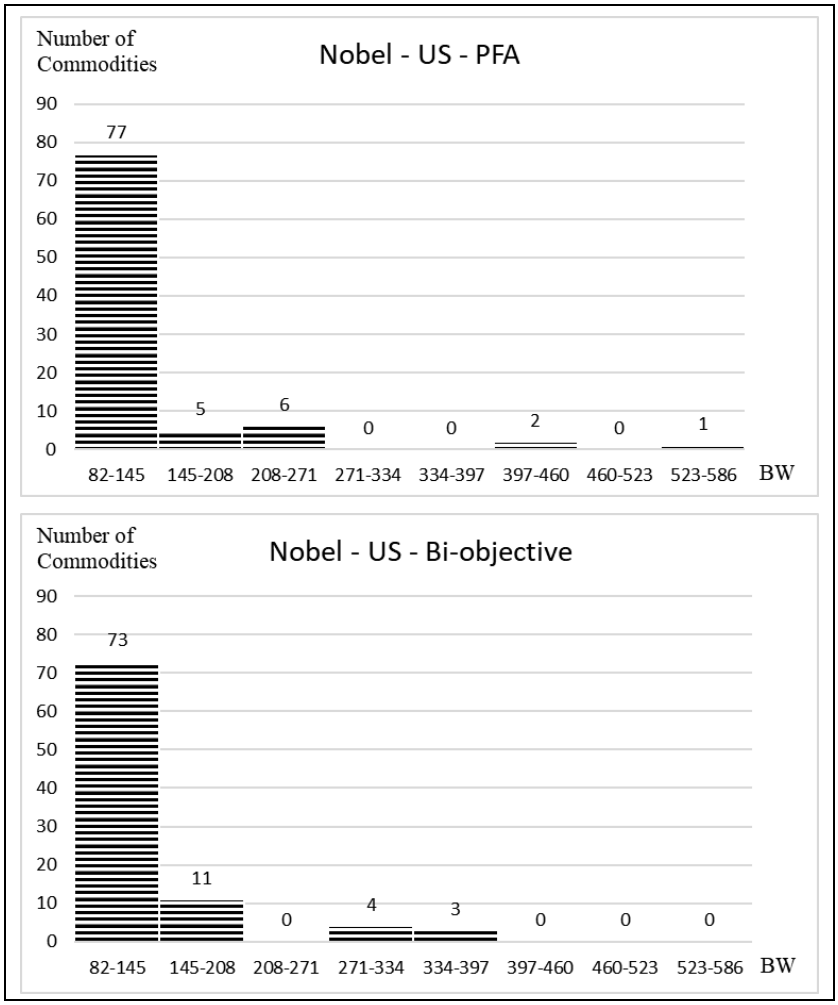

Figure A-0-4: The number of commodities in each bandwidth period using the progressive-filling algorithm and the bi-objective model for Nobel-US network

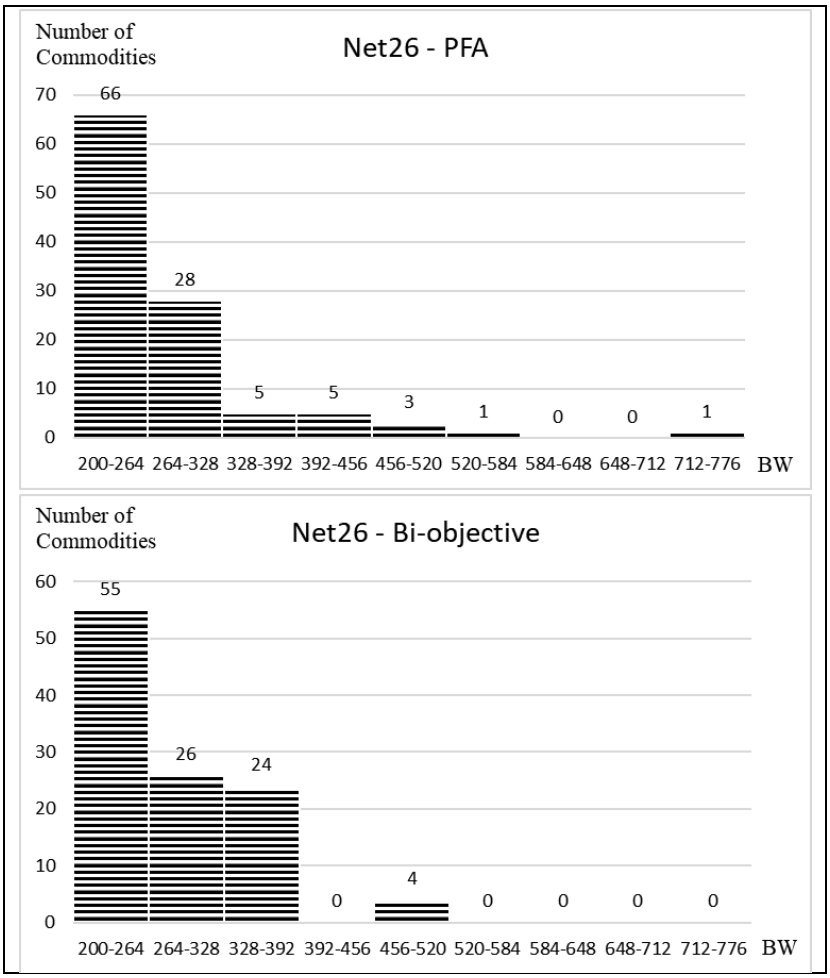

Figure A-0-5: The number of commodities in each bandwidth period using the progressive-filling algorithm and the bi-objective model for Net26 network

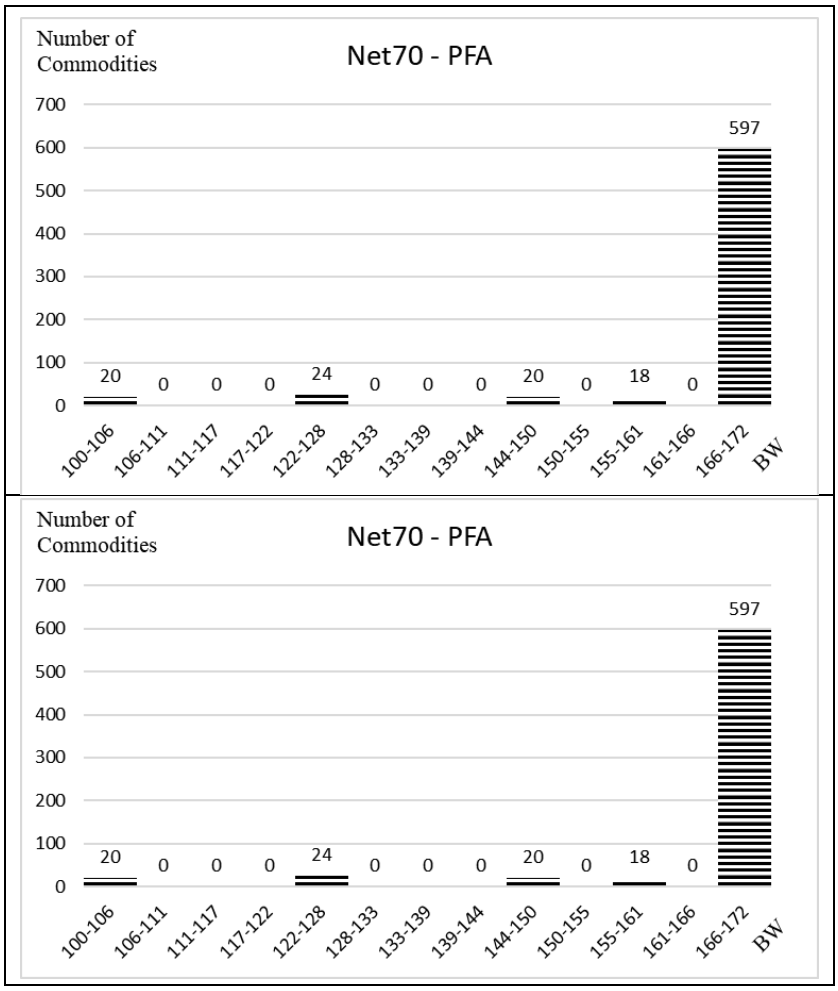

Figure A-0-6: The number of commodities in each bandwidth period using the progressive-filling algorithm and the bi-objective model for Net70 network

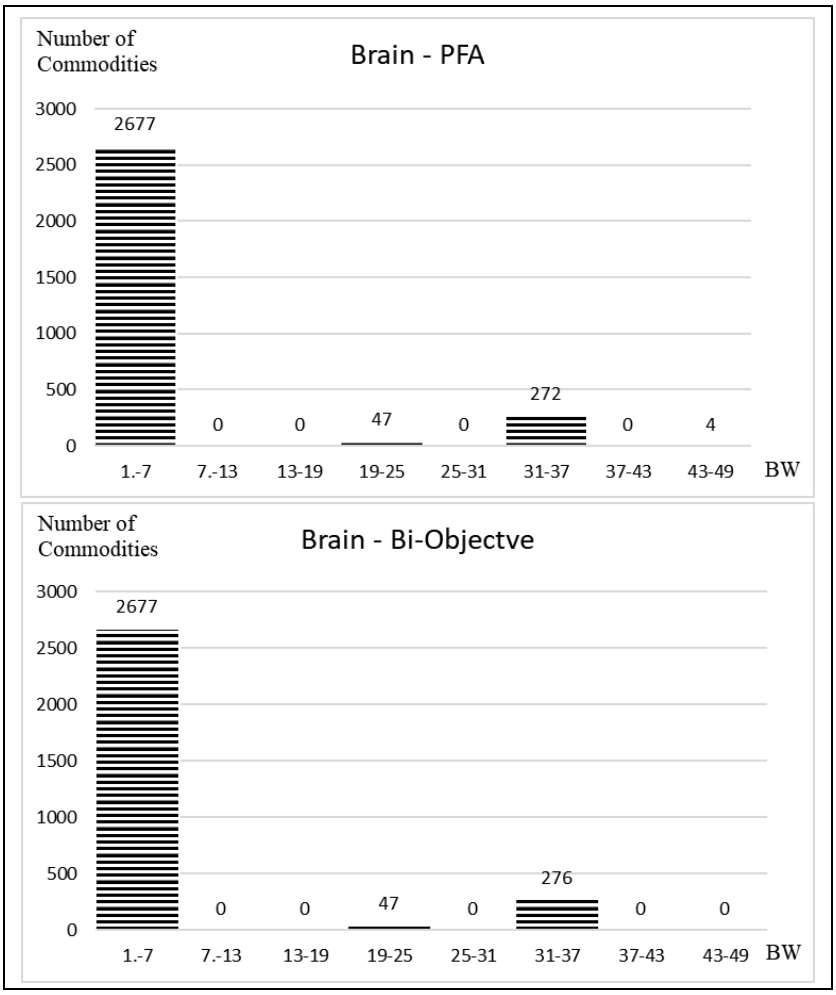

Figure A-0-7: The number of commodities in each bandwidth period using the progressive-filling algorithm and the bi-objective model for Brain network

A.2 Chapter 7 Additional Figures

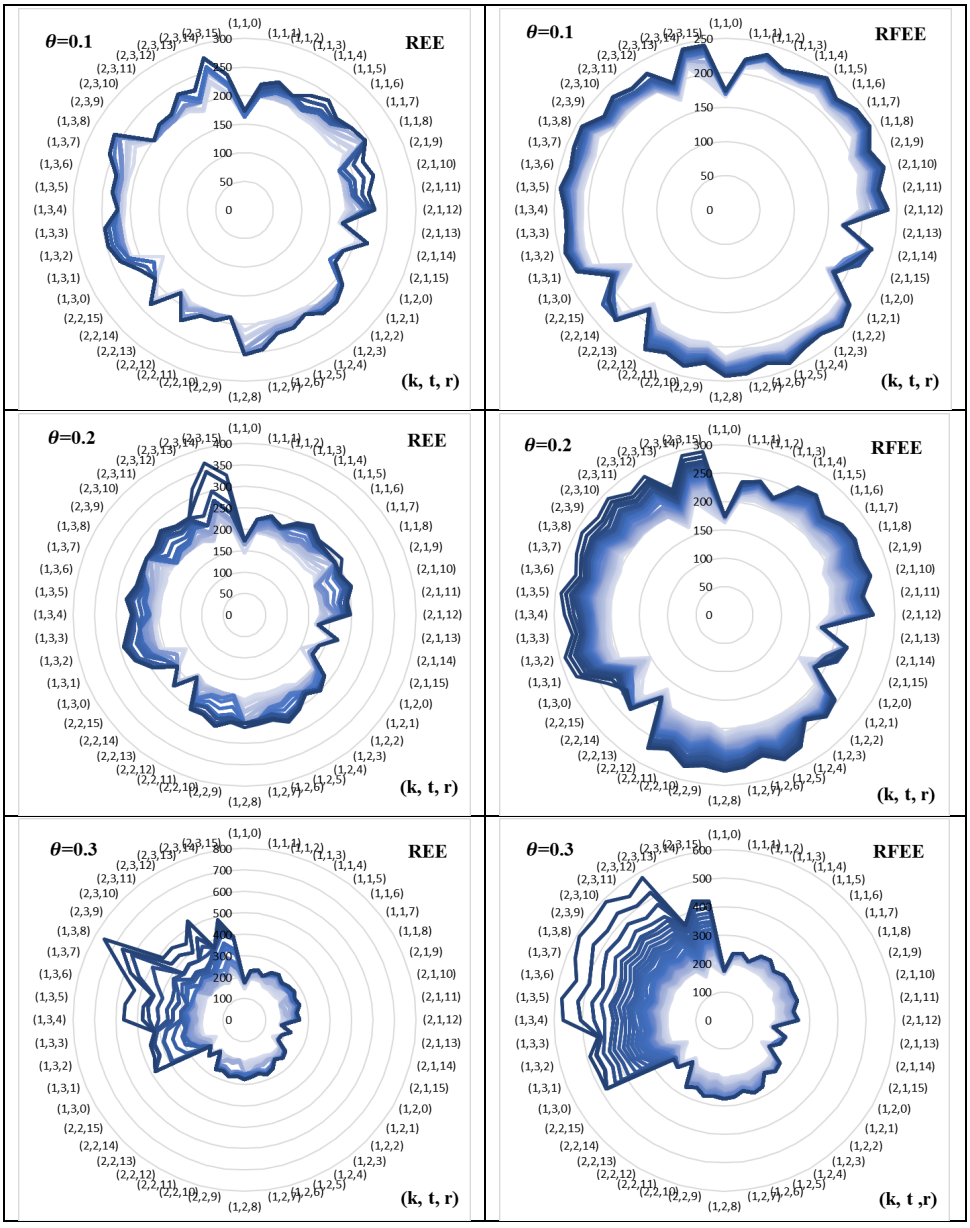

Figure A-0-8: The evacuation time for all groups evacuated from community k at time t on route r given controlled flow under REE and RFEE for the Nguyen and Dupuis network

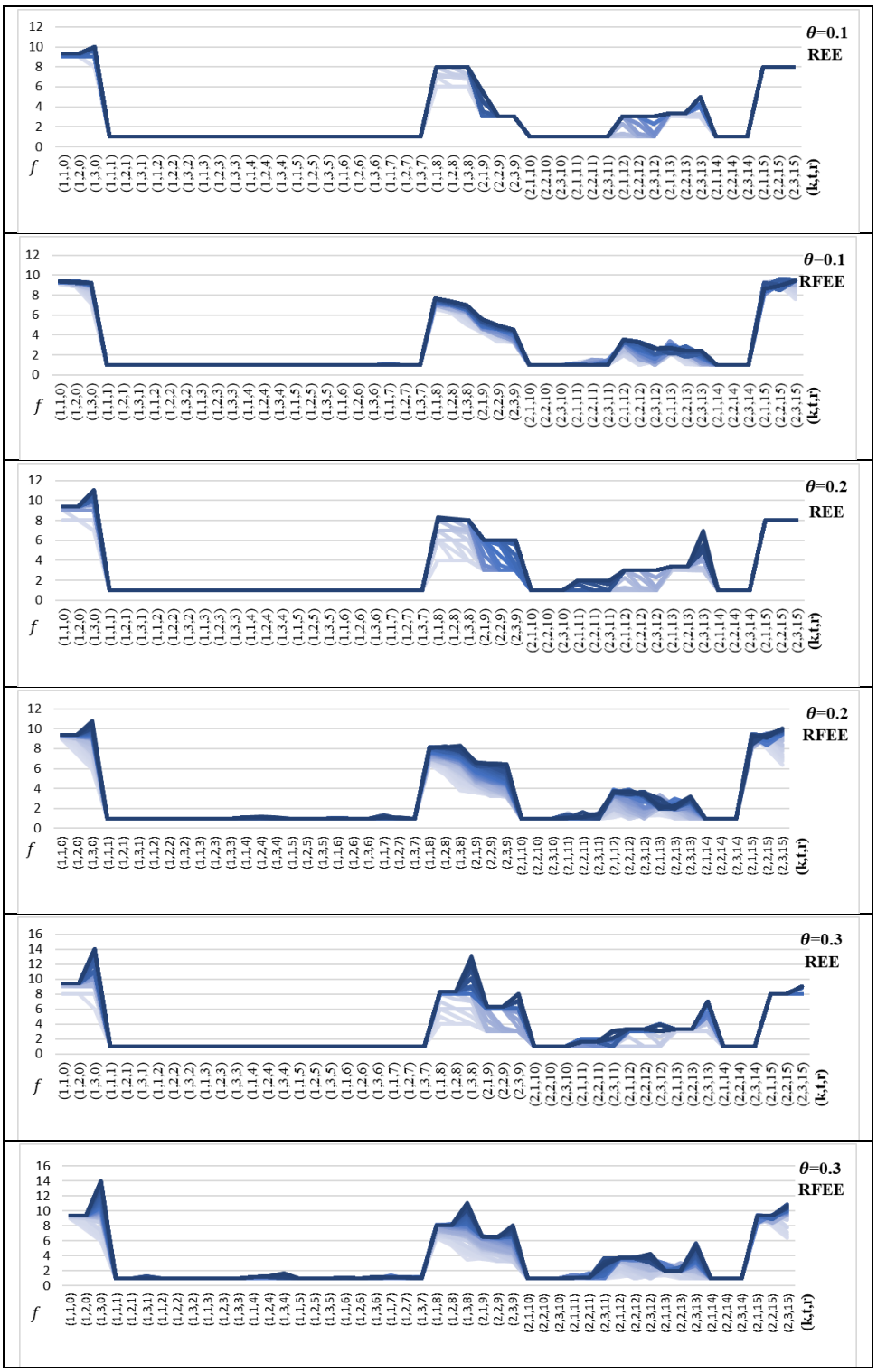

Figure A-0-9: The number of evacuees in each groups evacuated from community k at time t on route r given controlled flow under REE and RFEE for the Nguyen and Dupuis network

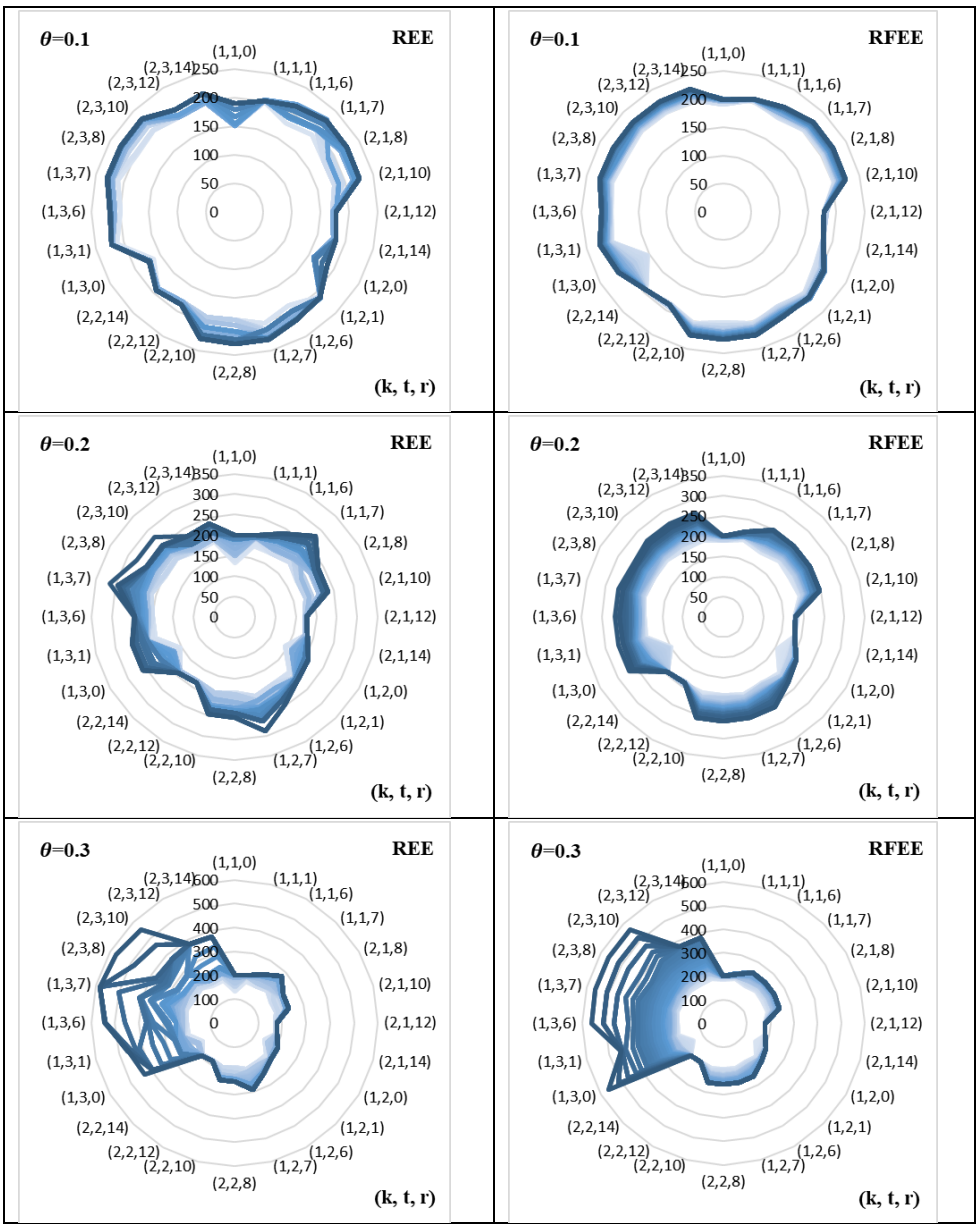

Figure A-0-10: The evacuation time for all groups evacuated from community k at time t on route r given controlled flow under REE and RFEE for the Nguyen and Dupuis network with optimal routes

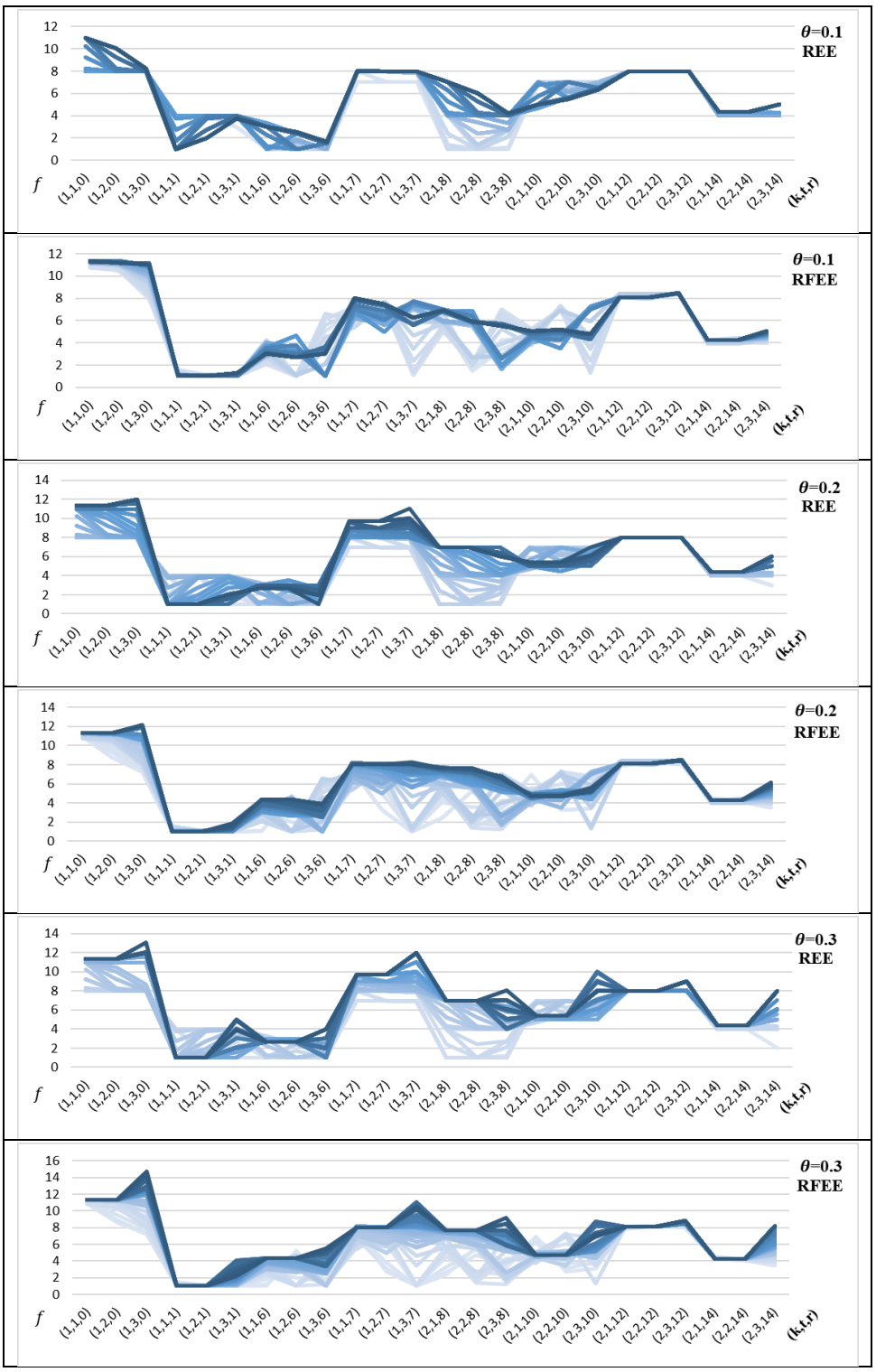

Figure A-0-11: The number of evacuees in each groups evacuated from community k at time t on route r given controlled flow under REE and RFEE for the Nguyen and Dupuis network with optimal routes

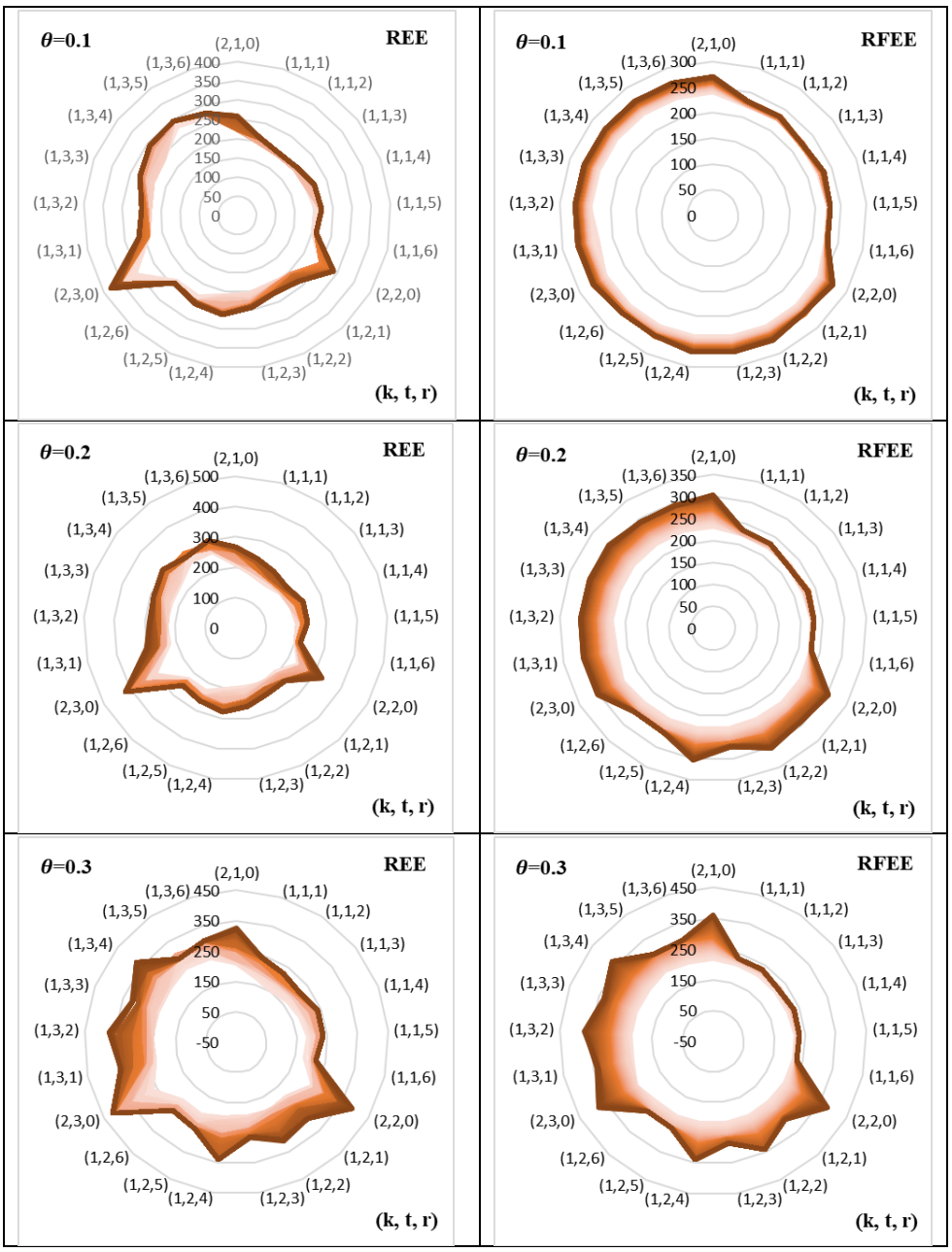

Figure A-0-12: The evacuation time for all groups evacuated from community k at time t on route r given controlled flow under REE and RFEE for the Tampa City network

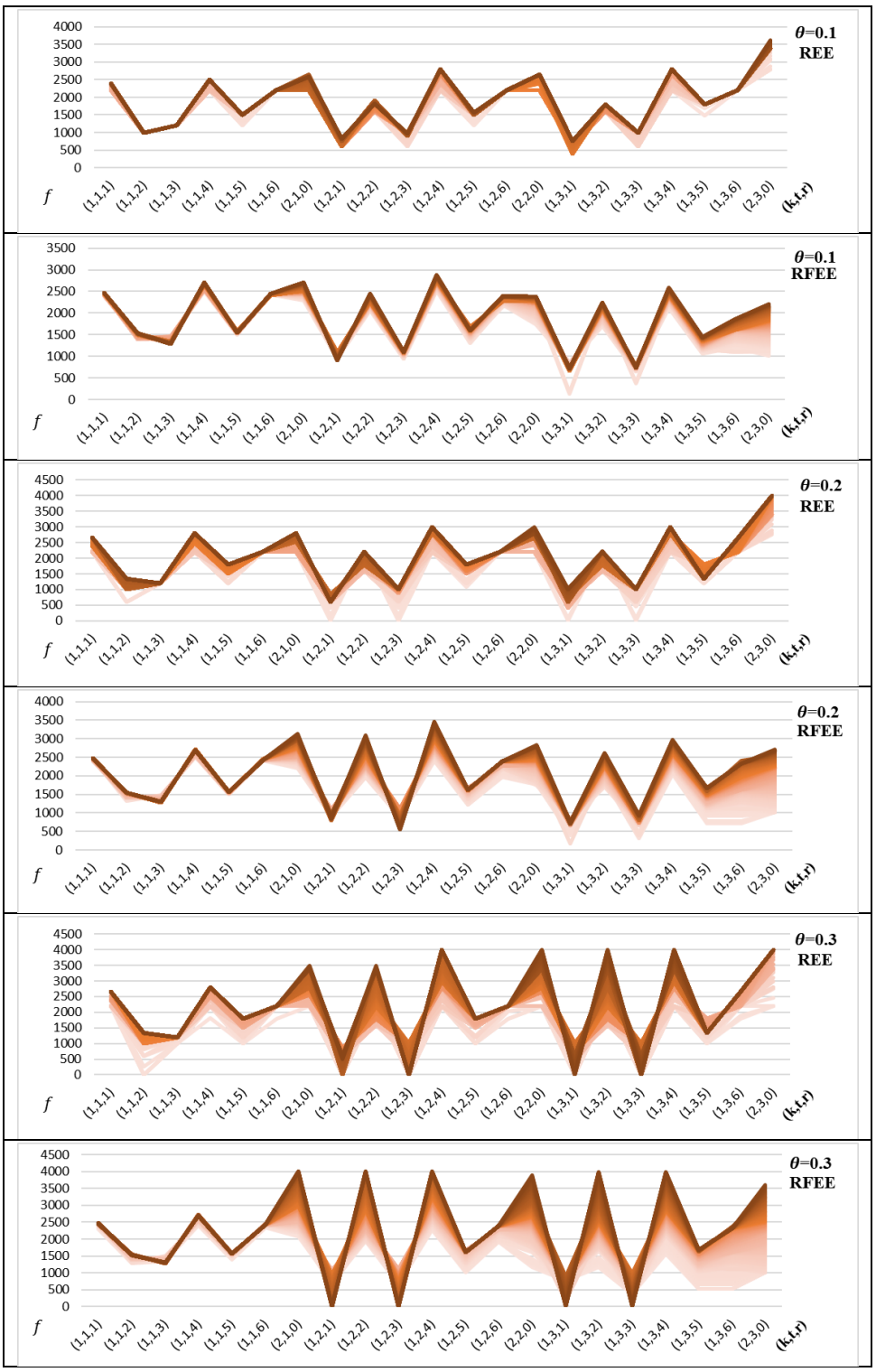

Figure A-0-13: The number of evacuees in each groups evacuated from community k at time t on route r given controlled flow under REE and RFEE for the Tampa City network

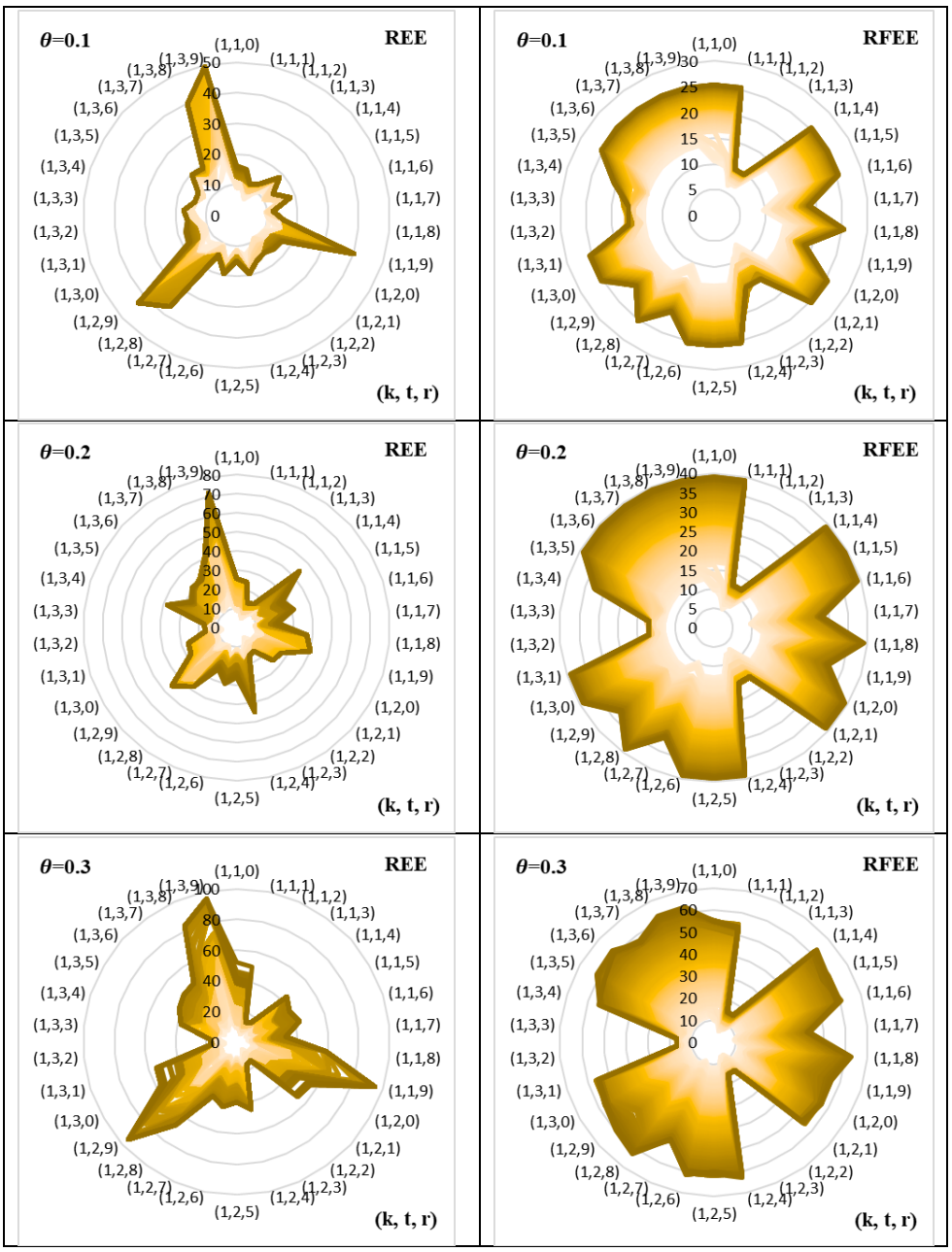

Figure A-0-14: The evacuation time for all groups evacuated from community k at time t on route r given controlled flow under REE and RFEE for the Fort Worth network

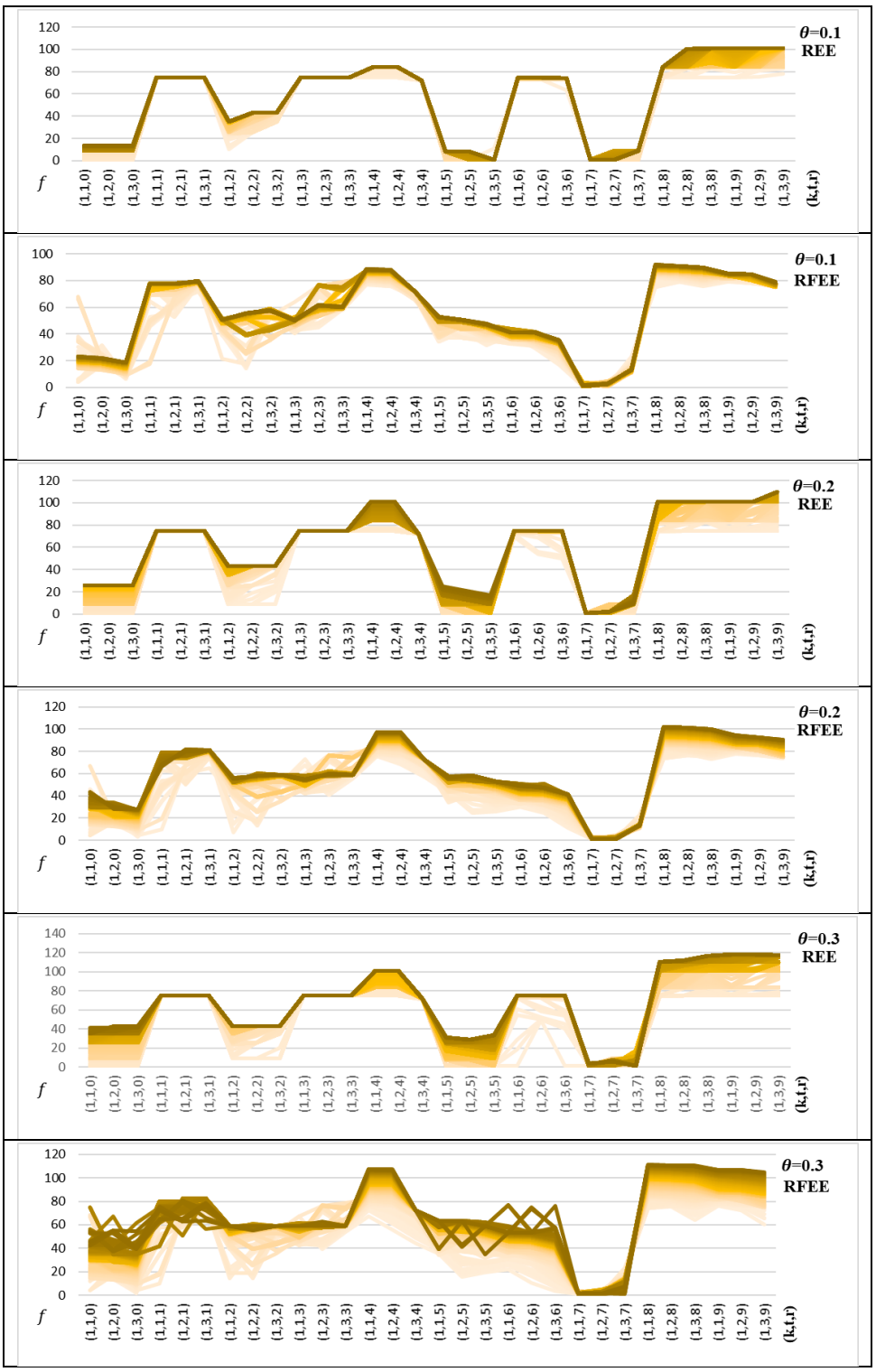

Figure A-0-15: The number of evacuees in each groups evacuated from community k at time t on route r given controlled flow under REE and RFEE for the Fort Worth network

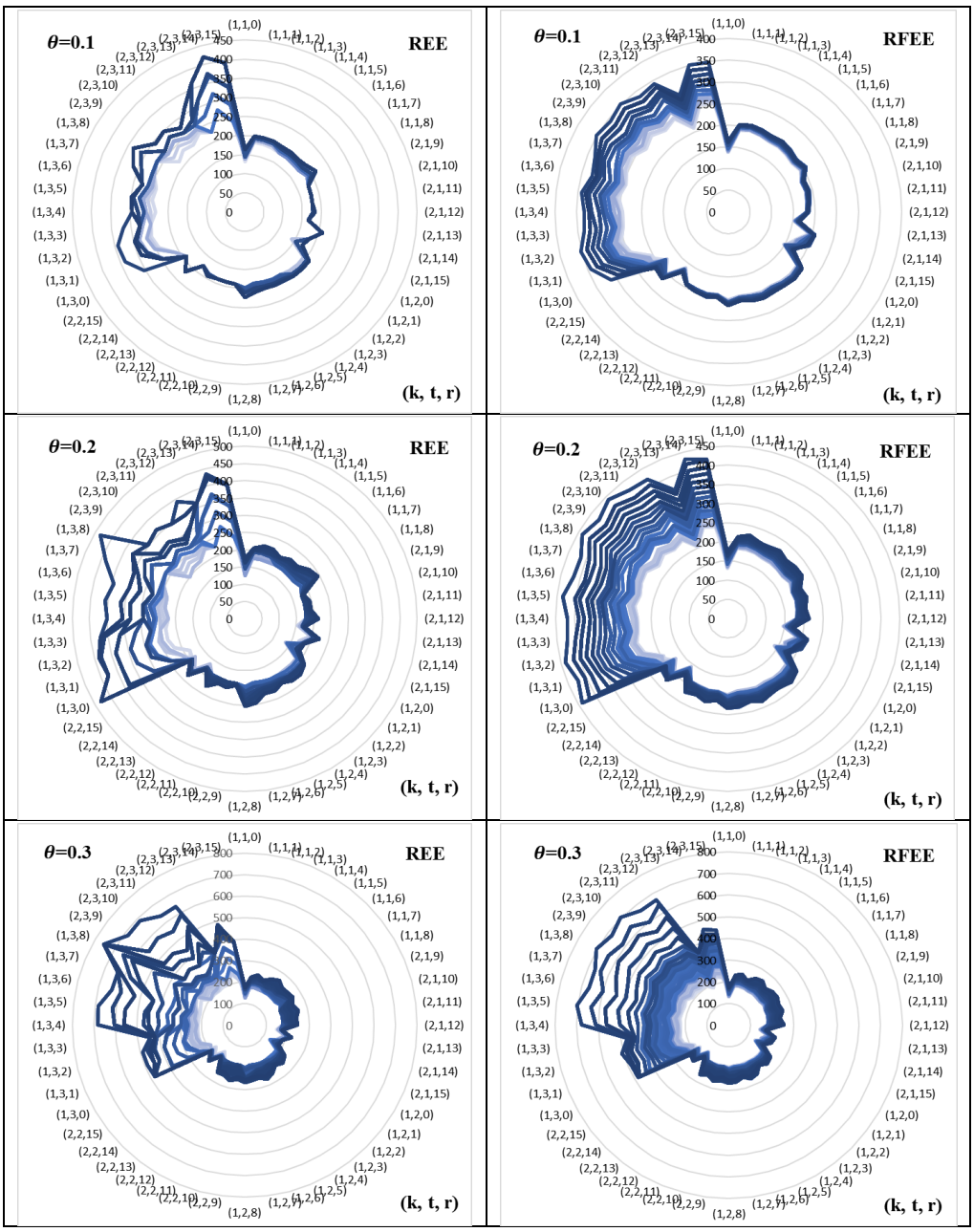

Figure A-0-16: The evacuation time for all groups evacuated from community k at time t on route r given uncontrolled flow under REE and RFEE for the Nguyen and Dupuis network

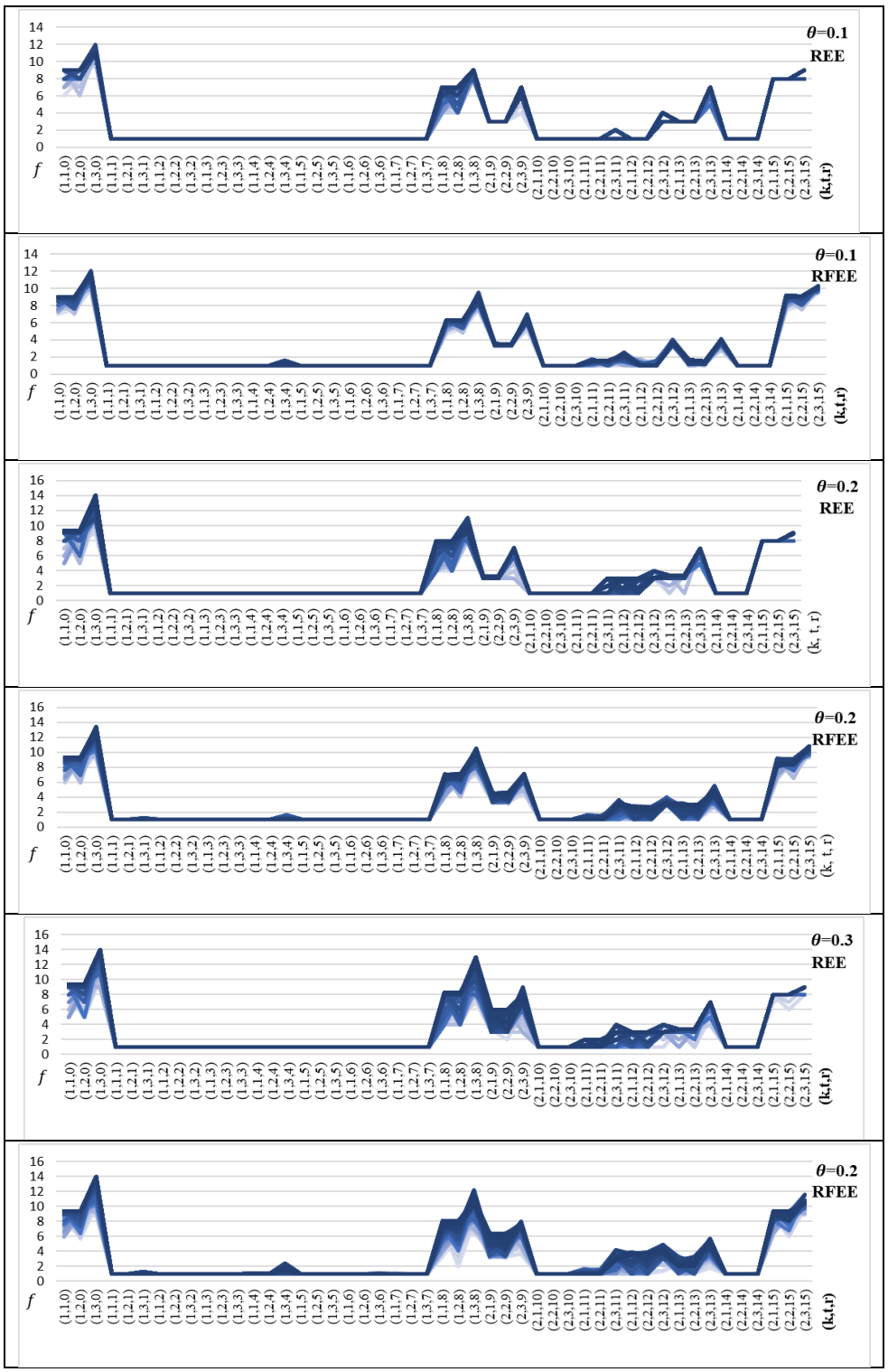

Figure A-0-17: The number of evacuees in each groups evacuated from community k at time t on route r given uncontrolled flow under REE and RFEE for the Nguyen and Dupuis network

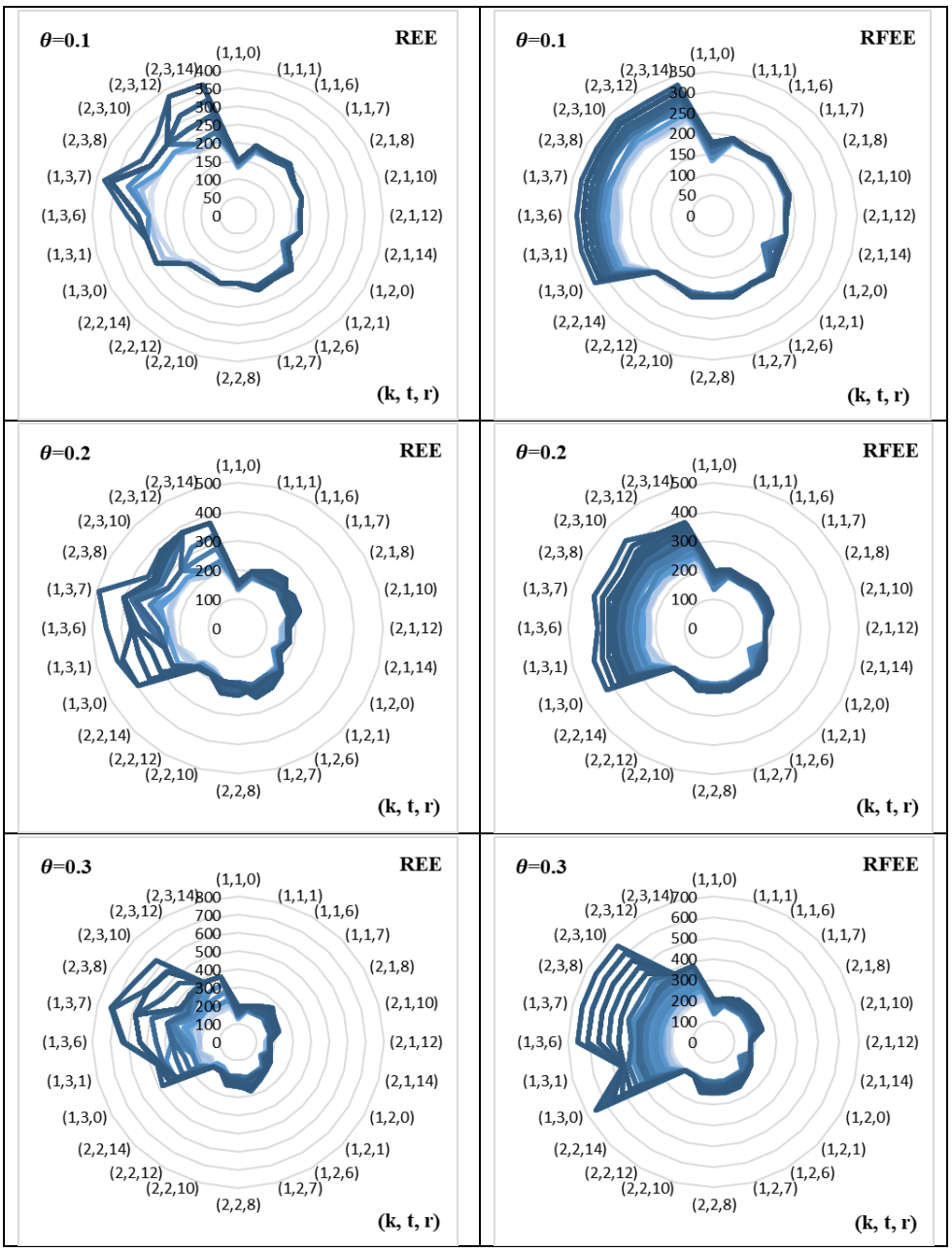

Figure A-0-18: The evacuation time for all groups evacuated from community k at time t on route r given uncontrolled flow under REE and RFEE for the Nguyen and Dupuis network with optimal routes

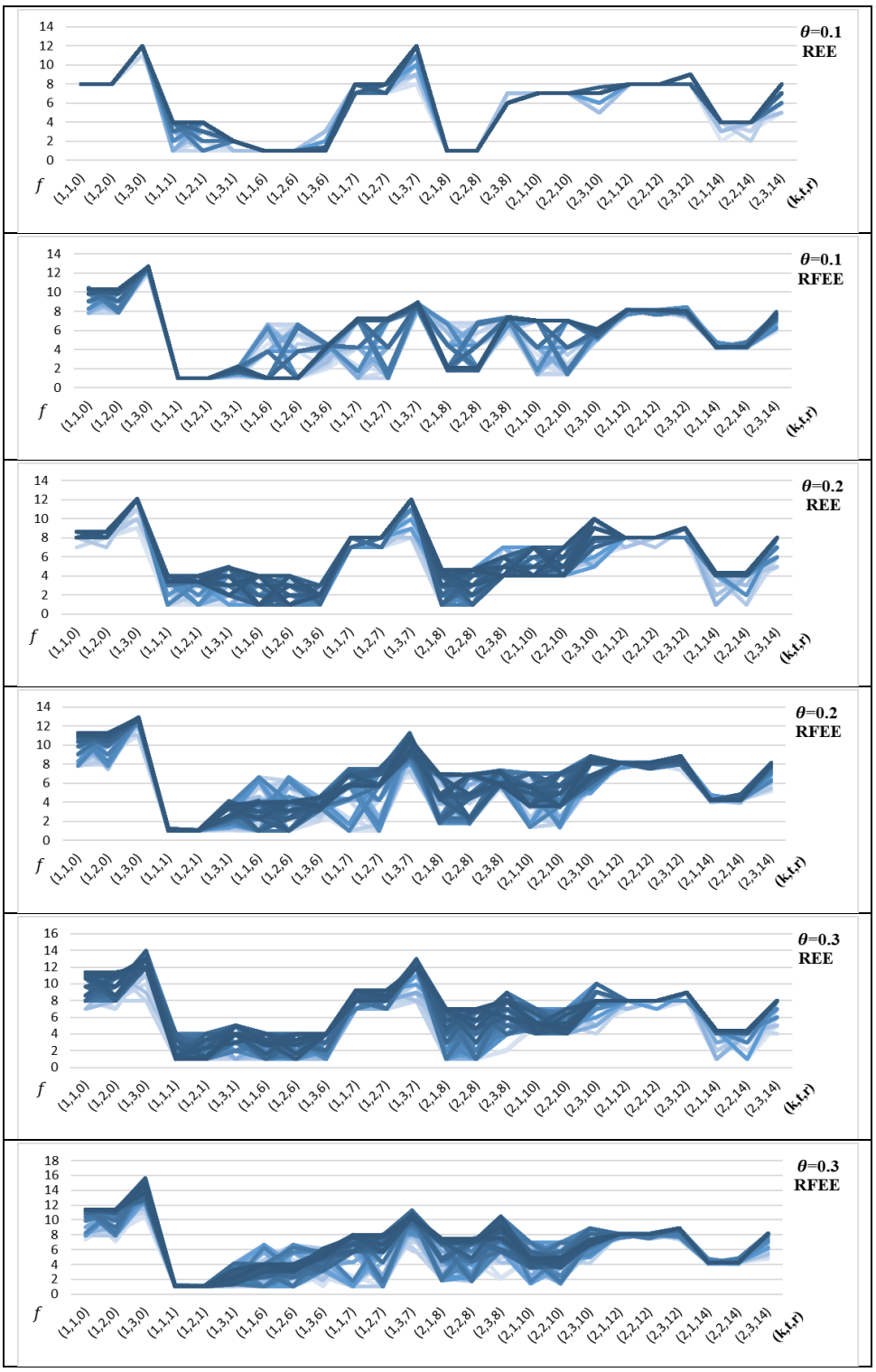

Figure A-0-19: The number of evacuees in each groups evacuated from community k at time t on route r given uncontrolled flow under REE and RFEE for the Nguyen and Dupuis network with optimal routes

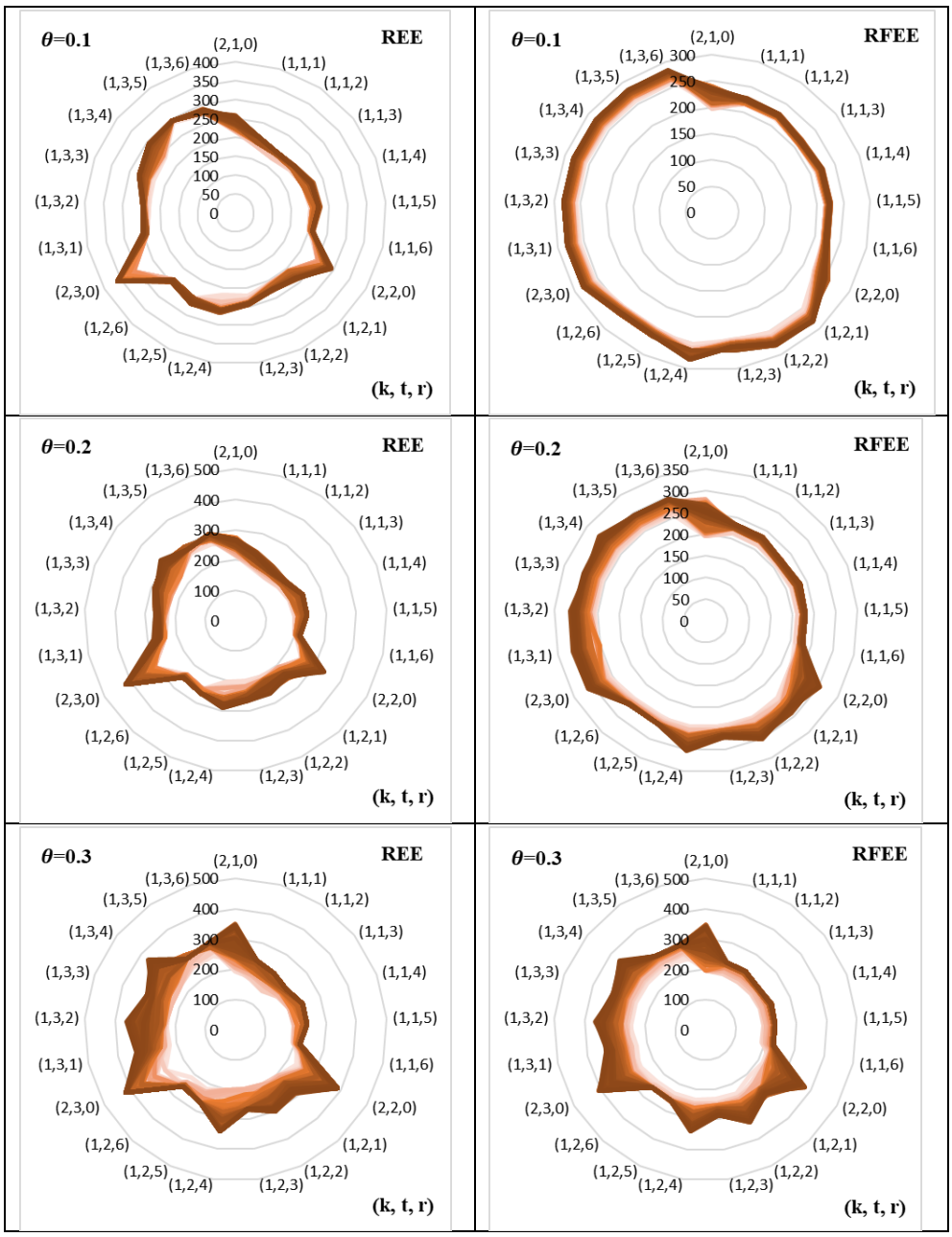

Figure A-0-20: The evacuation time for all groups evacuated from community k at time t on route r given uncontrolled flow under REE and RFEE for the Tampa City network

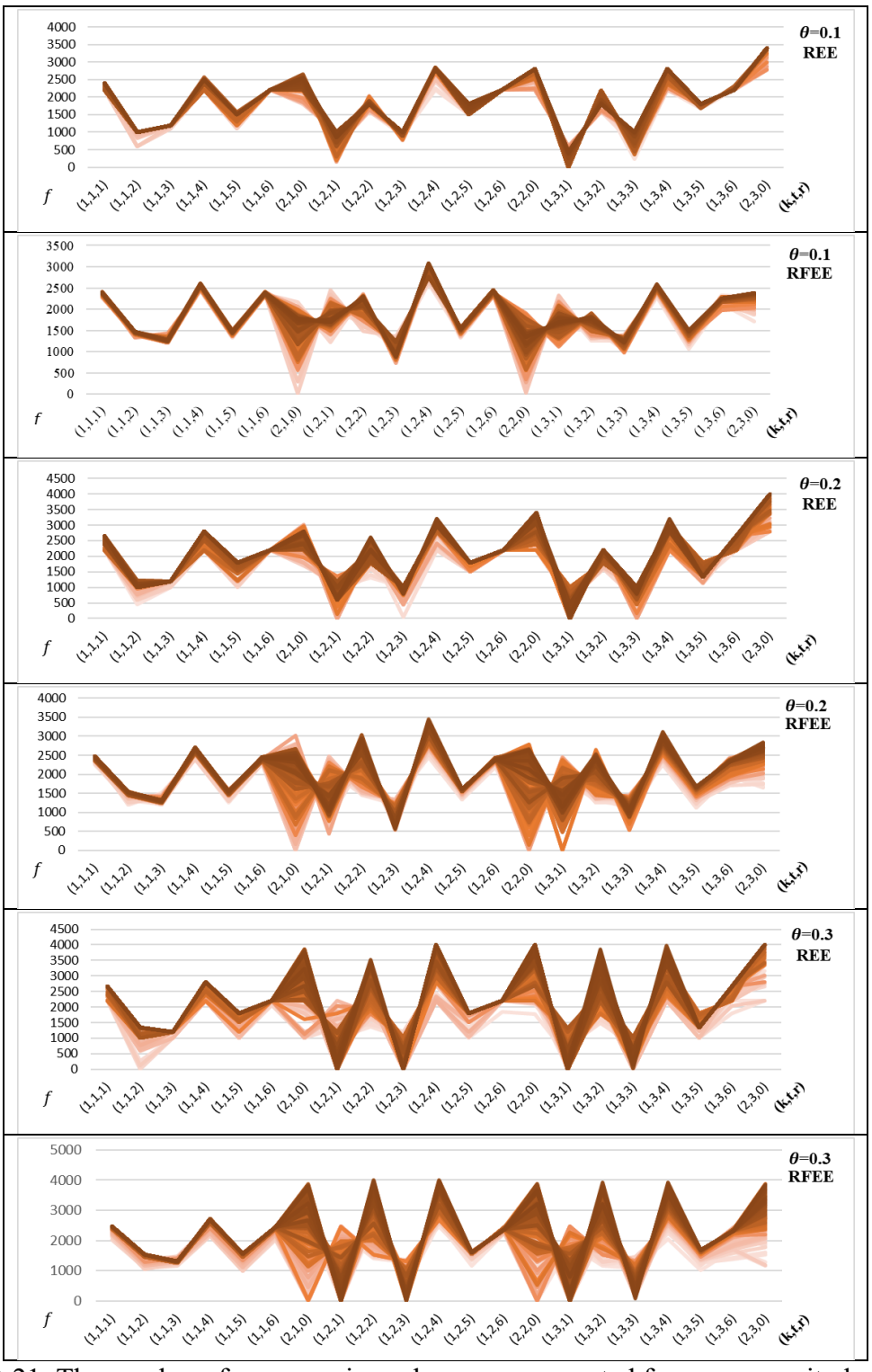

Figure A-0-21: The number of evacuees in each groups evacuated from community k at time t on route r given uncontrolled flow under REE and RFEE for the Tampa City network

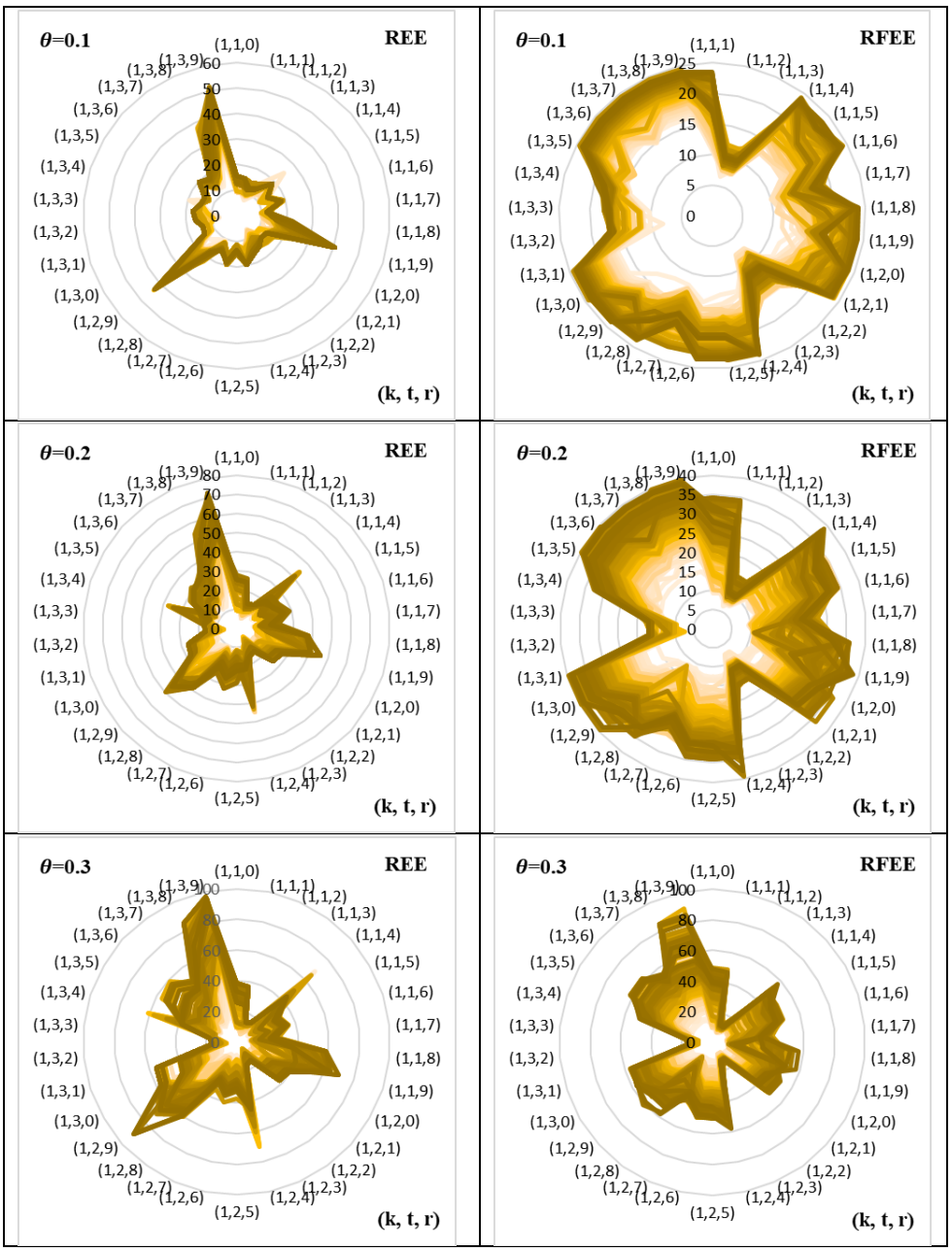

Figure A-0-22: The evacuation time for all groups evacuated from community k at time t on route r given uncontrolled flow under REE and RFEE for the Fort Worth network

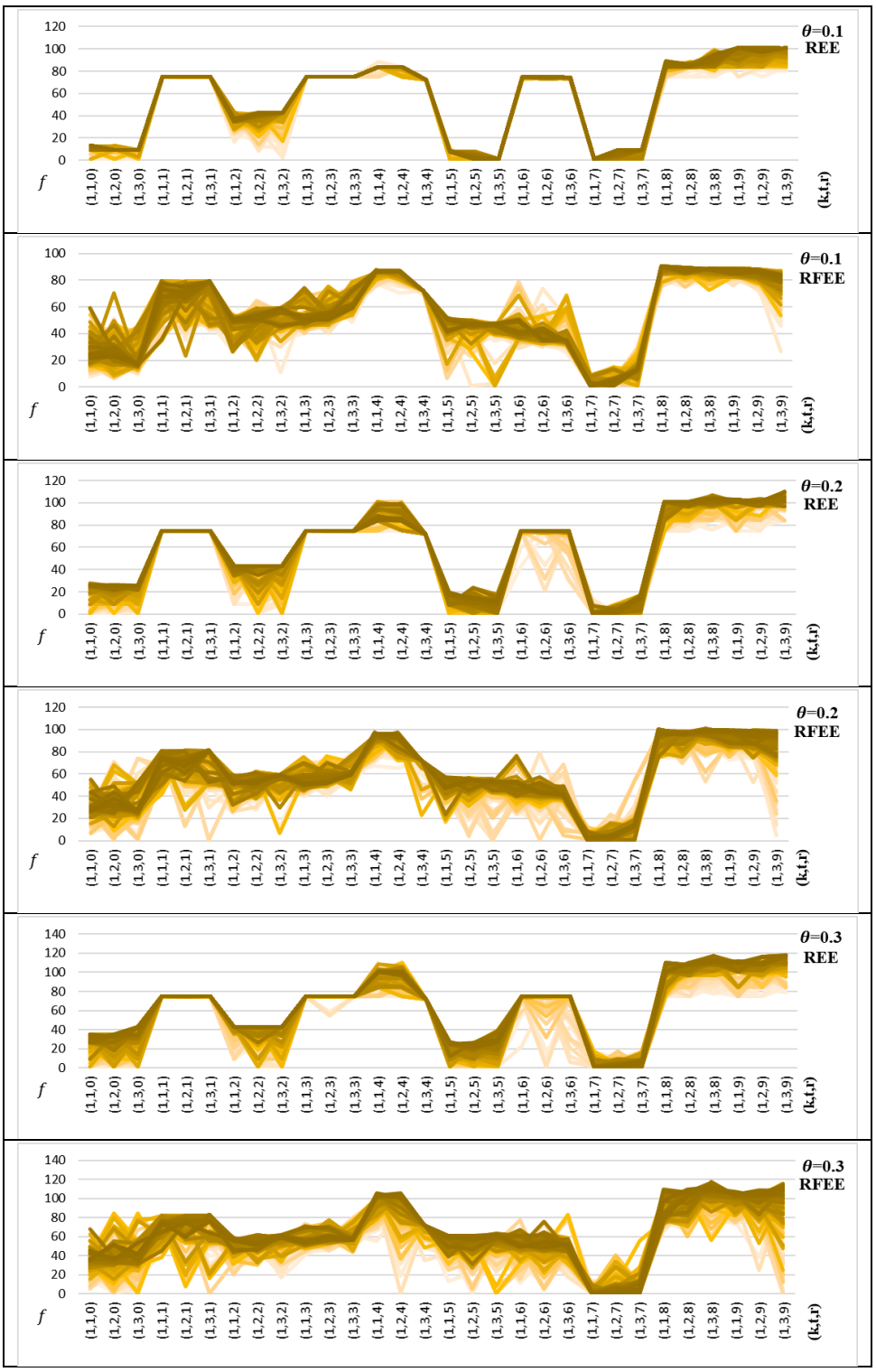

Figure A-0-23: The number of evacuees in each groups evacuated from community k at time t on route r given uncontrolled flow under REE and RFEE for the Fort Worth network